ADDIS ABABA UNIVERSITY

ADDIS ABABA INSTITUTE OF TECHNOLOGY

Effects of the Radius of Curved Rail and Vehicle Speed on Rail Friction and Wear

A Thesis Submitted to the School of Graduate Studies of Addis Ababa institute of Technology in Partial Fulfillment of the Requirement for the Degree of Masters of Science in Mechanical Engineering (Mechanical design)

by

Zemenu Tsehay Birhan

Advisor

Dr. Daniel Tilahun Redda

January, 2013

Addis Ababa

DECLARATION

Addis Ababa University

institute of Technology

This is to certify that the thesis prepared by Zemenu Tsehay entitled: Effects of the Rail Curve Radius and Vehicle Speed on Rail Friction and Wear and submitted in fulfillment of the requirements for the degree of masters of Science (Mechanical Design) compiles with the regulations of the university and meets the accepted standards with respect to originality and quality.

Signed by examining committee

Dr. Ing. Tamrat Tesfaye	_____	_____
External Examiner	Signature	Date
Dr. Ing. Zewdu igessa	_____	_____
Internal Examiner	Signature	Date
Dr. Daniel Tilahun	_____	_____
Thesis Advisor	Signature	Date
_____	_____	_____
Chairman	Signature	Date

ACKNOWLEDGMENT

My deepest gratitude goes to my advisor Dr. Daniel Tilahun, for his patience, concerned and valuable and constructive comments during the whole period of this thesis work.

I would also thank my family and friends for their unreserved encouragement and support they rendered to me during the entire period of schooling.

ABSTRACT

Effects of the Radius of the Curved Track and Speed of the Vehicle on the Rail Tribology

Zemenu Tsehay

Addis Ababa University

The aim of this work is to develop a theoretical background for the influence of the curved radius of the rail line and the vehicle speed on rail tribology. The mathematical equations are derived from the geometrical relations of the curved rail, the conic nature the wheels, speed and vehicle mass. This has two parts kinematic and dynamical analytical methods. The first one is focused on the geometrical constraint analysis with the vehicle motion. It helps to formulate equations that help to calculate lateral displacement of the vehicle over the rail, longitudinal slip, lateral slip and spin. In dynamical analysis the vehicle load due to its mass, velocity is added and friction and wear conditions are derived from the relations. The material which is applied on the study is UIC 60 standard carbon steel and their wear coefficients were taken from literature. All analysis of the equations was done by using MATLAB software. From the result of the study friction and wear are exponentially reduced as the curve radius increase and velocity decreases for the case horizontal curved track at the outer rail and the opposite is happened at the inner rail. The maximum load capacity of the rail has a direct and linear relationship with the radius of the track and an inverse exponential relationship with the increase of velocity of the vehicle. Result of friction and wear of canted curved track has two different patterns; the inner and outer rail friction and wear interchangeably increases as the vehicle speed is below and above equilibrium velocity respectively. The superelvation deficiency is linearly proportional for outer wear and inversely proportional for inner rail. Then the result will be utilized for designing appropriate curved rail roads, appropriate speed restrictions for the vehicles and to plan appropriate maintenance policy.

TABLE OF CONTENTS

List of Figure

List of Tables

Nomenclature

UIC	Union Internationale des Chemins (International Union of Railways)
D	Degree of the curve
α	Lateral force angle
F_N	Normal contact force per unit lateral length
v	Forward velocity of the wheelset
v_1, $v_2$and Ω_3	Actual velocities of the wheel longitudinal, Lateral and angular
v_1', v_2'andΩ_3'	Pure rolling velocity wheel longitudinal, lateral and angular
μ	Coefficient of friction
W_{ap}	Applied load (N)
K	Constant, referred to as a wear coefficient
A	Contact area
2l	Track gauge
ay	Lateral acceleration
az	Normal acceleration
∅	Lateral force angle
R	Radius of the curved track
R1	Right rail radius
R2	Left rail radius
λ	Conicity angle
Y	Lateral wheelset displacement
rr	Right wheel radius
rl	Left wheel radius
ro	Nominal wheel radius
Δr	Rolling radius differences between Right wheel and left wheels
t	Time
ω	Angular velocity of the wheelset
S	Arch length (perimeter for full circle)
ξx_l	Longitudinal creepage at left rail
ξx_r	Longitudinal creepage at right rail
ξ_{SP}	Spin creepage

V	Actual rolling velocity
ξy	Lateral creepage at both rails
φ	Cant angle
ht	Superelvation height
Veq	Equilibrium velocity
Θ	Angle of attack
ξ_{SP}	Spin creepage
$FA\vec{k}$	Left normal load
$FB\vec{K}$	Right normal load
$FA\vec{j}$	Lateral forces at left rail side
$FB\vec{j}$	Lateral forces at right rail side
ϕ	Roll angle of the wheelset.
$\overrightarrow{FA}$	Reaction force at rail A
$\overrightarrow{FB}$	Reaction force at rail B
$\overrightarrow{Fy}$	Lateral vehicle force at center of gravity of the vehicle
$\overrightarrow{Fz}$	Normal vehicle force at center of gravity of the vehicle
$\vec{i}, \vec{j}$ and $\vec{k}$	Unit vectors to the longitudinal, lateral and normal components
M	Vehicle total Mass [Kg]
W	Axle weight (N)
fWork	Frictional workdone
FR	Total load to be supported by the rails
$\sum M_A$	Total moment force about left rail
$\sum M_B$	Total moment force about Right rail
M_{sp}	Spin moment
Sy	Yield strength for the asperity
Veq	Equilibrium velocity
ξ	Sliding per unit length motion of the vehicle

FfB and FfA	Contact friction at the left and right rails
v	Wear volume per unit length per material constants
Q	Volume of wear [m^3]
PA	Normal pressure at left rail
PB	Normal pressure at right rail
al . bl	Contact Simi-axis dimension longitudinal and lateral at left rail
ar. br	Contact Simi-axis dimension Longitudinal and lateral at right rail
$V_{vehicle}$	Vehicle speed (m/s)
ξx	longitudinal slippage
ξxl	longitudinal slippage at left rail
ξxr	longitudinal slippage at right rail
ξxs	longitudinal slippage at rail side
MGT	Million (mega) Gross Tons

CHAPTER 1

1. INTRODUCTION

1.1 Background of the problem

Now, Ethiopians are concerned of the growth and development transformation plans which envision a big change for the country in to middle income countries in the coming five years. Growth rate of infrastructure is highly speedy. Railway engineering has crucial importance in solving transportation problems and to interconnect cities. Most educational institutions, recently, are showing interest to include railway study into their academic programs. The implication is that, attention is given for this system of transportation. Railway construction is very expensive, but has a long life and low operating costs **[1]**. Nowadays, the demand has led to the need to operate rolling stock on track with low as well as high radius curves; increased speeds and axle loads; and cope with a decrease in track quality due to a reduction in maintenance. These changes lead to an increase in the severity of the wheel/rail contact conditions, which may increase the likelihood of wear or damage **[2]**. New technologies and better safety standards are constantly being introduced associated with curve radius, speed and elevations but there will always some risk associated with accidents and early degradation of the components. These risks have multi-dimensional consequence on the system of transportation as well as for countries development which can be expressed in terms of loss of human life, infrastructure unavailability, traffic delay, penalty imposed by transport authority, and loss of assets and environmental impact when train carrying hazardous material is derailed. The track response for dynamic loading has different aspects of which one is rail tribology. Then the first step to design safe rails requires the idea of rail tribology. Rail way is preferable over the others due to:-it can handle a sufficient number of trains at a time; timetable that satisfies the customers' demands; low tariffs; reduced travel time; low environmental pollution. But lately, many derailments and train collisions were reported, which fortunately caused only material damage. The speed reduction is also another problem that prevents active transportations. By doing this research on the title effects of curve radius and speed of the vehicle on wear and friction properties of rails has many advantages for the global level and as well for the country 'Ethiopia' which is in the way to develop. Wear and friction take place at every rail and vehicle interaction but curves and speed assist the problem to be wrong. The Ethiopia Geographical nature looks constructing curved rail is mandatory since the country has many features that are inappropriate to construct a deserved tangent tracks such as rivers, cities, and steep slopes. So studying curved track wear and friction properties at different vehicle speed and track parameters is

very relevant. Then the result will be utilized for designing appropriate curved rail roads, appropriate speed restrictions for the vehicles and to plan appropriate maintenance policy. Degradation due to wear and which cannot be completely eliminated, it needs continues effort to put more the system safe. A detailed analysis for the situation a track is mandatory to get optimum friction which can balance the cost due to high damage that comes from high friction and the derailment risk due low friction. Cost effective is coming when the maximum operation efficiency of geometrical parameters is designed before actual rail construction. The rail tribology here is to mean the change in friction and wear property due to the various changes in numeric values of superelvation height, track radius and speed of the vehicles. Therefore, it is important to assess the geometrical relation with the tribology of the rail.

1.2 Objective of the thesis

1.2.1 Major objective

- Analyze the influence of the radius of curve and vehicle speed on friction and wear conditions of rails

1.2.2 Specific objectives

- ✓ To determine the effect of variation curve radius of rail in friction property of wheel rail contact
- ✓ To determine the effect of variation curve radius in rail wear.
- ✓ To assess effects of changing speed on friction, wear of rail within curved track.
- ✓ To assess the influence of superelvation on friction and wear.
- ✓ To predict the life of the rail based on allowable wear limits.

1.3 Organization of the thesis

This thesis is organized in to six chapters. In the first chapter, background and justification of this thesis work and the objectives to be achieved are discussed. In chapter two, a review of literature relevant to this thesis work, which has been investigated by different researchers, is given. Chapter three is about formulating analytical relations which deal with the interaction between vehicle and curved rail by using kinematic and dynamic analysis. In chapter four, materials, methods and conditions that applied for result analysis and interpretations of the study are presented. In chapter five results of the analysis are summarized and discussions are made based on using deferent ranges of a radius of a track, velocity of a vehicle and superelvation height by doing graphs using MATLAB software. Finally, chapter six gives conclusion achieved from this thesis work and propose future work in this field of study.

CHAPTER 2

2 LITERATURE REVIEW

Tribology is the study about friction and wear, which is one of the most important properties of matter; and helps to determine the cost and energy saving potential of the system. This is possible by minimizing energy consumption and wear. Friction occurs when two bodies are in relative rubbing motion; and rubbing means that the bodies are in actual contact. It generates wear and heat. Wear takes place on both rubbing surfaces. It depends on interactive force and geometry of contacting mates. Geometry of a track has a vital effect on life of both wheel and rail materials. For example the fatigue life of standard 280 to 290 HB hardness rail on tangent track is about 800 MGT and the wear life on medium radius curves is accepted to be only around 350 MGT under local conditions, due to side wear. From this the wear life of the rail is lower than fatigue life The wear life of sharp curves is accepted, also due to severe side wear, to be between 13-27 MGT **[3]**. Lubrication on sharp curves has been commonly adopted as a method of reducing friction between the wheel flange and rail gauge face to minimize wear and energy consumption **[4, 5].** Study shows 10% to 20% additional wagons can be hitched to a train for the same tractive effort when the line is consistently and properly lubricated **[3].** The achievement found is done on field observation and yet there is no formal theoretical relation that shows effects of curve radius on rail-wheel tribology. Many friction models show that friction is affected by the rheology of the third body, slip distance and load with the shear stress, of which slip distance exhibits the dominant influence **[6]**. In curves there can be a large sliding component on the contact patch at the gauge corner of the rail head since the wheel flange is in contact with the gauge corner of the rail. Flanging results causes large sliding motion in the contact patch **[7]**. Sliding increases wear rate in the contact under the poorly lubricated condition that is typical of wheel/rail contact. During sliding wear, an increase of the severity of loading (normal load, sliding velocity, or surface temperature) leads to a sudden change in the wear rate (volume loss per sliding distance). It was found that mild wear dominated at the rail head, but at the rail edge severe wear was clearly occurring. For horizontal curved track radius below 1500 m at any of case of vehicle run with flange contact whereas within elevated track of curve radius of 700 m rather than 1500 m any of the cases with lower conicity wheel/rail combinations run in flange contact. Where there are separate flange and tread contact points, the conditions at the point with the higher contact stress and traction coefficient. At the tighter 700 m radius, the wheels are much closer to full slip and the traction coefficient changes much more markedly. Therefore, curve radius of the track has a strong influence on rail wear. The influence also depends on the vehicles and their behaviors especially speed **[8]**. Speed can adversely influence

the curving performance of the vehicle and, in turn, lead to wear and stresses in rail and wheel **[9]**. It is because the point of application of the load moves with the running speed. Due to the centrifugal forces at the curves, the outer rail bears substantial amount of forces that wears it out. By applying a superelvation, wear can be decreased **[10].** It helps prevent overturning of the vehicle, to overcome the centrifugal force of the vehicle on curves. Degradation on either the high rail or low rail lying in the same curve radius depends on the speed of the vehicle. The higher the speed, the more the degradation will be on the high rail. This is because much of the wheel flange is in contact with the inner surface of the high rail than the inner surface of the low rail due to centrifugal force acting on the vehicle. The lower the speed, the more the degradation will be on the low rail **[1]**. The narrow curved rail highly affected by vehicle loading to wear and plastic deformation. Figure 2.1 shows the transformation of the profile of a UIC 60 high rail over a period of two years in a narrow curve with a radius of 303m and trafficked by commuter trains **[10]**. In general, rail wear is classified into vertical and lateral wear. Vertical wear occurs on the upper head of the rail. This type of wear is evident along the straight track or on the inner rail of the curves. Lateral wear occurs on the railhead side. At curves, this type of wear is the most important parameter determining the operating life of wheel and rail.

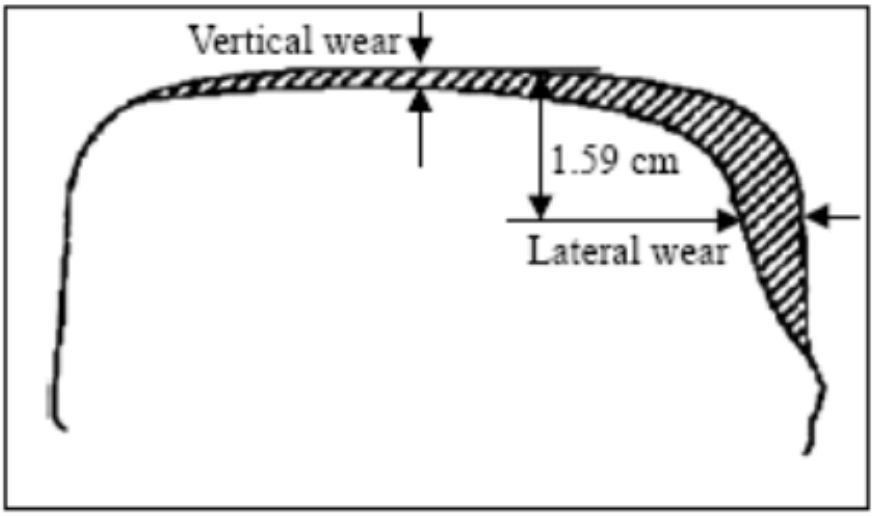

Figure 2.1: Vertical and Lateral Rail Wear due to Two Point Contact **[10]**

The influence of curve radius can be clearly seen when comparing rail wear rate as a function of curve radius and the rail wear rate seems to increase exponentially for decreasing curve radius, **[11]** as shown in fig. 2.2

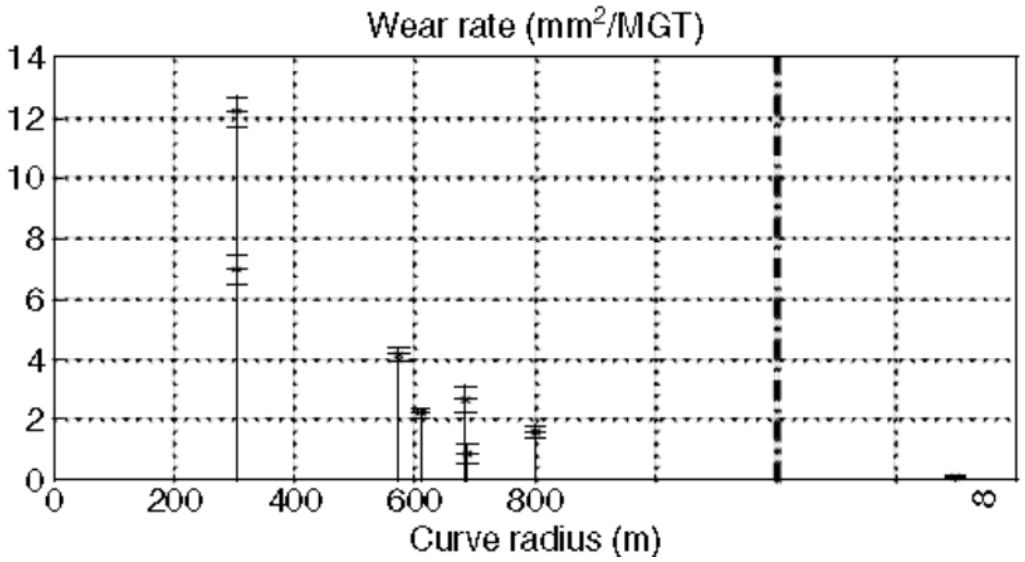

Figure 2.2: Wear Rate for High Rail as the Function of Curve Radius **[11].**

Similarly Table 2.1 and fig. 2.3 are the taken from **[6]** which shows the influence of curved radius on wear conditions of the rail at both rails.

Table 2. 1 Cross-sectional area loss at both rails from field measurement

		Traffic Wear	
	Total area [mm2]/MGT		Total area [mm2]/MGT
	High Rail	High Rail	Low Rail
Curve radii [m]	Non Lubricated	Lubricated	Non Lubricated
0<R<300	10.56	2.57	1.14
301<R<450	5.13	1.41	0.63
451<R<600	2.79	0.85	0.38
601<R<800	1.39	0.48	0.21
801<R<1500	0.36	0.15	0.07
1501<R<9999	0.25	0.11	0.05
10 000<R	0.14	0.06	0.03
Tangential track	0.03	0.02	0.01

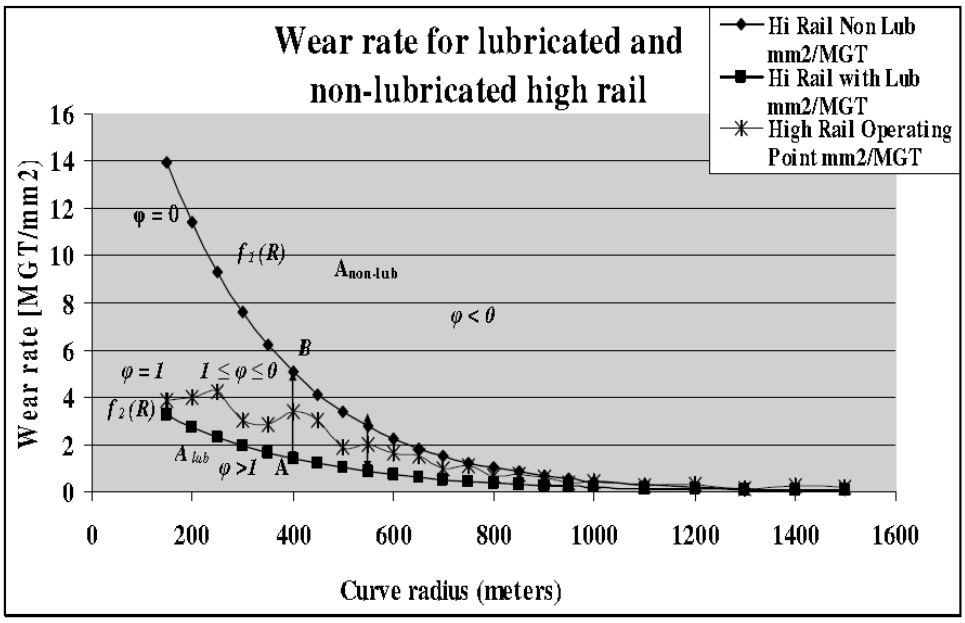

Figure 2.3: Traffic Wear Rate for Lubricated, Non-Lubricated operating Point

Track curves are observed with high wear rate and the intention of this paper is to see the influence of curve radius and vehicle speed on friction and wear rate in curved rail.

CHAPTER 3

3 ANALYTICAL METHODS

3.1. Curved rail properties

The main elements of rail way industry are track structure and rolling stock as shown in fig. 3.1. A track consisting of rails, fasteners, sleepers, ballast plus underlying subgrades **[12].** Sleepers hold the rails to correct the gauges and transmit loads, fasteners are used for the purpose of fastening against sleepers and the ballast is a part of foundations. Among these, rail is a central discussion point in this paper. It is the main bearing element of track, is made of longitudinal steel members that help to accommodate wheel loads and distribute these loads over the sleepers or supports.

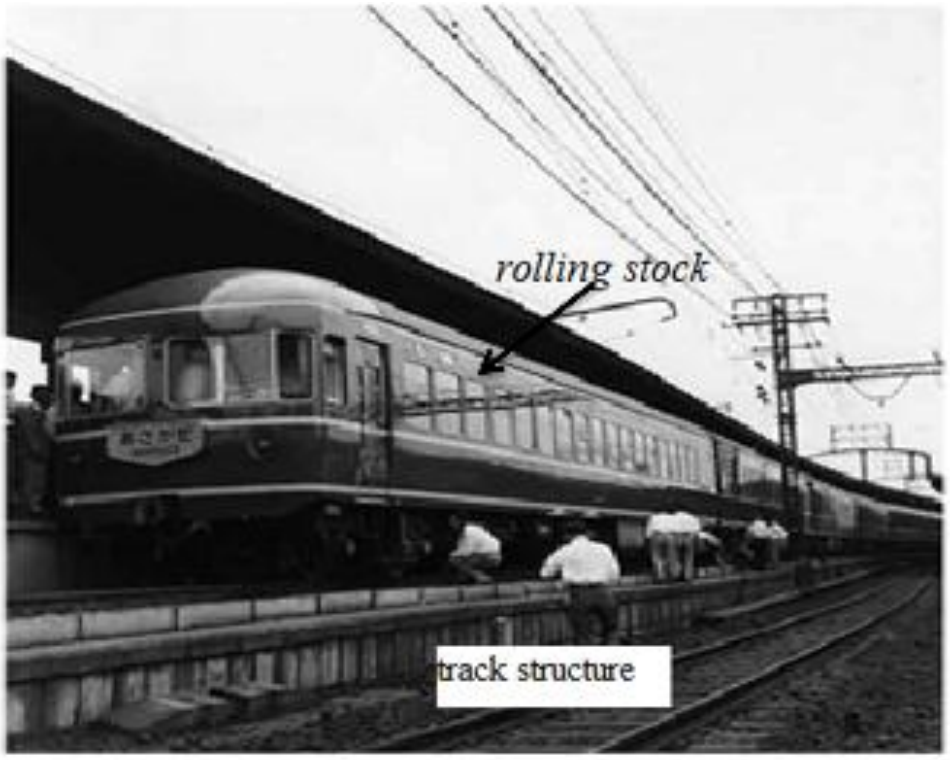

Figure 3.1: Track Structure and Rolling Stock

It withstands large dynamic loads in vertical, longitudinal and lateral direction. Strong and wear proof rails are required for safe railroad traffic. The rails are the most important element in railway study. Their function is to guide the wheel-sets, to support the loads and to damp the vibration generated during motion. The rails where wheel-sets are in contact have transverse section 'T' to guarantee the maximum moment of inertia. The rails are classified based on mass in Kg per 1m, it may call 21, 27, 30, 36, 46, 50, and 60.UNI 60 is the most widely used and produced in 36 and 48 m length. All rails are inner tilted with a cone angle (mostly 1/20 or 1/40), used for stability during

motion, to maintain contact of wheel-set to the center of the track and adjust velocity within the same angular velocity of wheel-set axle. The rail can be divided into three parts: the rail head, rail web and rail foot as shown in fig.3.2.

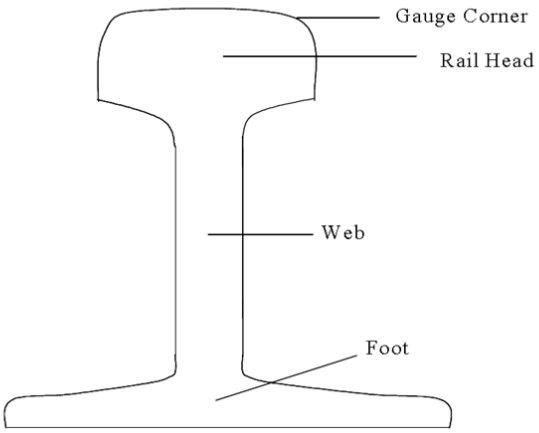

Figure 3.2: Parts of Rail **[13]**.

Similarly in rolling stock profiled-flanged steel wheels are in contact with the rail and are used for support, guidance and traction. Rail-wheel material plays a very important role in rail degradation. When a railway wheel rolls across a smooth rail track with sufficient hardness to support its weight, it is generally observed that there is only a small amount of friction to oppose the rolling motion. The rails must possess sufficient stiffness so that they can act as beams and transfer the concentrated wheel loads to the spaced sleeper supports without excessive deflection between supports.

Track geometry has a great influence on the tribology of rails by changing the vehicle load and force transmission. Railroad track geometry is intrinsically three-dimensional. For practical purposes the vertical and horizontal components of track geometry are usually treated separately. In this thesis only horizontal circular curves which use a uniform radius for the entire distance between adjacent tangent sections are used.

A circular curve used on railway system is identified with the following parameters:

- Direction of curve may be considered as clockwise or anti-clockwise depending on the motion of the trains through the curved rails. And in this thesis outer rail is at the right side of the driver and the inner rail is at the left side considering clockwise movement of the vehicle over the rail.
- Radius, R or degree, D: - The radius, R is the radius of the circle at the center line of the track and the degree D is another term used to describe the curve by curvature in place of radius it also illustrated in fig.3.3. A D-degree curve turns the forward direction by n degrees over some agreed-upon distance. The usual distance in US road work is 100 ft (30.5 m) of arc.**[21]**

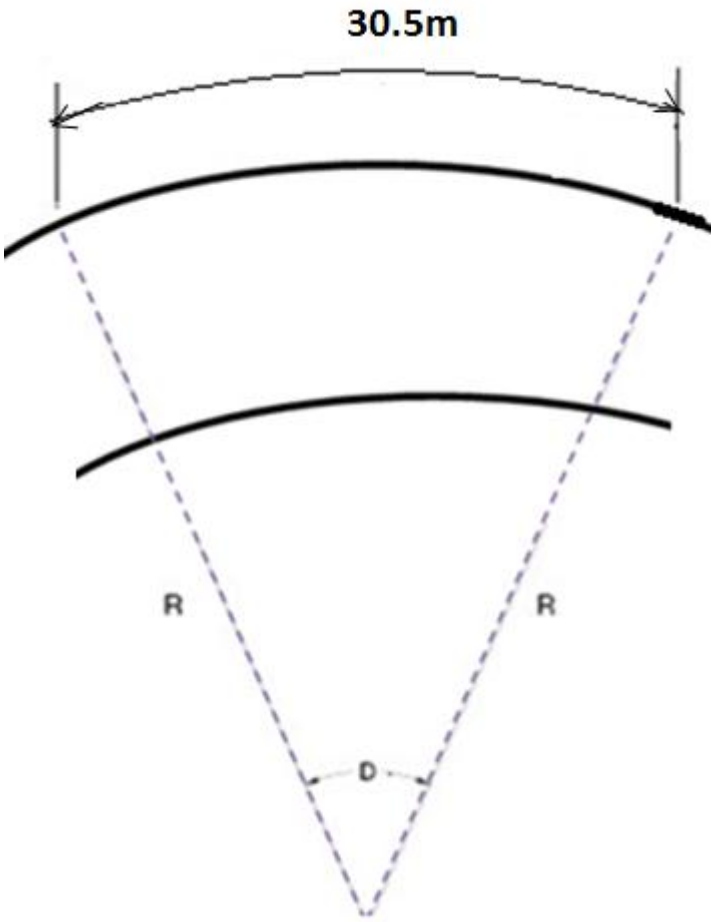

Figure 3.3*:* Degree of Curved Track

Degree of curve (D) can be derived as follows, the circumference of the full circular curve is $2 \times \pi \times$ R. For which the angle at the center of the curve is $360^{o}.2\pi R \rightarrow 360^{0}$, $\frac{2\pi R}{360^{0}} \rightarrow 1^{0}$.Since arc length of 30.5 m corresponds to D^{0}. It is derived from $\frac{30.5}{R} = 2\pi \times \frac{D}{360^{0}}$i.e.

$$D = \frac{1747.5}{R}$$

This can be approximated

$$D = \frac{1750}{R} \qquad (3.1)$$

The fundamental component common in all conventional railway vehicles is the wheelset which are rigidly fixed with a common axle as seen in fig.3.4 that means they are not free to rotate independently, they have the same rotational speed and a constant distance between the two wheels is mentioned. The wheels treads are conical and profiled, in order to allow them to negotiate curves without slipping. The wheel profile is composed of two parts, the wheel tread and the wheel flange. The wheel tread is usually conned at 1/20 or 1/40 and is in contact with the rail head. The wheel flange is provided on the inside edge of the tread which limits the wheel lateral motion and

reducing the probability to derailment **[14].**The kinematic analysis is the vehicle is a representation of the vehicle movement on a curved track while lateral force is either null or balanced by some mechanism other than rail side reaction force but the analysis of the slip rate is equally important for case of either the vehicle is moving on equilibrium speed or not.

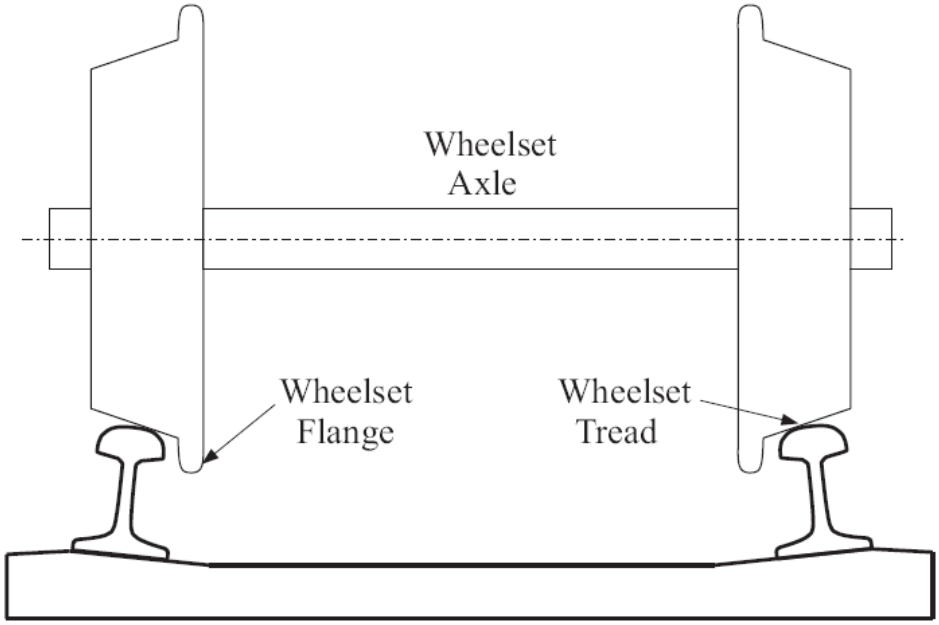

Figure 3.4: the Two Wheels Rigidly Fixed to a Common Axle

The curving motion of the vehicle on horizontal track or canted track is accompanied with wheelset laterally movement. This causes other changes that are going to be discussed in the next subsequent units such as on rolling radii of the wheels, contact angles in between wheel and rail and wheelset roll angle etc.

3.2. Horizontal curved track

This track constructed on level horizontal plane without an introduction of superelvation. The vehicle passing over the curve continuously changes its direction over a curve. Due to the inertia, the vehicle tends to continue moving in the straight lateral acceleration acting outwards so that vehicle should be constrained to move in track. The vehicle moving in horizontal curved track uses the conicity and flange of the wheel as a means of guidance and it is shown in fig. 3.5.

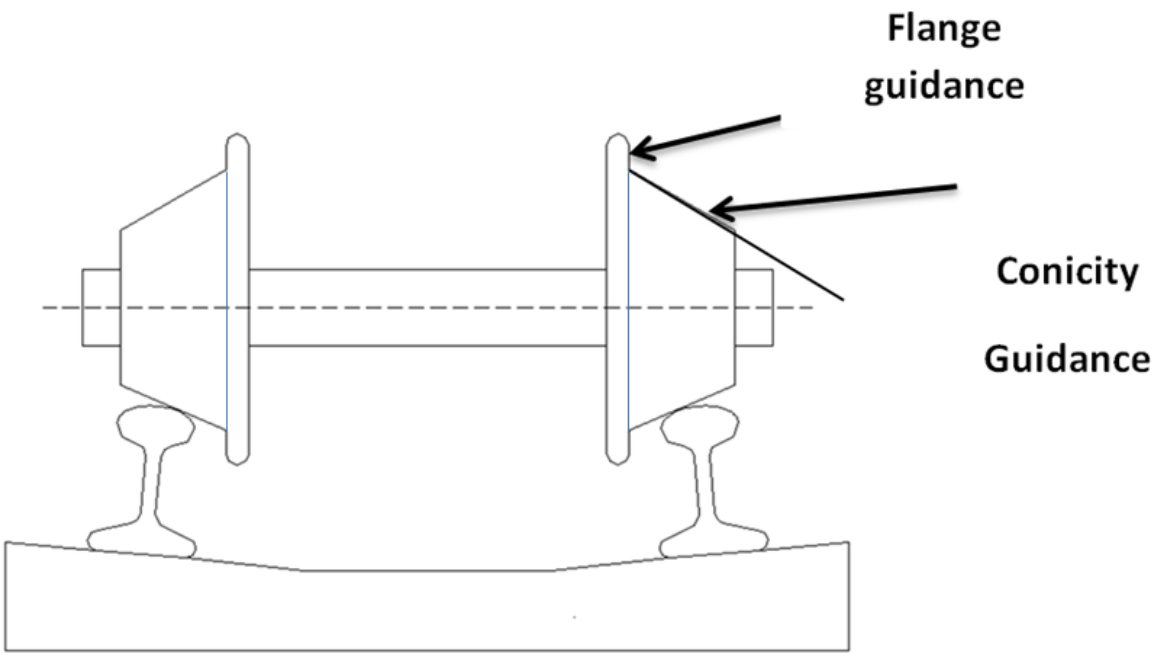

Figure 3.5: Flanges and Conicity Guidance for the Wheelset on the Rail

Primary means of guidance is conicity which constrained small displacements from the center of straight or slightly curved track. But as the curve becomes sharper, the flanges become the essential mode of guidance. The actual vehicle movement on curve is quite complicated but the vehicle traverses the curved path without appreciable slip due to coning in the wheels, which causes larger diameter to travel on the outer rail and smaller diameter on the inner rail by slight movement of the center of gravity of the vehicle towards the outer rail. In a curve the leading wheelset will tend to roll towards the outside of the curve, and the trailing wheelset will tend to roll towards the inside as shown in fig. 3.6.

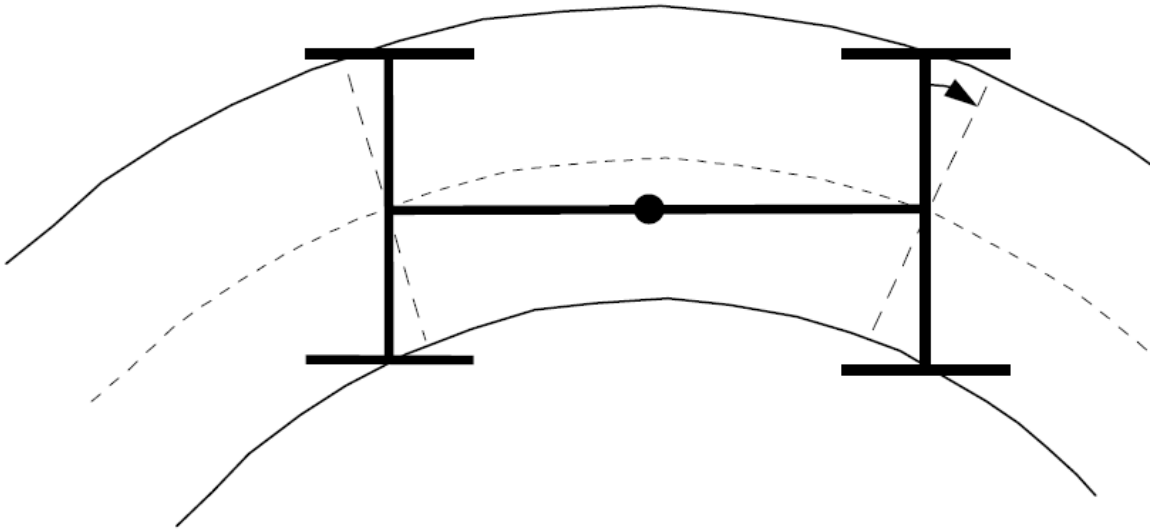

Figure 3.6: Systematic Representations Vehicles on a Curved rail

Because of the coning of the wheels, as the leading wheelset moves outwards, the radius of the outer wheel becomes greater than the inner wheel, as shown in the fig. 3.7. As both wheels are rotating at the same angular velocity, the larger radius wheel tries to roll further than the smaller radius wheel, thus steering the wheelset towards a radial alignment, when it will roll smoothly around the curve. The opposite process happens on the trailing wheelset as it moves inwards on the curve. The outer rail on the curve is longer than the inner rail, so that unconstrained wheelsets can curve freely by running along the equilibrium rolling line, where the rolling radius difference balances the difference in the lengths of the rails.

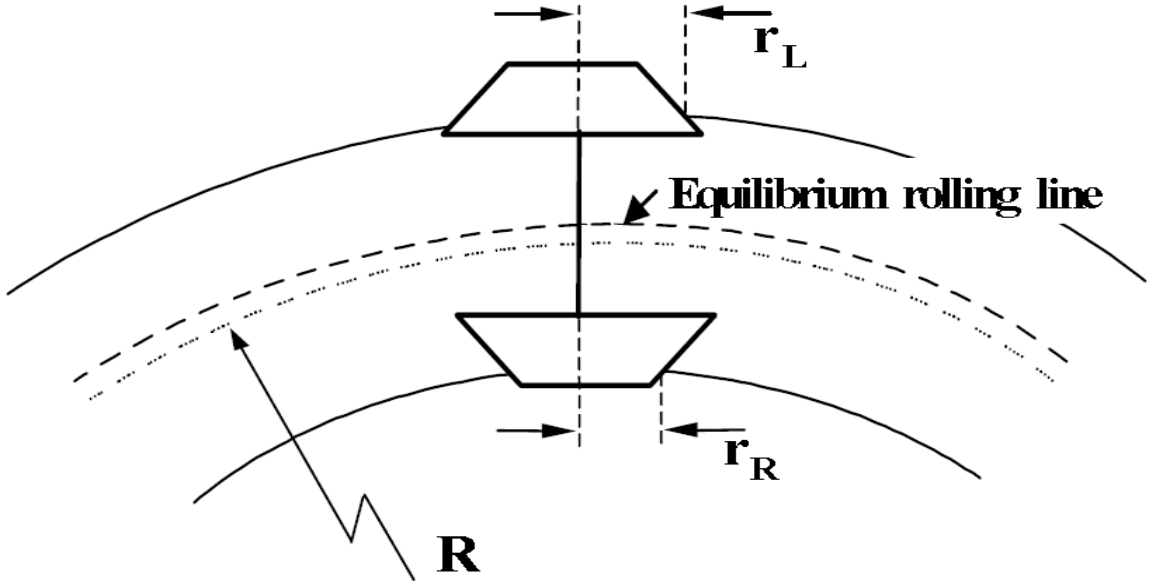

Figure 3.7: Rolling Radius Difference Vehicle Wheels over the two Curved Rails

The leading wheel of a bogie moves with positive angularity, attacking the outer rail of the curve. The outer rail causes the wheel to change direction. However, the above is possible only up to a certain radius of curves and if the radius is going to smaller, the outer wheel will skid and inner wheel will slip in order to ensure that the axle moves as a unit in the desired direction. Due to this, and additional lateral forces on track causes flange contact and the kinematic analysis of obtaining equilibrium rolling line by increasing rolling diameter of the wheel is not valid any more. But the contribution of conicity should under consideration though the contact condition changed to flange contact. So this analysis combined with flange reaction form the vector sum effect centrifugal loading and normal load will help to model wear and friction property of the rail.

3.3. Canted curved rail

The above two types of guidance in railways are not enough for vehicles moving with high speed on the sharped curved rail because of the added centrifugal force due to vehicle mass and all

passengers/ things inside. There is a must to have an additional guidance to be able to constrain the vehicle to move properly. This is done by the raising of outer rail with respect to inner rail to counter act lateral centrifugal force by centripetal force. The forces by a vehicle on the curve having cant (ht) are shown in fig. 3.8 and dynamic analyses are presented **[14]** and discussed below.

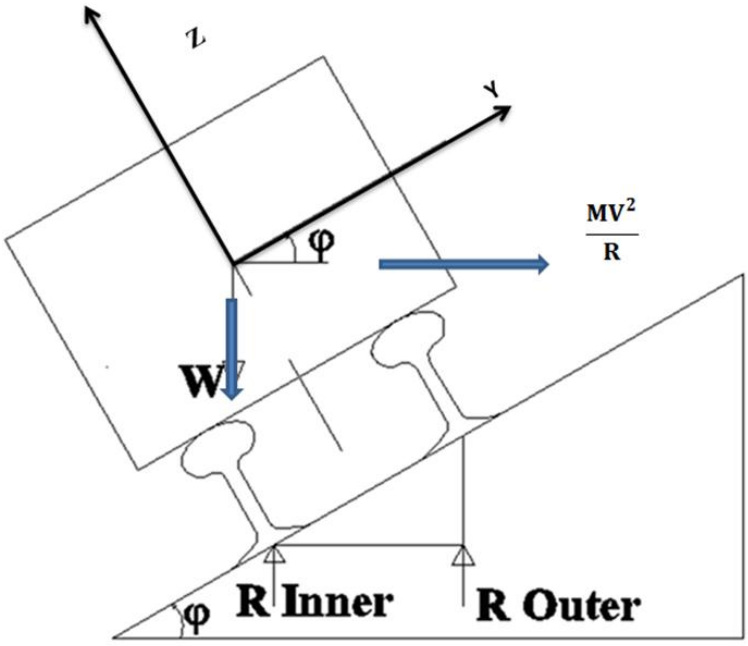

Figure 3.8: Forces of the Vehicle on the Canted Curve

For a vehicle moving on a curved track there is centrifugal force by amount equls to $\frac{M.v^2}{R}$. this force is acting at center of gravity of the vehcle in perpendicular dierction away from the center of the curve. If the curve is having cant, centripetal force will be acting towards the inner rail. When the two force is acting in the lateral dierction match with each other, the vehicle is in equilibrium as far as lateral forces are concerened. The cant at which the equilibrium is there on a curve is called equilibrium cant. Conversely, the speed corresponding to cant in any curve is called equilibrium speed. The angle can be determined by:

$$\varphi = \sin^{-1}\frac{ht}{2l} \qquad (3.2)$$

By assuming the two forces (centrifugal and centripetal forces) are equal, the relation between equilibrium speed and equilibrium cant can be designed.

$$\frac{M.v^2}{R} = W\tan(\varphi) \qquad (3.3)$$

In case of quasistatic curving the vehicle is exposed to two accelerations i.e., normal and lateral which is vector sum effect of horizontal centrifugal acceleration and vertical gravitational

acceleration. The resultant of the acceleration is the vector sum of these two components as shown in fig. 3.9.

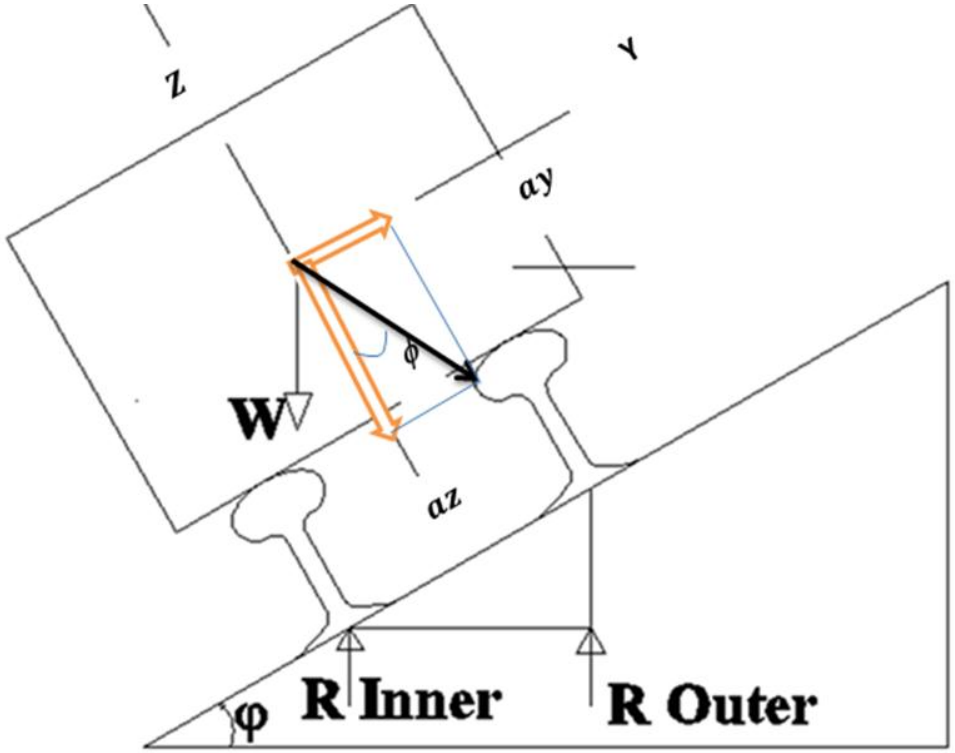

Figure 3.9: Lateral Acceleration 'at' and Lateral Force Angle' ϕ'

$$ay = \frac{mv^2}{R}\cos\varphi t - W\sin\varphi t \qquad (3.4)$$

$$az = \frac{mv^2}{R}\sin\varphi t + W\cos\varphi t \qquad (3.5)$$

The lateral force angle ∅ in figure 3.9 are related to the acceleration ay and az in accordance with the following equation

$$\emptyset = \tan^{-1}\frac{ay}{az} \qquad (3.6)$$

3.4. Kinematic analysis

3.4.1 Lateral Displacement

A. Without superelvation

Conicity of the wheels helps to balance the difference in the lengths of the rails for the outer and inner rail up to when the wheel flange in contact to the rail side. Look fig. 3.10 below.

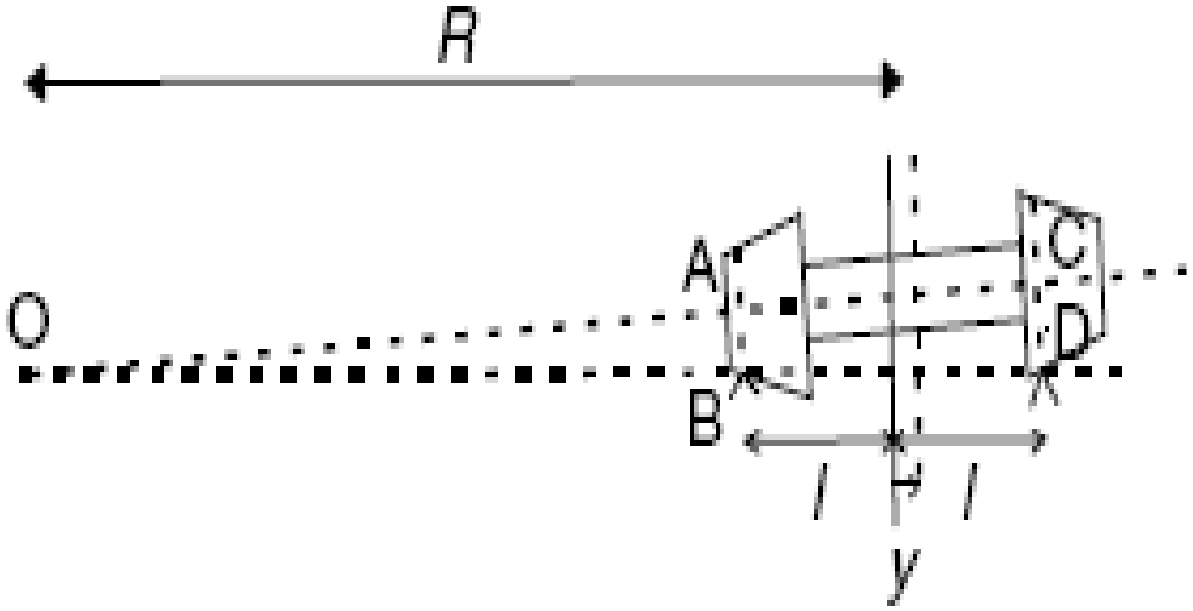

Figure 3.10: the Lateral Shift for Horizontal Curved Track

From the geometrical relations of fig. 3.10

$OAB \approx OCD$ From Similarity of triangle

$$(r_0 - \lambda y)/(R - l) = (r_0 + \lambda y)/(R + l) \quad \text{since} \frac{AB}{OA} = \frac{CD}{OC} \text{ assum } \lambda \text{ in Rad}$$

$$y = \frac{r_0 * l}{R * \lambda} \qquad (3.7)$$

B) With superelvation

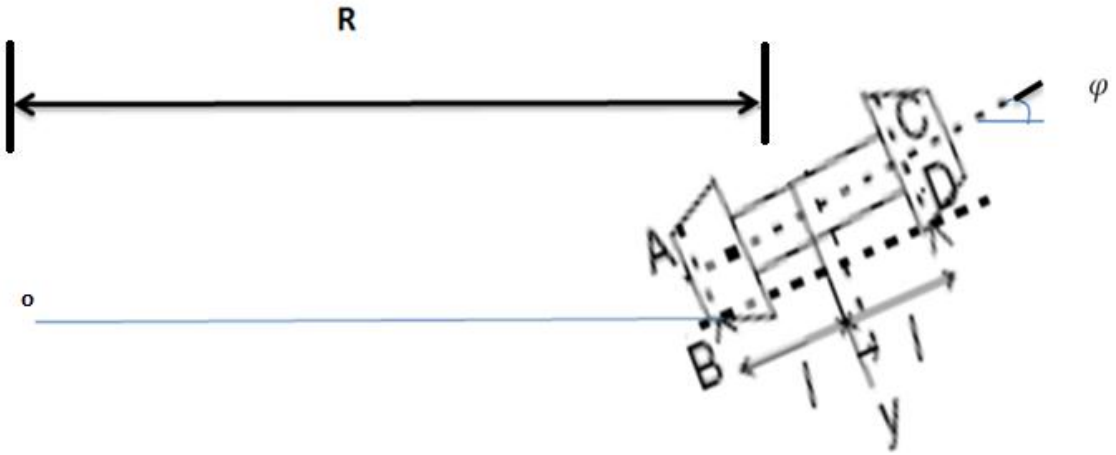

Figure 3.11: Lateral shift for canted curved track

Friction work is done by self steering which helps to adjust the differenc of the two eccentric different radius circles since the conical shape of the wheel.

$$Wf = \mu F_N \times y$$

But unlike horizontal curved rail the force that makes the shift can be decomposed to normal and lateral direction by cant angle and the gravitational force also constrained the lateral shift by some amount i.e.the net normal load (to the inclined surface) is equal to the summation of the centrifugal and the weight components which is high when it is compared with horizontal curved track (weight of the object). The shift 'y' determines from geometry horizontal curved track will relate by using dynamic analysis. The vehicle starts lateral motion when the lateral traction is equal to frictional load μF_Z. So it is logical think that the vehicle is doing equal amount of work to that of frictional work done for given wheelset shift since to the sytem is in equlibrium i.e. the normal component of force becomes:

$$\sum Fz = \frac{mv^2}{R}\sin(\varphi) + W\cos(\varphi)$$

And from equilibrium speed on canted curved track the lateral force becomes

$$\sum Fy = 0,$$

$$\rightarrow \frac{mv^2}{R}\cos(\varphi) - W.\sin(\varphi) = 0$$

Therefore,

$$W = \frac{mv^2}{R\tan\varphi} \rightarrow \frac{mv^2}{R} = W\tan\varphi.$$

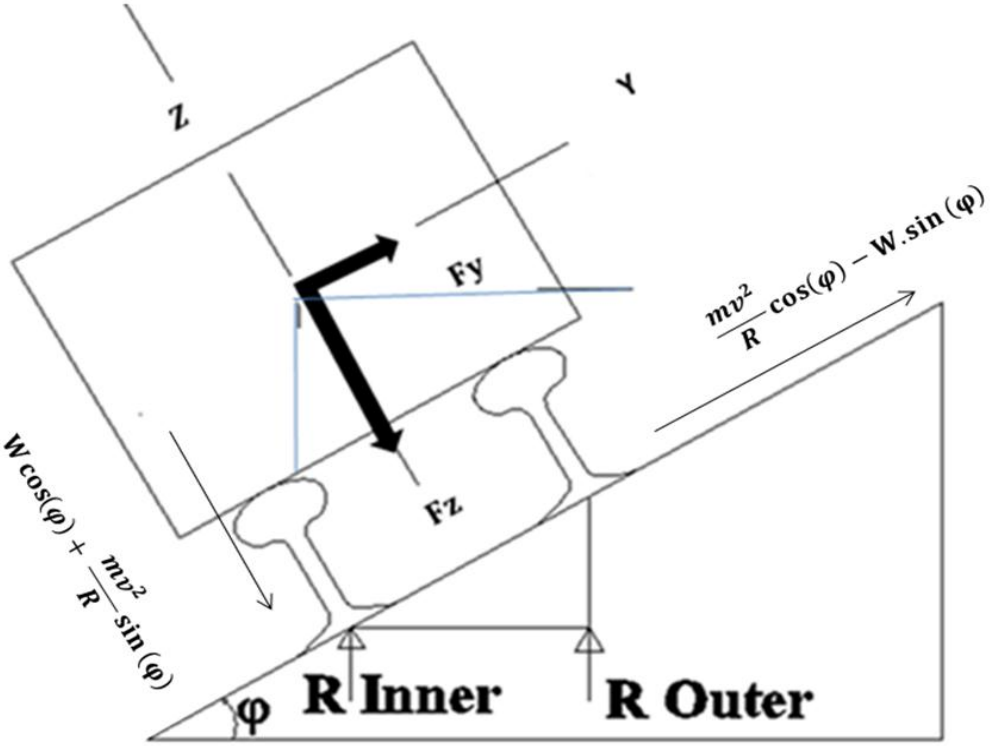

Figure 3.12: Normal and Tangential Forces on Canted Track

Let y′wheelset displacement for canted rail. Assuming the same frictional workdone for the two cases Y can be related as:

For the horizontal curved rail, $\text{Work} = \mu F_N\, y \rightarrow \text{Work} = \mu W.y$

For canted track and for the same work done y is raleted with y′ by the equation

$$\text{Work} = \mu y'\left(W\cos(\varphi) + \frac{mv^2}{R}\sin(\varphi)\right)$$

$$\rightarrow \mu y'\ (W\cos(\varphi) + W\tan(\varphi)\sin(\varphi)),$$

$$y = y'(\cos(\varphi) + \tan(\varphi)\ \sin(\varphi))$$

But $\sin(\varphi) = \tan(\varphi)\cos(\varphi)$ and by substituting it on the above gives $y = y'\cos(\varphi)(1 + \tan^2(\varphi)) =$ but $1 + \tan^2(\varphi) = \frac{1}{\cos^2(\varphi)}$, $y = \frac{y'}{\cos(\varphi)}$

But substuting eqution 3.7 to the above gives,

$$y' = \frac{(r_0 * l) * \cos(\varphi)}{R * \lambda}$$

So the lateral shift for canted track becomes

$$y = \frac{r_0 \times l}{R \times \lambda}\cos(\varphi) \qquad (3.8)$$

Unlike the horizontal curved rail here the determination of shifting distance depends on both the cant angle in addition to the curve radius and other requirement that the vehicle should move with

equilibrium speed. At low velocity the wheel flanges are in contact with the inner rail, on the other hand at high velocity the wheel flanges are in contact with outer rail so that the wheel travels from one side of conical wheel to the other. That shows minimum track radius that the wheel moving without flange contact. Determination of whether wheels of vehicles to be rail side contact or not is done by: -

From

$$\varphi' = \tan^{-1}\frac{v^2}{gR}$$

And

$$\varphi = \sin^{-1}\frac{ht}{2l}.$$

If the two equals the vehicle is moving with equilibrium speed and the vehicle is enjoying flange free curving. If ($\varphi' < \varphi$), the vehicle is moving with cant excess and there is a flange contact at the inner Rail. If ($\varphi' > \varphi$), the vehicle is moving with cant deficiency there is a flange contact at the outer Rail. When the vehicle is moving with rail side contact the effect of the vehicle weight and centrifugal force is assumed to be supported by the rail side reaction force.The motion also constrained by the flange contact.

3.4.2. Longitudinal slippage

The difference in the circumference of two curved rails (right rail and left rails) when assuming is equals

$$2\pi(R2 - R1) = 4\pi l$$

It is assumed to be compensated by the conicity of the wheels up to a certain level of lateral displacement (look fig.3.14) but when maximum possible lateral distance is shifted the wheels are exposed for longitudinal slip. It implies the wheels longitudinal sliding distance are responsible for the two wheels to be placed on the same radial position.

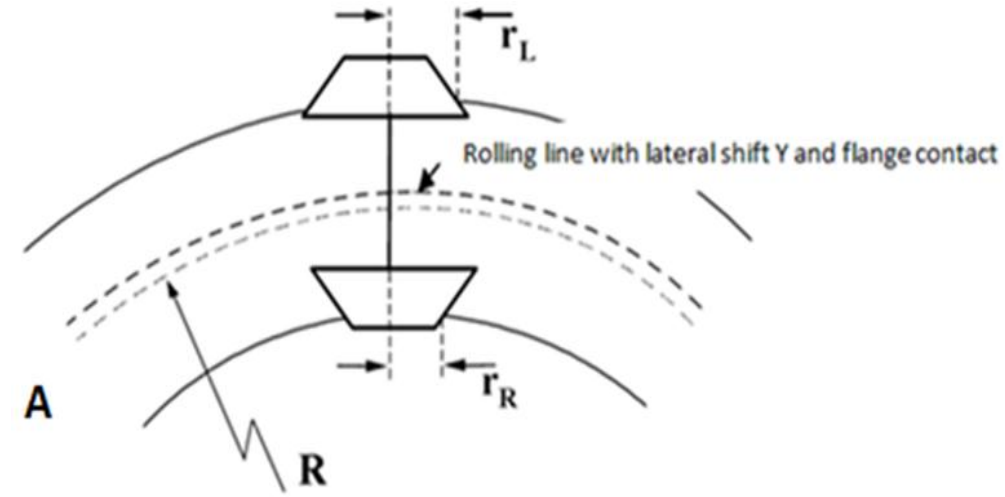

Figure 3.13: Lateral Shift of wheel to Reduce Slip by changing the Rolling Radius Differences

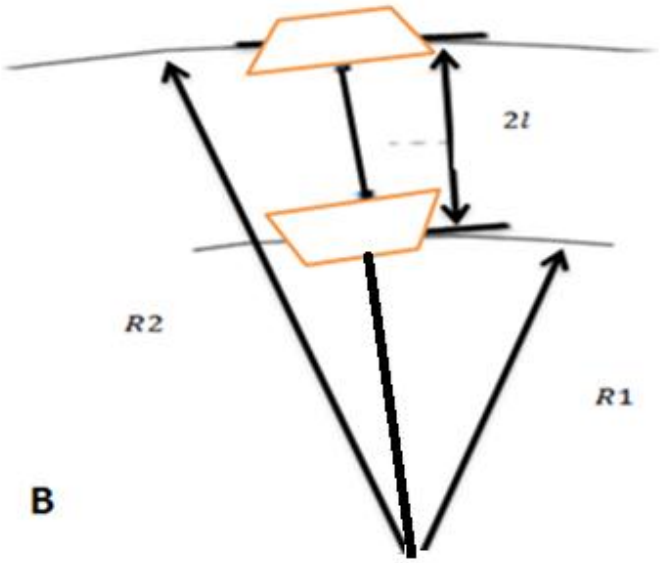

Figure 3.14: the Two Rail Radius's with Gauge Width 2l.

Therefore the longitudinal slippage can be calculated from rolling radius differences and the two curved rails as follows $rr = ro + y\lambda$ and $rl = ro - y\lambda$.

Their difference becomes

$$\Delta r = 2y\lambda \qquad (3.9)$$

From the two wheels the distance travel difference for same time and same angular velocity of the wheelset, the rolling radius difference creates this amount linear displacement

$$\omega t \times 2\lambda y$$

And therefore this amount of slip is saved due to the radius difference for a circular motion distance $'\omega t'$ of the wheelset. Let the wheel makes displacement equals the circumference of curved track with the same angular velocity angular displacement becomes

$$\theta = \omega t = \frac{S}{ro}$$

But this also related with the radius of curved road.

$$S = 2\pi R.$$

It becomes

$$2\lambda y \times (2\pi R/ro)$$

And it is the amount of reduction not to slide on the rail by the help of conicity from full curved motion. So, sliding for one full revolution

$$4\pi(l - \lambda y \frac{R}{ro}),$$

It can be re-writing per unit length by dividing the circumference of the full track $4\pi(l - \lambda y \frac{R}{ro}) \Big/ 2\pi R$

and equally shared for both rails since there are two rails. Therefore longitudinal slip at right rail and left rail respectively as follows

$$\xi x_r = \left(-\frac{l}{R} + \frac{\lambda y}{ro}\right) \qquad (3.11)$$

$$\xi x_l = \left(\frac{l}{R} - \frac{\lambda y}{ro}\right) \qquad (3.12)$$

Therefore the vehicle wheels are slipping the inner rail forward and the outer rail is slip backward. But when the vehicle wheels are in flange contact to the inner side of the rail the advantage gain by conicity affects the system negatively since this creates with larger rolling diameter at the inner rail.so slip for left flanging becomes

$$\xi x_r = -\frac{l}{R} - \frac{\lambda y}{ro} \qquad (3.13)$$

$$\xi x_l = \frac{l}{R} + \frac{\lambda y}{ro} \qquad (3.14)$$

The wheel set has one point of contact on the wheel that travels on the left rail and two points of contact on the wheel that travels on the right rail or the reverse also true according to the vehicle speed and superelvation is applied. The sliding distance on two point contact is by outer wheel is determines by assuming that rail side contact is completely sliding. The sliding distance on two point contact is by wheel flange is determines by assuming the rail side contact is completely sliding. So the longitudinal creepage at side point contact becomes

$$\xi xs = 1 \qquad (3.15)$$

3.4.3. Lateral slippage

$$\xi y = \frac{v_2' - v_2}{V} \qquad (3.16)$$

For the instantaneous time the distance difference in the vehicle lateral displacement (v2) and the wheels supposed travel (v_2')can be related as

$$(v_2' - v_2) * t = -S \sin \Theta \qquad (3.17)$$

And when dividing both sides by a product of circumferential velocity and time gives

$$\xi y = -\sin \Theta \qquad (3.18)$$

Assuming small angle Θ in rad;

$$\xi y = -\Theta \qquad (3.19)$$

Longitudinal creepage can be related as

$$\xi x = \frac{V - \text{Forward velocity}}{V}$$

$$= 1 - \cos\Theta$$

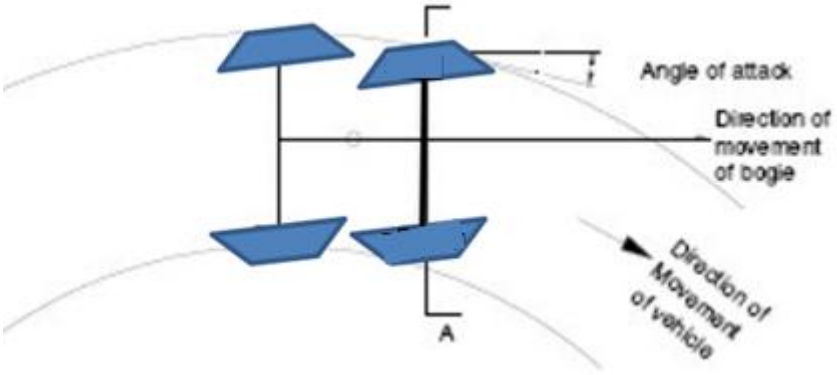

Figure 3.15: Angle of Attack

From the point vehicle dynamics angle of attack which dependent on the steering capacity of the vehicle and driver is the causes for slippage. In quasi static approach the assumption with in within the perfect steering capacity, the angle of attack becomes

$$\Theta = \cos^{-1}(1 - \xi x) \qquad (3.20)$$

3.4.4. Spin Slippage

$$\xi_{SP} = \frac{\omega_{R/W}}{V} = \frac{\omega 2 - \omega_1}{V} \qquad (3.21)$$

It is the difference in angular velocity of wheel within contact patch. The angle of contact is high on the flange to give lateral curving forces that guide the wheelset around the curve of the outer rail. At this point the region of contact is inclined and it produces the significant difference in rotational

velocity within the area of contact. That means the innermost and the outer most parts of the region spent an equal time in contact with the rail. To do this, the outermost point slips backwards and the innermost slips forwards. A two-point contact was analyzed where the differences between the contacts on rail-head to wheel tread and rail edge to wheel flange can be attributed primarily to the relative velocity differences in regard to both magnitude and direction. It is derived with contact angle (lateral force angle) α

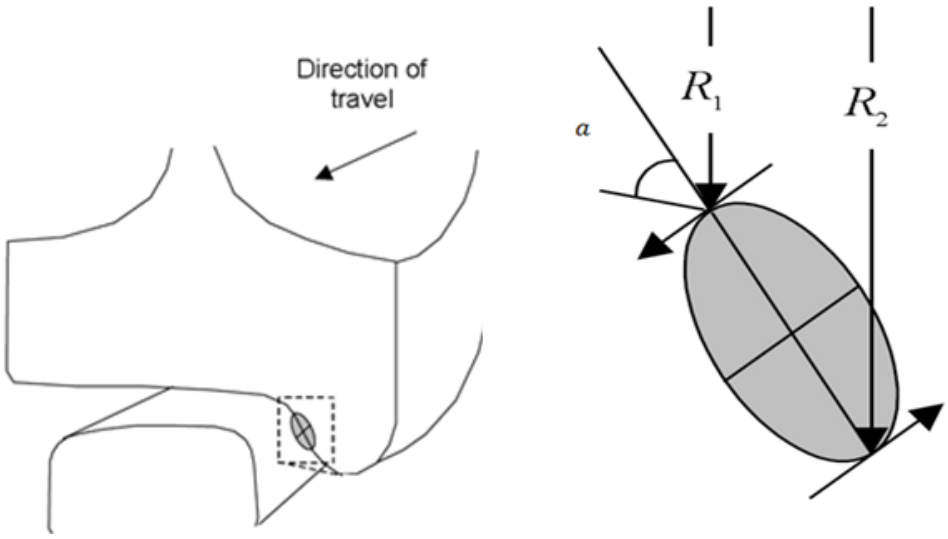

Figure 3.16: the Wheel Radius Difference due to Flange Contact

Let assume the velocity of the wheel $'V'$, which equals to $R1\omega_1 = R2\omega2 = \omega \times ro$

$\omega_1 = \frac{V}{R1}$ and $\omega_2 = \frac{V}{R2}$ And substituting this equation to the above equation 3.21 gives

$$\frac{\frac{V}{R2} - \frac{V}{R1}}{V} = \frac{1}{R2} - \frac{1}{R1} = \frac{2 \times ro \times \sin\alpha}{R2 \times R1}$$

But $R2 \times R1 \approx {r_0}^2$ and assuming the upper and the lower limit of the wheel shares the spin equally equation 3.22 can be written as

$$\xi_{SP} = \frac{\sin\alpha}{r_0} \qquad (3.23)$$

It is very significant when the maximum contact angle at flange contact

3.5. Dynamic analysis

3.5.1. Vehicle loads

When the vehicle moving on the curved track, the lateral centrifugal force are added on the system and it makes a change in rolling radius difference, angle of contact, and lateral force angle. For the case $\varphi = 0$, it represents horizontal curved track, at same time lateral force Fy becomes $\frac{mV^2}{R}$, normal force $Fz = mg$, and the motion would be either of one point contact or two point contact depending

on lateral loading and friction conditions. Whereas if $\varphi > 0$ a track is called canted track. Similar to the above the motion would be either of one point contact or two point contacts depending on vehicle speed. The difference with the former case is the flange contact may happen on both sides of rails (at inner rail when the vehicle speed is lower than equilibrium speed and outer rail at speed is greater than the equilibrium). The general case for the vehicle moving on the curved track is shown as in fig. 3.17 below. Center of mass a vehicle considered from A located (750j+1653k) and from B located at $-0.750j + 1.653k$.

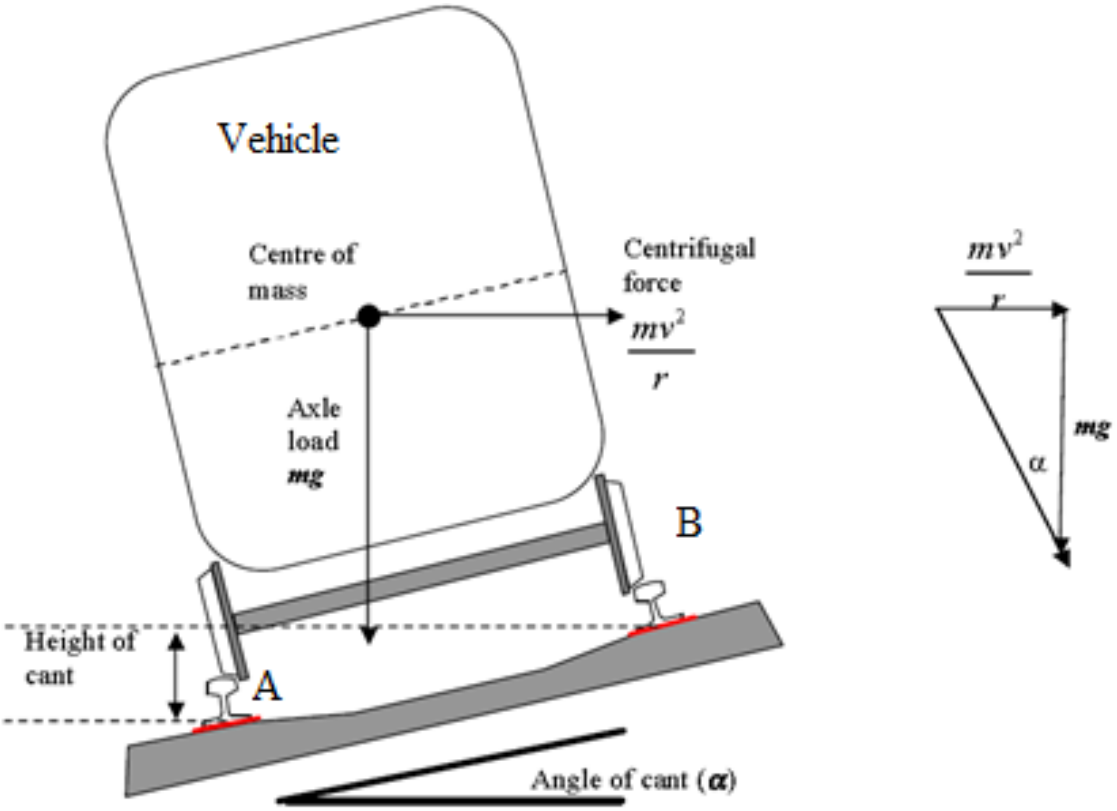

Figure 3.17: Vehicle Loads

3.5.2 Contact force at left and right rails

A) Normal load: it systematically represented as fig.3.18 by FA and FB

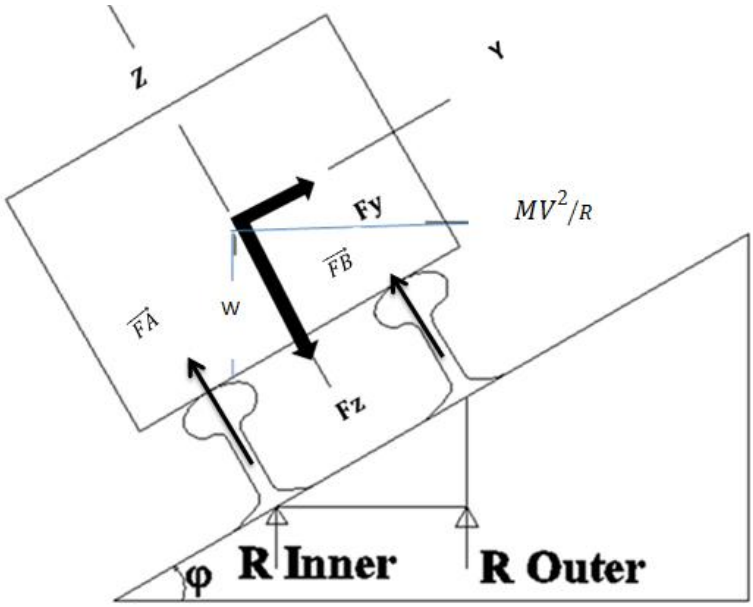

Figure 3.18: Loadings in the Inner and Outer rails

$$\emptyset = \tan^{-1} {}^{Fy}/_{FZ} \qquad (3.25)$$

$$R = \sqrt{FZ^2 + FY^2} = -R\cos\emptyset\,\vec{k} + R\sin\emptyset\,\vec{j} \qquad (3.26)$$

From 1st law of equilibrium $\sum FZ = 0, \rightarrow FA\vec{k} + FB\vec{k} = FZ$

From 2nd law of equilibrium

$$\sum M_A = 0, \rightarrow \left(0.750\vec{j} + 1.653\vec{k}\right) \times \left(-R\cos\emptyset\,\vec{k} + R\sin\emptyset\,\vec{j}\right) + 1.5\vec{j} \times FB\vec{k}$$

$$\left(0.750\vec{j} + 1.653\vec{k}\right) \times \left(-FZ\vec{k} + FY\vec{j}\right) + 1.5\vec{j} \times FB\vec{k}$$

$$(-0.750FZ\vec{i} - 1.653FY\vec{i}) + 1.5FBi$$

$$FB\vec{k} = 0.5FZ + 1.1Fy \qquad (3.27)$$

$$\sum M_B = 0, \rightarrow (-0.750\vec{j} + 1.653\vec{k}) \times \left(-R\cos\emptyset\,\vec{k} + R\sin\emptyset\,\vec{j}\right) + (-1.5\vec{j} \times FA\vec{k})$$

$$(-0.750\vec{j} + 1.653\vec{k}) \times \left(-FZ\vec{k} + FY\vec{j}\right) + (-1.5\vec{j} \times FAk)$$

$$(0.750FZ\vec{i} - 1.653FY\vec{i}) - 1.5FAi$$

$$FA\vec{k} = 0.5FZ - 1.1Fy \qquad (3.28)$$

Case 1: When cant angle is zero

When superelvation is zero, the conicity of the wheel is the only guidance for the lateral forces and in this case the influence of conicity in the rolling effect of the wheelset is considered (see fig.3.19) below.

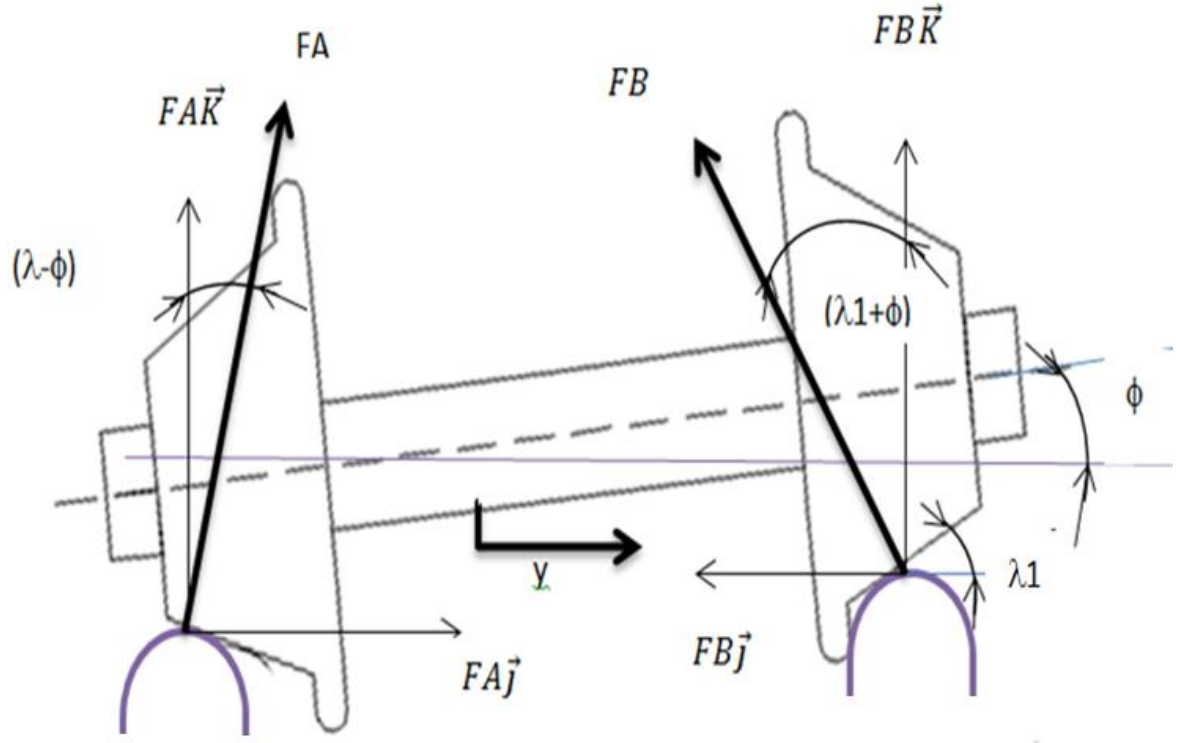

Figure 3.19: Vehicle Loads on the Rail at Horizontal Curved Rail

The angle ϕ is made due to the wheelset shifts laterally. When the vehicle translates by 'y' the degree ϕ is added on the right and the same ϕ deducted to the left from the conicity of the wheels.

Determine 'ϕ'

From right and left wheel radii at contact points and lateral shift distance the roll angle can be calculated. If y = 0 the two radii are equal, that is ro = rl = rr. Then there is no elevation difference in between the two wheels. If for $y \neq 0$, there is a rolling radius difference, there is an elevation difference which equals to 2yλ (see eqn. 3.9). That makes angle with gauge length

$$\phi = \sin^{-1}\left(\frac{2y\lambda}{2l}\right)$$

For small lateral displacement and conicity in rad, it can be approximated as

$$\phi = \frac{y\lambda}{l} \qquad (3.29)$$

Equating lateral components of axle load and assuming horizontal centrifugal load is only happen at right rail.

$$FB\vec{j} = -FB\sin(\lambda - \phi) + \frac{MV^2}{R} \qquad (3.30)$$

$$FAj = FA\sin(\lambda + \phi) \qquad (3.31)$$

So the total lateral force becomes

$$FY = FBj - FAj \qquad (3.32)$$

If we assume equal FA, FB, and their sum W

$$FY = \frac{MV^2}{R} - W\sin(\phi) \qquad (3.33)$$

Then the normal components of the forces that perpendicular to rail head becomes

$$FZ = W\cos(\phi) \qquad (3.34)$$

- **Normal loads at the rail head**

  FAK=0.5FZ-1.1Fy, &FBK=0.5FZ+1.1FY.From the above relations formulated (eqn. 3.27 and 3.28)

- **lateral loads at rail sides**

  For horizontal curved track it can be concluded that the lateral force is always at right rail side. It is also equals to flange reaction force at the wheels that is approximately equals to FY (eqn. 3.33). It is generally assumed equilibrium speed is only achieved at slow velocity i.e.

$$0 \leq Veq \leq \frac{W\sin(\phi)}{M \times R} \qquad (3.35)$$

Case 2: When there is superelvation

In this case the component of forces due to conicity is assumed negligible and then vehicle normal loads and lateral loads (see fig.3.19) below becomes

$$FY = \frac{MV^2}{R}\cos\varphi - w\sin\varphi \qquad (3.36)$$

$$FZ = W\cos(\varphi) + \frac{Mv^2}{R}\sin(\varphi) \qquad (3.37)$$

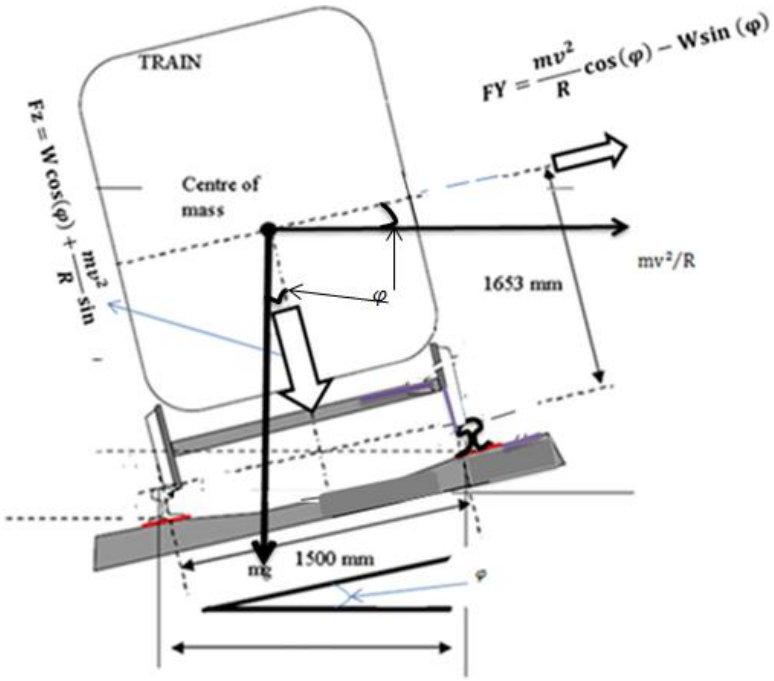

Figure 3.20: the Vehicle Load on the Canted Rail

A) Normal loads at the Rail Head

$FAK = 0.5FZ - 1.1Fy$, $FBK = 0.5FZ + 1.1FY$ from eqn. 3.27 and 3.28

B) Lateral load at the Rail

Right side contact for vehicle moving above equilibrium speed of the vehicle

From 1st law of equilibrium

$$\sum FZ = 0, \rightarrow FA\left(\vec{k}\right) + FB\left(\vec{k}\right) = Fz$$

$$\sum Fy = 0, \rightarrow Fy\vec{j} + FB\vec{j} = 0$$

$$FBj = -FY = -\frac{MV^2}{R}\cos\varphi + w\sin\varphi \qquad (3.38)$$

If the direction is towards left then similarly

$$FAj = -FY = -\frac{MV^2}{R}\cos\varphi + w\sin\varphi \qquad (3.39)$$

And the load supported by the rails becomes

$$\overrightarrow{FA} = FA\vec{k} + FA\vec{j} \qquad (3.40)$$

$$\overrightarrow{FB} = FB\vec{k} + FB\vec{j} \qquad (3.41)$$

3.5.3. Modelling friction

Modelling of friction for vehicle moving in equilibrium speed an easy task and it is only localized friction due to creep that can be calculated using nonlinear heuristic creep force theory **[15]** but for the case friction is saturated due to unbalance in normal load due to centrifugal loading adhesion theory is used instead of creep forces. Contact friction at the left and right rails can be calculated by the normal force multiplied by friction coefficient when the vehicle is deviated from the equilibrium speed.

$$FfB = \mu . FB \qquad (3.42)$$

$$FfA = \mu . FA \qquad (3.43)$$

3.5.4. Modelling of wear rate

The Archard equation can be derived from examining the behavior of a single asperity. Assumed the rail plastically deformed at contact patch which is equal to the yield strength of the material. For rail elliptical contact patch area and the load supported by asperity equals becomes:

$$\delta w = Sy . \pi . a . b \qquad (3.44)$$

If the volume of wear debris,δv, and assuming the depth equals 'a' for half ellipsoid which an asperity is changing to fragment from the rail for one full sliding motion in longitudinal directions becomes

$$\delta v = \frac{2 . \pi . b\, a^2}{3} \qquad (3.45)$$

Hence δQ, the wear volume of a material produced from this asperity per unit length is:

$$\delta Q = \frac{\delta v}{2a} = \frac{\delta w}{3P} \qquad (3.46)$$

However not all asperities have had material removed when sliding distance 2a. Therefore the total wear debris produced per unit distance moved Q will be lower than the ratio of W to 3Sy. This accounted for the dimensionless constant K, which also incorporates the factor 3 above.

$$Q = \frac{K \times W \times L}{Sy} \qquad (3.47)$$

A simulation scheme is developed that calculates the wear at a detailed level. The removal of material follows Archard's wear law, which states that the reduction of volume is linearly proportional to the sliding distance, the normal load and the wear coefficient **[16]**. Dividing both sides of this equation by total distance the object moved and wear coefficients wear volume per unit distance per coefficient of wear rate of motion becomes

$$\frac{Q}{K.L} = \frac{W.l}{\text{total length}} \qquad (3.48)$$

$$\xi = \frac{\text{total sliding distance during the vehicle motion}}{\text{total distance covered by a vehicle}}$$

$$\nu = \xi.W \qquad (3.49)$$

Therefore longitudinal creepage for rails is similar to sliding per unit length of motion per this model. Wear coefficients are found in laboratory experiment, interpolating the values is depending on slip and contact pressures are used while modelling wear as seen in fig. 3.21. Wear coefficients modelling results in different laboratory works in dry conditions is presented below. So careful attention is paid to pressure (stress) properties in the normal direction in addition to slip. The following relations are used for considering the pressure conditions of the two rails and sliding velocity then linear interpolation is used for finding the approximated wear coefficients from fig.21.

> *The wear coefficient for the high contact pressure regime has been estimated based on interpolation from other regimes and from past experience, since neither of the mentioned laboratory measurements featured such extreme contact pressures* ***[16]***

The pressure at the head of rails can be calculated as

$$PA = FA\vec{k}/\ \pi.al.bl \qquad (3.50)$$

$$PB = FB\vec{k}/\ \pi.ar.br \qquad (3.51)$$

At the rail side lateral force divided by respective contact area and the area approximately equals with 15% rail head contact area **[17]**.

Sliding velocity (V_{slip}) can be calculated from:-

$$v_{Slip} = V_{vehicle} \times \xi x \qquad (3.52)$$

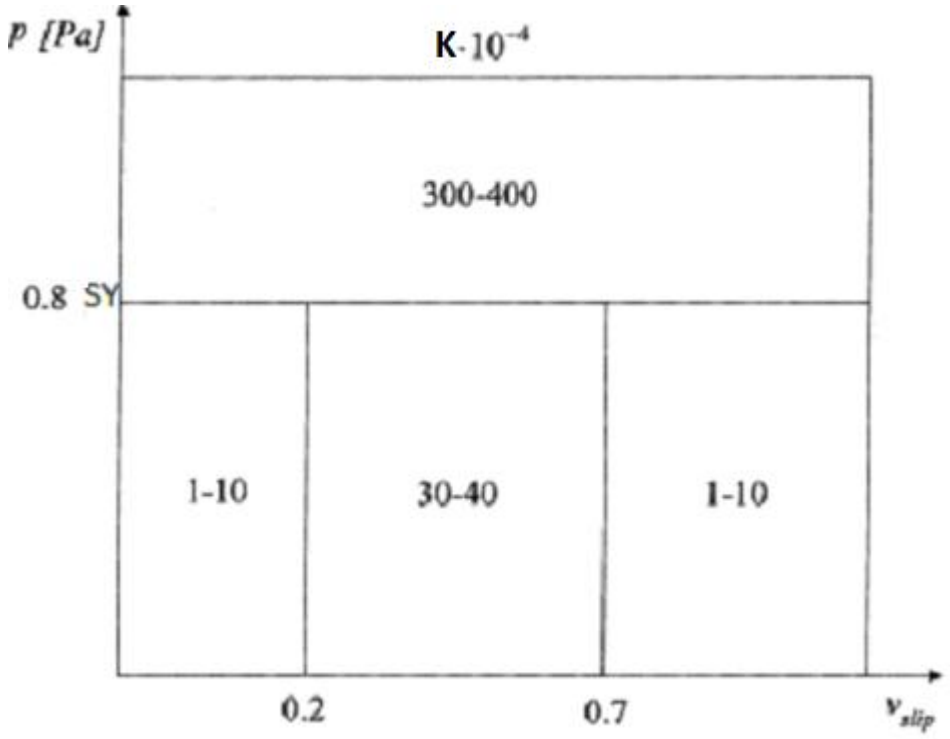

Figure 3.21: Wear Chart for the Wear Coefficient k Based on Laboratory Measurements with Wheel and Rail Steels **[16]**.

All the above data (measurements) didn't consider lubricants since any kind lubricants were not considered in laboratory researches so that the following compensating factors will be added on while studying lubrication effect.

For lubrication

• For sharp curves, 300–400m radius or so, the wear rate is about 10–15 times lower in a lubricated curve.

• For curves with radius around 600 m, the wear rate is about two–five times lower in a lubricated curve.

It is also important to remember that lubrication often is applied only to the outer rail of the curve. For the rest of the track the wear coefficients are reduced to compensate for natural lubrication in the form of rain and contamination. **[16].**

Estimation of rail wear limit

So assuming that parabolic area loss at both contacts which means maximum wear rate is at the centerline of the contact, dropping to zero at the edges of the contact. The average wear rate across the full width of the contact is about 75% of the wear rate at the centerline. Then it is possible to calculate the wear depth and which used for estimations of wear limits. The cross-sectional area loss due to wheel motion on the curved rail can be explained in terms of wear per unit motion of the rail as shown in the fig. 3.22.

Wear per unit vehicle motion=the cross sectional area loss

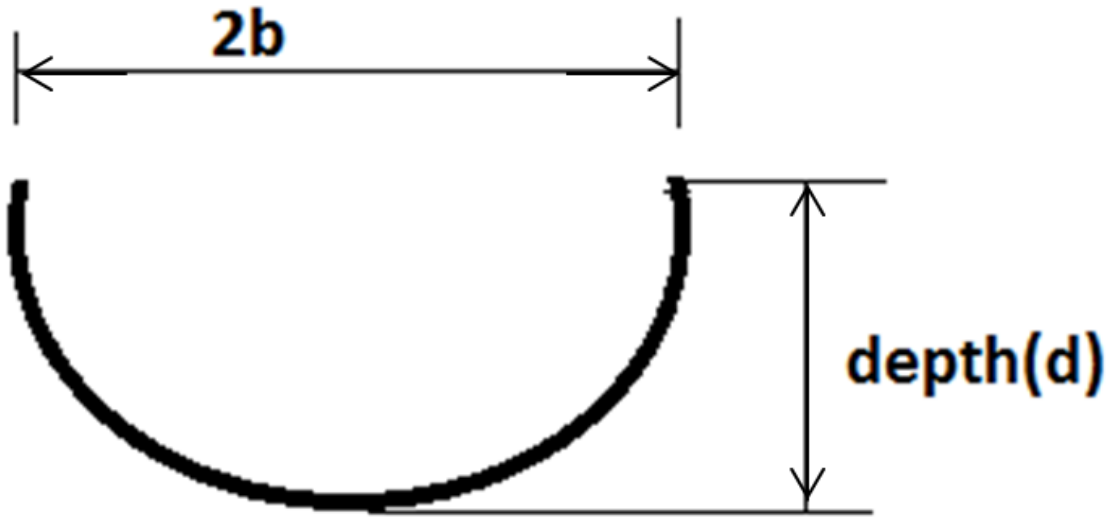

Figure 3.22: a Magnified Area Loss at the Contact (Wear per Unit Length Motion)

Elliptical dimensions 'a' and'b'.

Wheelsets can laterally move +3 (right) and -5 (left) at the left rail with changing the contact dimensions. The fig below shows the elliptical dimensions at respective lateral shift. The right +3 mean the rail profile doesn't change in area elliptical dimensions when it shifts more than this distance in the right direction. But when opposite happens, these dimensions are varied as the wheel flange close to the rail side.

> *In GENSYS the contact between wheel and rail is by default modelled by the Hertzian theory (elliptical contact surface) in combination with tabulated results calculated with Kalker's simplified theory (FASTSIM). One great advantage with this method is that all solutions can be tabulated once and for all. The solution of the contact problem is thus only a matter of data interpolation, which in general is a very fast operation.* ***[15]***

Fig. 3.23 shows the nature of the functional dependence between these geometrically constrained variables and the wheelset lateral position depends on the wheel and rail profile as in contact patch is shifts on both rails the two rail elliptical dimension can be found as follows **[15].**

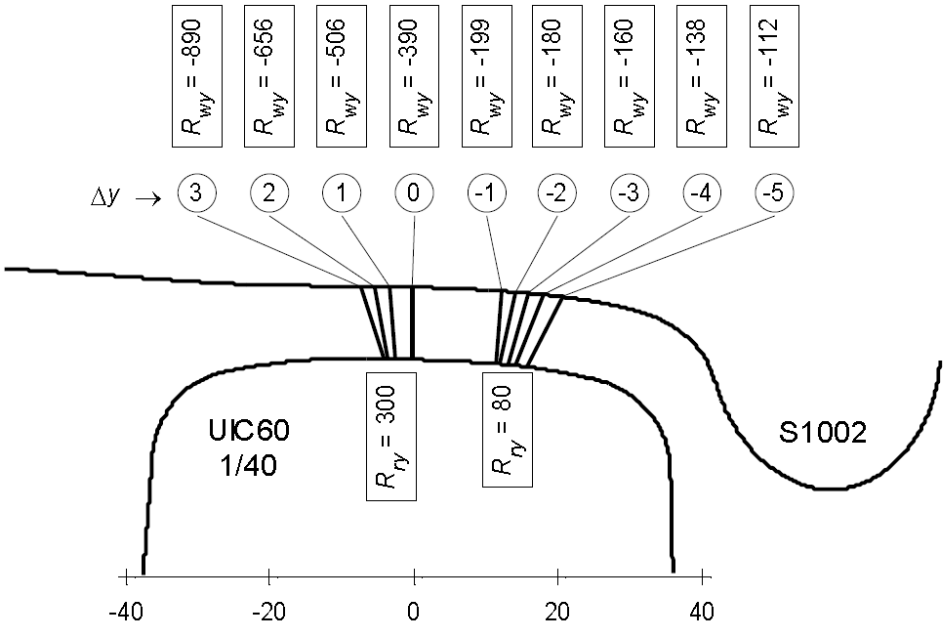

Figure 3.23: Contact Point Positions and Profile Curvatures for Different Lateral Shifts of the Wheelset Relative to the Track, Values in mm. **[15]**

Table 3. 1 Elliptical semi-axis dimensions for lateral shift of the wheelset (y) on the left rail

Y	**al[mm]**	**bl[mm]**
3	**6.5**	**6.4**
2	**6.3**	**7.1**
1	**6.0**	**8.2**
0	**5.4**	**10.7**
-1	**7.8**	**3.4**
-2	**7.7**	**3.5**
-3	**7.6**	**3.7**
-4	**7.4**	**4.1**
-5	**7.1**	**4.9**

When the two rails have the same profiles, the axis dimensions have some paternal relationships for same lateral displacement since the rails at the left profile is mirrored image the right rail.

CHAPTER 4

4. MATERIAL, CONDITIONS AND METHODS

4.1 Materials

In this paper the material property is taken from standard rails. UIC 60 Rails that is made from high carbon steel (up to 0.82% carbon), which provides high fatigue toughness. Since the analysis in wear analysis requires rail strength and has the following properties **[6]**

Table 4.1 Standard rail properties

No	Name of the parameter	Values (range)
1	Rail strength (Sy)	between 1300-1400N/mm^2
2	Equivalent young's modulus rail ($E_{1)}$	210 GPa
4	Distance between rail axis(2l)	1500mm

4.2. Conditions

- The wheel set angular velocity about its axis is constant. In other words starting, braking and tangential acceleration in between the motion of the vehicle wasn't considered in the analysis.
- The other important assumption is curving motion with maximum curving potential of the vehicle and the perfect driver otherwise their effect significant than that the curved nature of the track.
- A vehicle has a nominal static position of center of mass or loading and unloading should have some strict rules, since it may affect the position of center of mass of the vehicle.
- Dynamic effects is ignored and only assumed by using quasi-static approach.
- Throughout this paper a vehicle represents a vehicle which has two bogies one front the other behind. As seen in the fig.4.1 below there are a four wheeler (should be expected for axle load 10 tons services).The mass is assumed equally shared for each axle of the bogie. For example for 120 tons wagon then the axle load becomes of 30 tones.

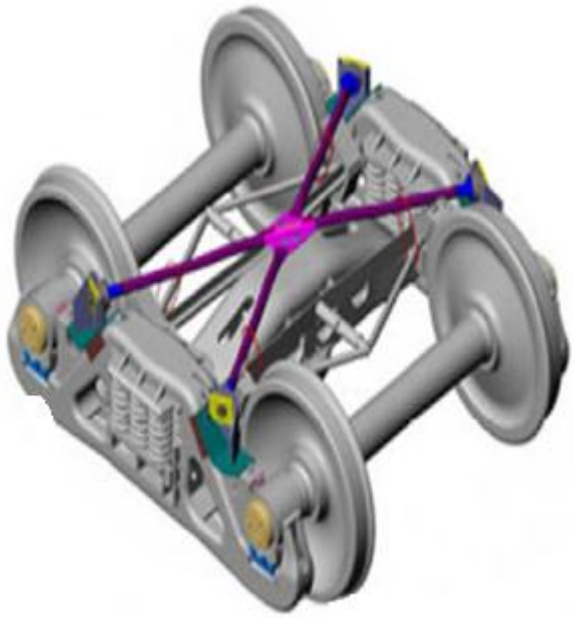

Figure 4.1: Leading Wheelset of the Vehicle (as Putt Upside Down)

- The tribology of curved rail determinate from the leading wheelset. Since the trailing wheelset is assumed always move to the center of rail axis. The leading wheelset only affect the behavior of curved track. The calculation is based on centrifugal loading only neglecting other forces such as wind. So all calculation from the point of axles loads and forces generated due curving motion of the vehicles.
- As a vehicle traverses a curve, the vehicle transmits a centrifugal force to the rail at the point of wheel contact. This force is a function of the radius of the curve, speed of the vehicle and the mass (weight) of the vehicle (look fig 4.2 below). This force acts at the center of gravity of the rail vehicle. This force is resisted by the track. If the vehicle is traveling fast enough, it may derail due to rail rollover, the vehicle rolling over or simply derailing from the combined transverse force exceeding the limit allowed by rail-flange contact. To avoid this difference in normal load to the rail heads of both sides of rails is only up to 30% **[18].**

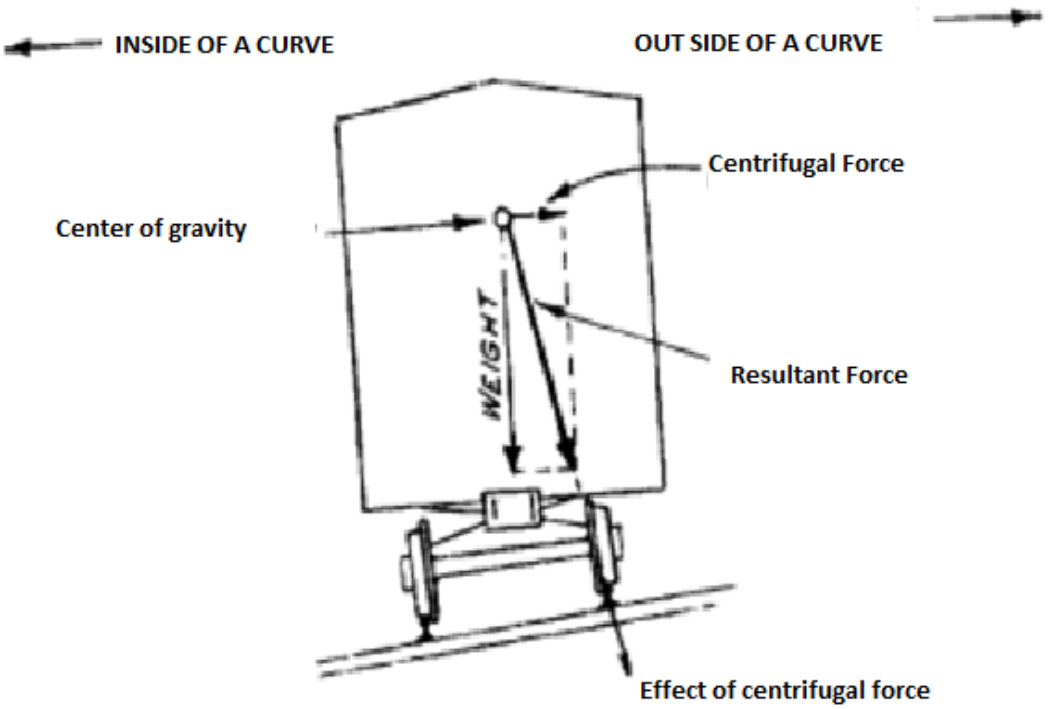

Figure 4.2: loadings on curved track

- All mechanisms of friction and wear assumed as adhesive mechanisms. Wear occurs on both wheel and rail as a result of the relative velocity difference of the two contacting bodies in the contact zone, where part of the contact is in adhesion and the rest is sliding **[19]**.So throughout the paper wear means a removal of debris which is produced from microscopic level sliding at each unit of a vehicle travel.
- The vehicle on the track assumed left hand travel and the wheel set on the left is as inner rail and right is the outer rail
- Practically curved track are designed to work with $\pm$100%superelvation differences. Here in this paper 100% mean the vehicle is moving within equilibrium superelvation to avoid negative percentages.
- Here in this paper the allowable limit for side wear is about 11mm and head wear is 16mm **[20].**
- For the case of superelevated track the effect conicity angle is very small and considered as no effect when comparing to the cant angle.
- The unbalanced lateral moment in the total vehicle equilibrium is assumed to be balanced by the twisting moments of trailing wheels set so the system only focused on the leading wheelset.
- The lateral force exerted by the flange and it is assumed to be applied on the leading wheelsets and this assumption may show clearly the difference between the steady state curving behaviors discussed by other authors.

4.3 Methods

Mathematical model is developed using different theories in chapter 3. Now using equations derived in chapter 3 and analysis is made by using MATLAB involving different track parameters like radius and cant angle; Vehicle wheel parameters speed, conicity, wheel radius; traffic parameters like load and traffic. The researcher were tried to cover all kinds of track and speed to deal on both horizontal and canted curved track. The major classification as to simplify the study is either the track is horizontal or canted. Result interpretation phase are deduced responses of curved track for radius change and velocity change. Finally according to the result found within prescribed conditions of the vehicle on the curved track the influences of speed and curve radius can be generalized.

CHAPTER 5

5. RESULT AND DISCUSSIONS

5.1. Introduction

This paper analyses the mechanism of curving motion, generation of lateral forces and their influence on tribological condition of the rail within the absence of wheel derailment and passenger discomfort. Now, in this part it discussed the influences of the curve radius and the speed of the vehicles by using derived formulas in the chapter 3. In this investigation, mathematical models are simulated using MATLAB program and most results have positive relation with field measurements **[6]** or laboratory experiments **[7].** The result analysis is done for 10 tone axle load and 0.4 friction coefficient throughout. Result interpretation is the word descriptions of the results found in the graphical way. The analysis procedure is classified as horizontal curved track and canted curved track. Except that there are additional superelevation parameters for the case of canted track, in both cases all friction, wear and maximum traffic /load carrying capacity are described in terms radius of a track and velocity of a vehicle for both rails at heads and sides.

5.2. Result Analysis

5.2.1 Horizontal curved rail Analysis

5.2.1.1 Friction property as a function of radius

From **fig.5.1** as the radius increases the friction at right rail decreases. The slope of the curves increases as the radius of the curve decreases. As the vehicle speed becomes more, the right rail exposed to high friction condition. It implies the vehicle moving at lower speeds the friction at right rail becomes lower. From **fig.5.2** the left rail behaves differently according to the vehicle speed. Friction at left side increases as radius increases. The slope of the curves increases as the radius of the curve decreases for high vehicle speed. As the vehicle speed becomes slower, the rate of change of friction at left rail becomes lesser.

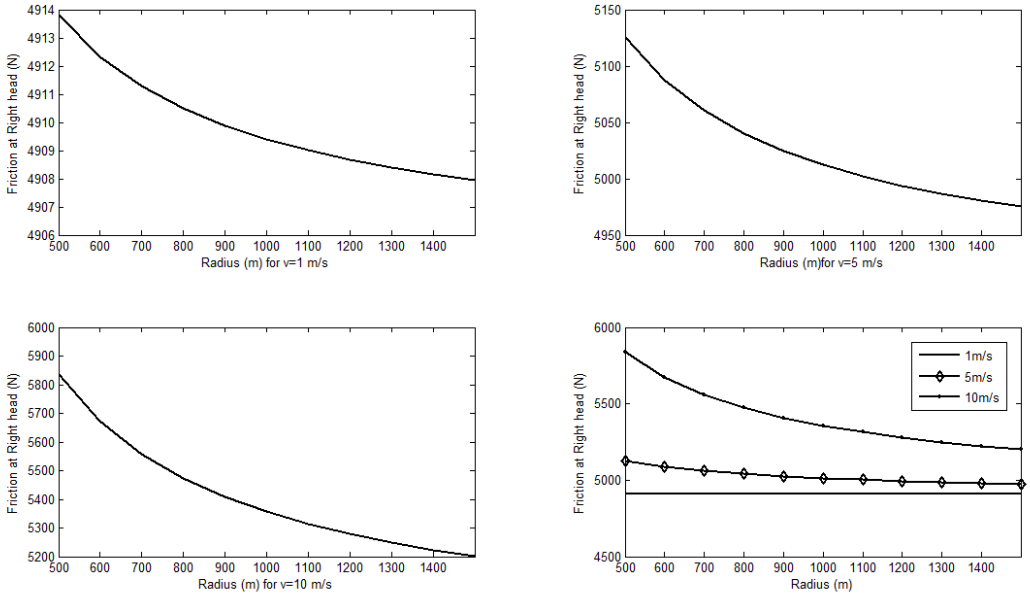

Figure 5.1: the Graph Shows the Effect of Curved Track Radius on Friction Force at Right Rails on Horizontal Curved Track at Velocity v=1, 5,10m/s

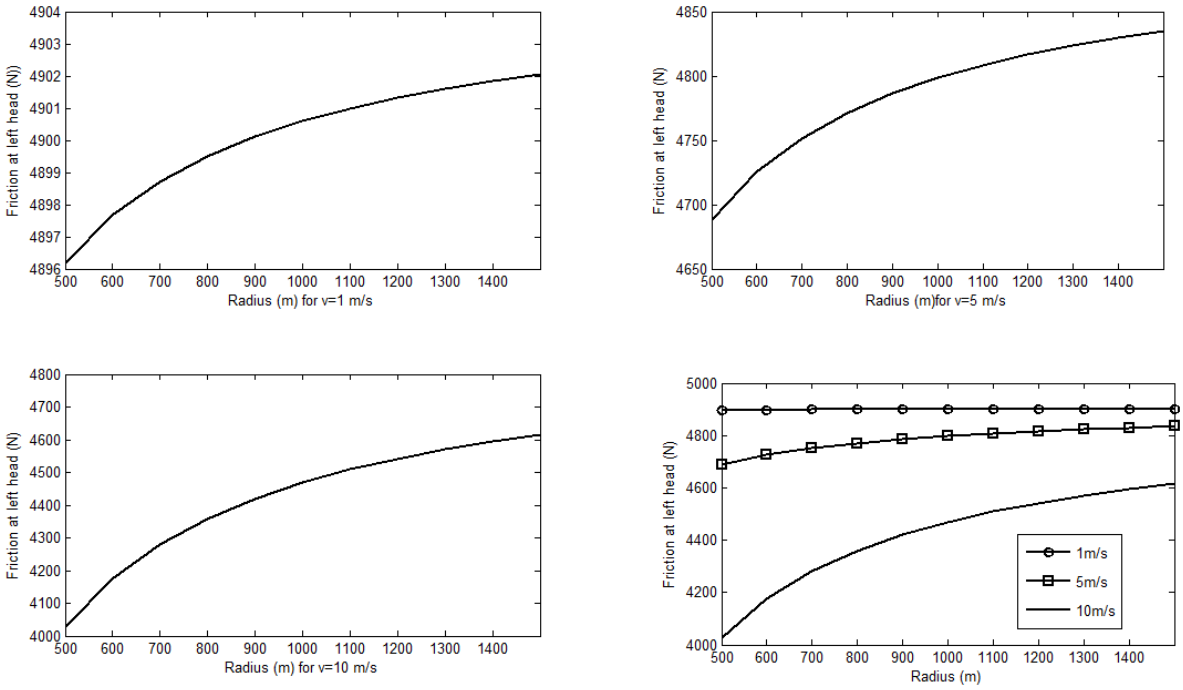

Figure 5.2: the graph shows the effect of curved track radius on friction force at left rails on horizontal curved track at velocity v=1, 5,10m/s

5. 2.1.2 Wear property as a function of radius

From **fig. *5*.3** the right rail head cross-sectional area loss after one million ton is passed over it, the property of the rail wear have similar behaviour for different vehicle velocity i.e. the slope of the

curves increases as the radius of the curve decreases. The slope (the rate of change) of the curves increases as forward velocity increases. The vehicle moving with high speed is more exposed to right rail head wear.. Similarly From **fig. *5*.4** the left rail head cross-sectional area loss after one million ton is passed over it, the property of the rail wear have behaviour of the slope (the rate of change) of the curves decrease as forward velocity increases. The slope of the curves increases as the radius of the curve decreases for low velocity. The property of wear at left rail for high velocity has look like upside down parabolic graph which shows there are certain radius which have a high wear conditions but generally smaller wear exposure when compared to vehicle travelling at low velocity. From **fig. *5*.5** the cross-sectional area loss at right rail side due to flanging contact. At low velocity there is no side wear. Right side only occurs at certain forward velocity which is equivalent to above equilibrium speed for canted track. The slope of the curves increases as the radius of the curve decreases.

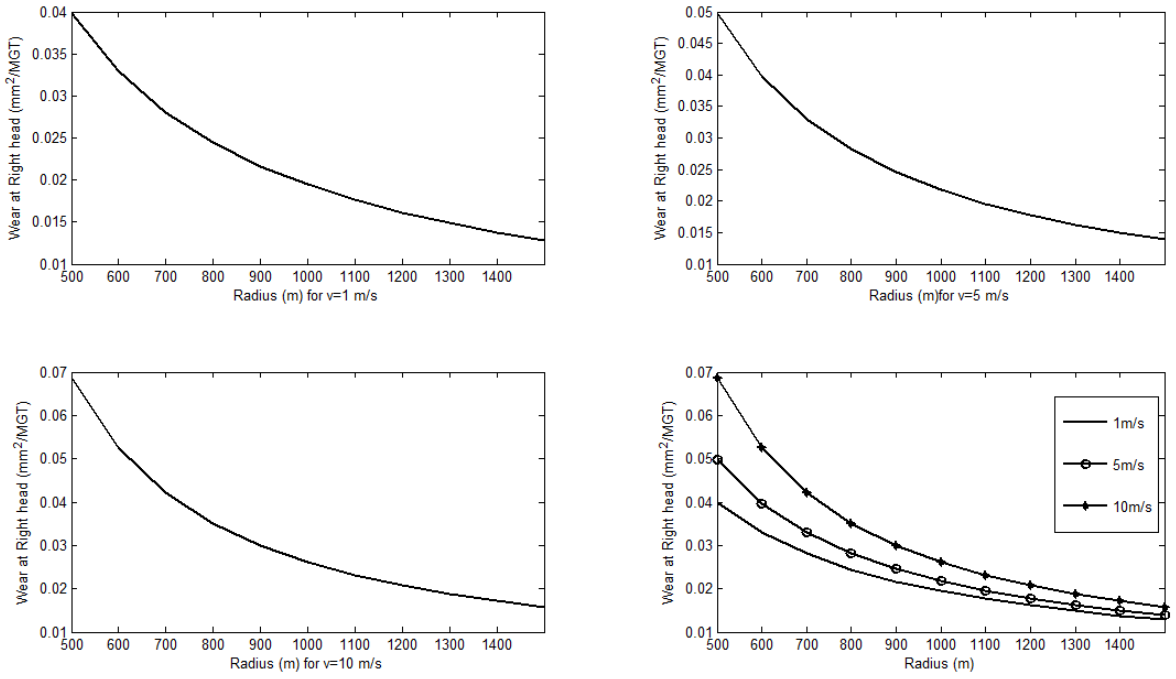

Figure 5.3: the graph shows cross-sectional area loss as a function of radius of curved track of horizontal curved track at velocity v=1, 5,10m/s

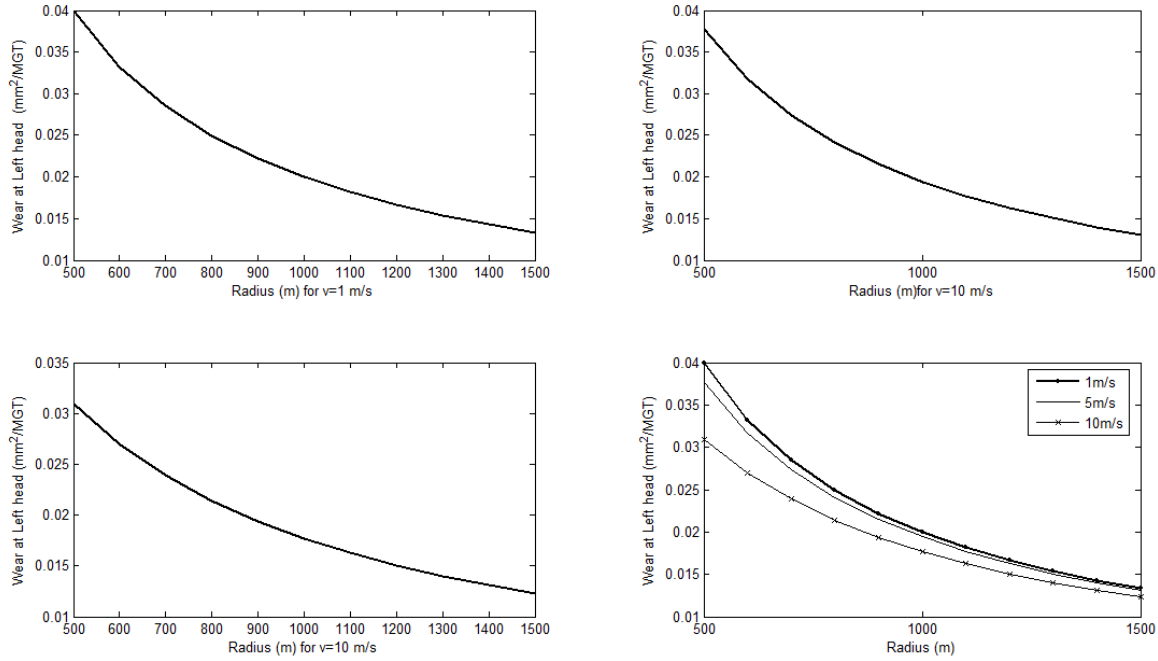

Figure 5.4: the Graph shows Cross-sectional Area Loss as a Function of Radius of Curved Track at Left Rails of Horizontal Curved Rail at Velocity v= 1, 5, 10m/s

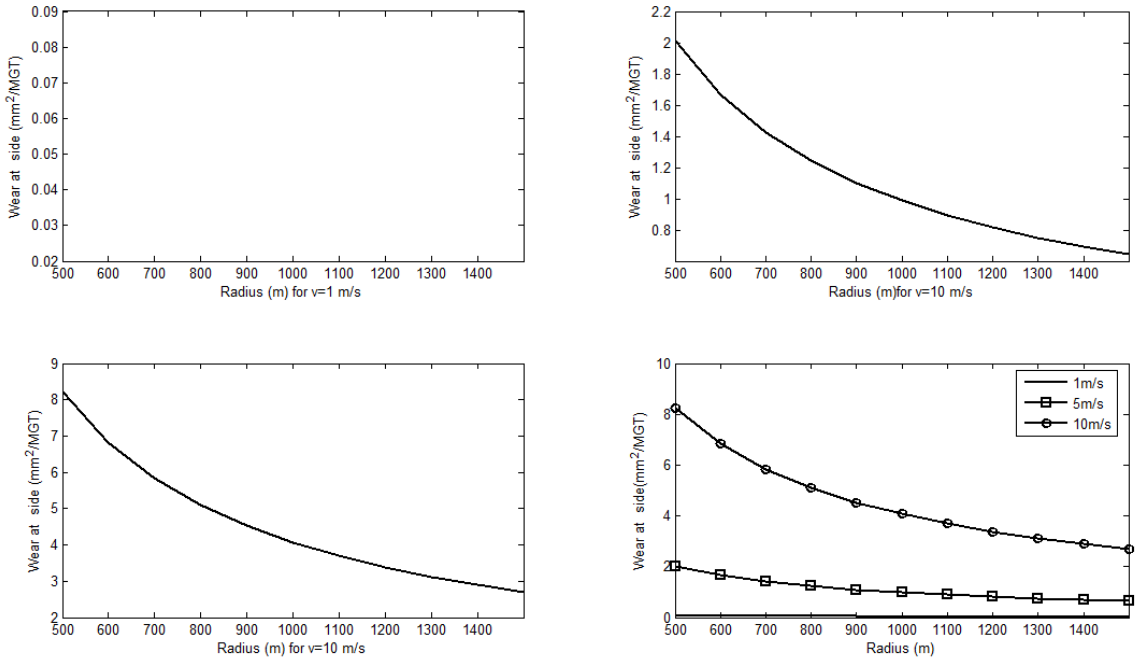

Figure 5.5: the Graph Shows Cross-sectional Area Loss as a Function of Radius of Curved Track at Right Rail Side on Horizontal Curved Track at Velocity 1, 5, 10m/s.

5.2.3.1 Predicting rail life as a function of radius on Horizontal curved track

From the **fig. 5.6** the maximum wear is occurred at right side, the life of the rail calculated at this contact. Assuming dry contact the life of the rail is under 200 MGT for vehicle velocity above 10m/s of a track radius is less than 1500m. If the rail has traffic load of 20MGT per year the life span is only 10 year. As the radius becomes smaller this life time is linearly reduced.

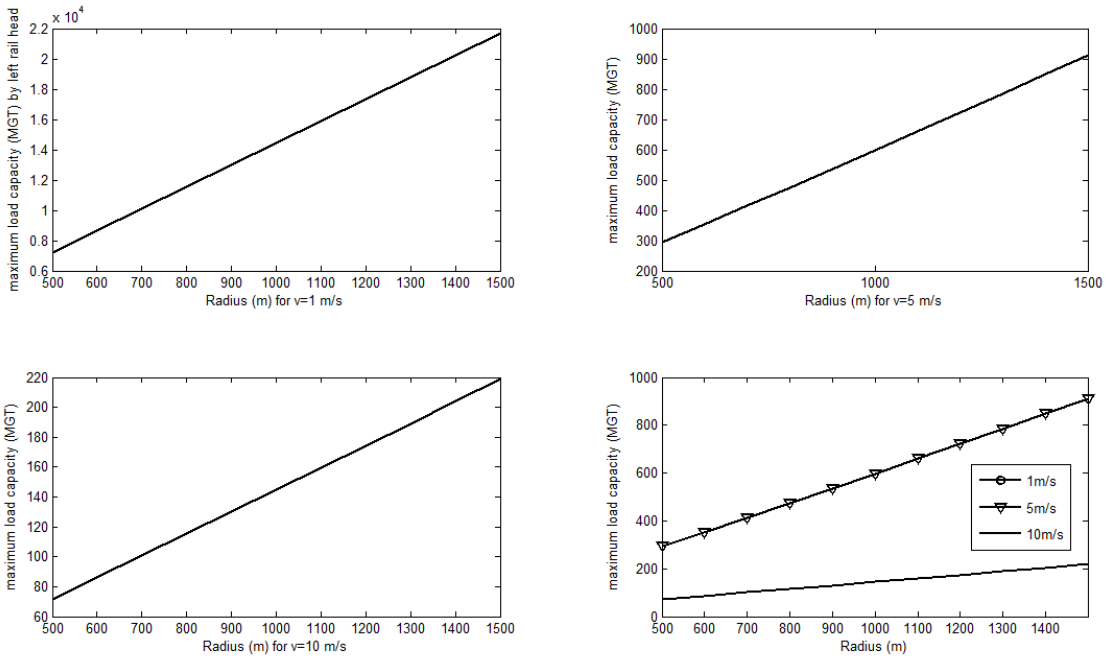

Figure 5.6: the Graph Shows Predicting the Maximum Tonnage of Rail using Right Side Cross-sectional Area Loss as a Function of Radius.

5.2.1.3 Friction property as a function of velocity

Fig. 5.7 is about the effect of forward velocity at right rail and it behaves. As the velocity increases the right rail friction increases. The slope of the curves increases as forward velocity increases at the right rail. There is more friction force as the radius becomes sharper within the same forward velocity. The **fig. 5.8** the effect of forward velocity at left rail and it behaves. As the velocity increases the left rail friction decreases. The slope of the curves increases as forward velocity increases at the left rail. There is more friction force for large radius curves.

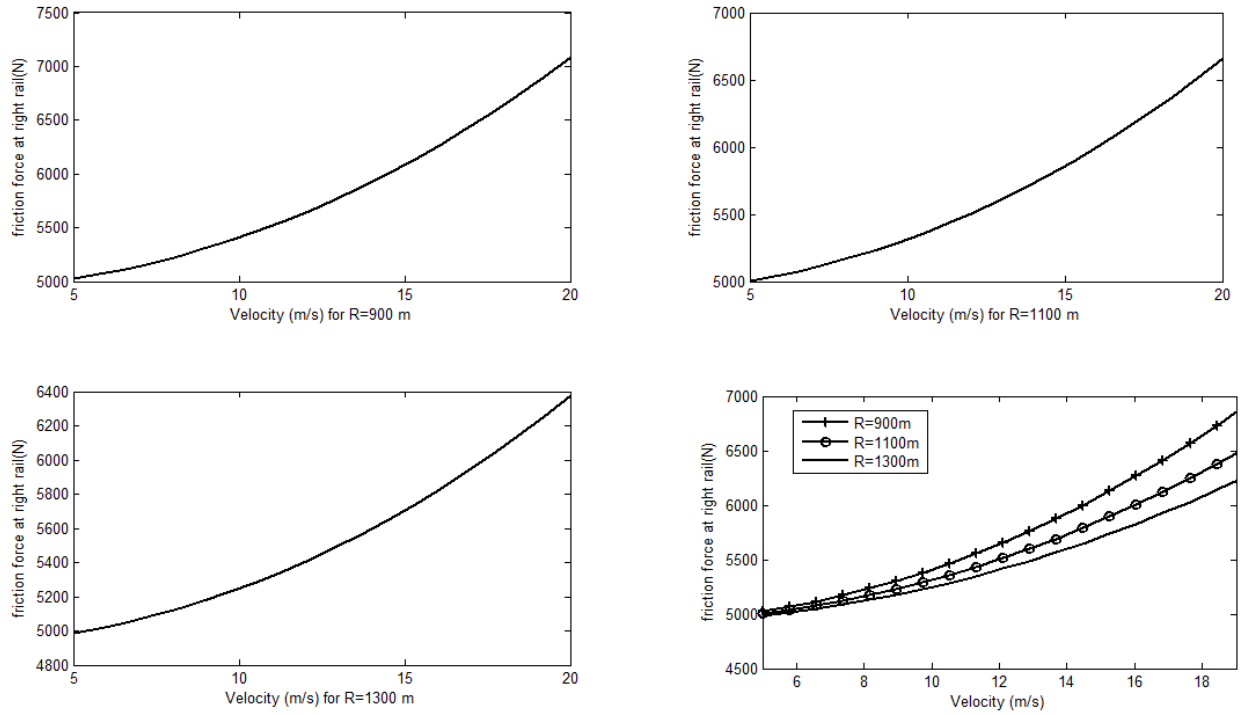

Figure 5.7: the graph shows the effect of forward velocity on friction property of right rails at different radius curves (900, 1100 and 1300m) for horizontal curved track.

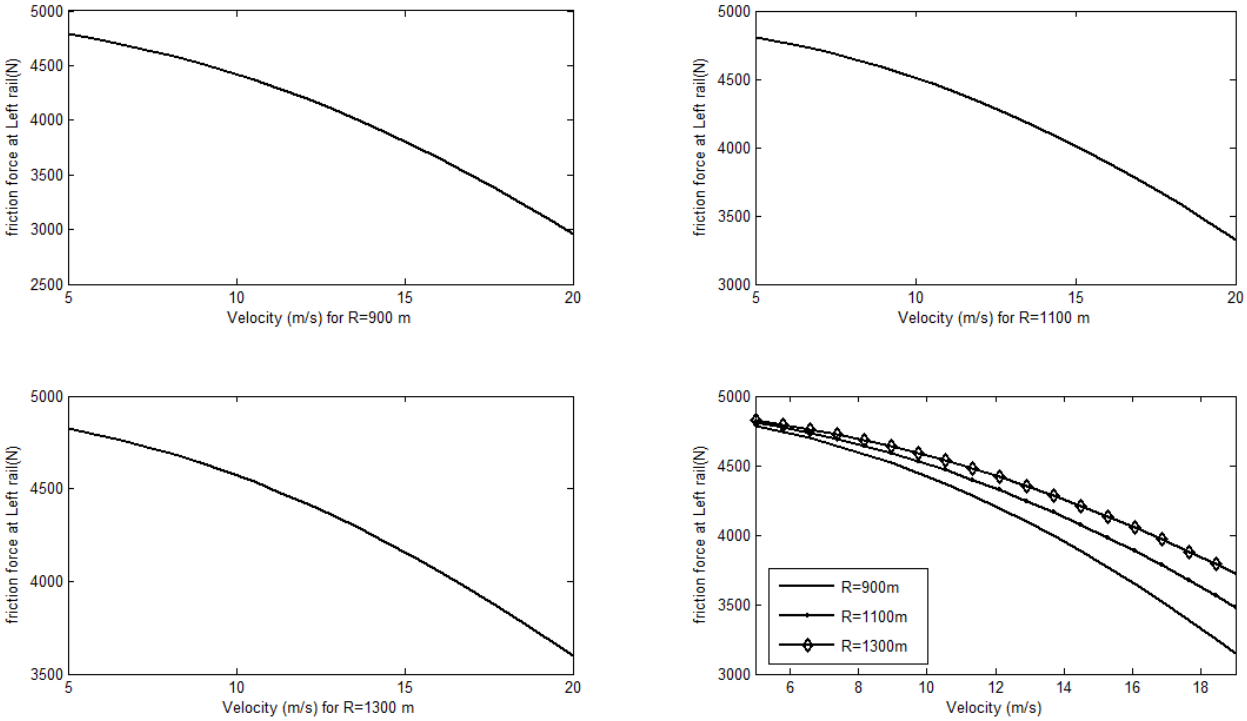

Figure 5.8: the Graph Shows the Effect of Forward Velocity on Friction Property of Left Rails at Different Radius Curves (900, 1100 And 1300m) for Horizontal Curved Rail

5.2.1.4 Wear property as a function of velocity

The **fig. 5.9** below shows about the effect of forward velocity on cross-sectional area loss at right rail head with in different track radius. As a velocity increases the right rail exposed to more wear conditions. The slope of the curves is constant (linear relationships). There is more wear at small radius curves within the same forward velocity. Similarly from **fig. 5.10** the effect of forward velocity on cross-sectional area loss at left rail head with in different track radius. As a velocity increases the left rail less exposed to wear conditions. The slope of the curves increases in absolute value as forward velocity. There is more wear at small radius curves within the same forward velocity but as the velocity increases the wear conditions at large radius is more exposed to wear. The graph shows (**fig. 5.11)** below shows about the effect of forward velocity on cross-sectional area loss at right rail side with in different track radius. As a velocity increases the right rail side is more exposed to wear. The slope of the curves increases as forward velocity increases. There is more wear at small radius curves within the same forward velocity. At low velocity there is no side wear

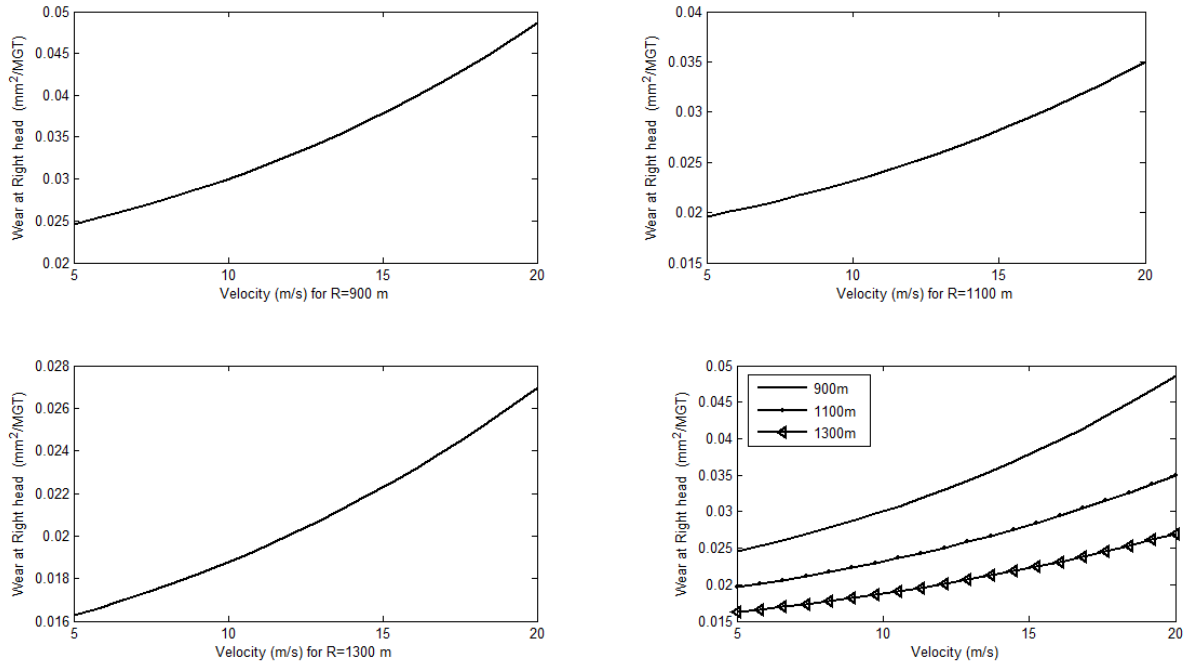

Figure 5.9: the Graph Shows Cross-Sectional Area Loss as a Function of Speed of the Vehicle in Different Radius (900, 1100 and 1300m) of a Track at Right Rail Head on Horizontal Curved Rail

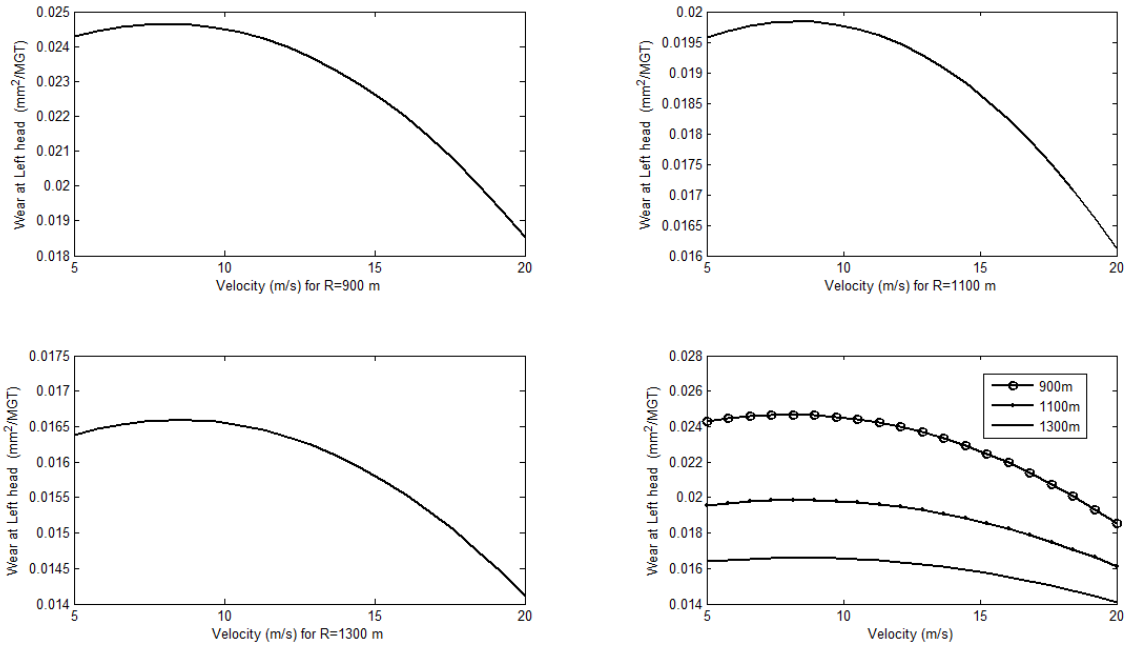

Figure 5.10: the Graph Shows Cross-Sectional Area Loss as a Function of Speed of the Vehicle in Different Radius (90, 1100 And 1300m) of a Track at Left Rail Head on Horizontal Curved Rail

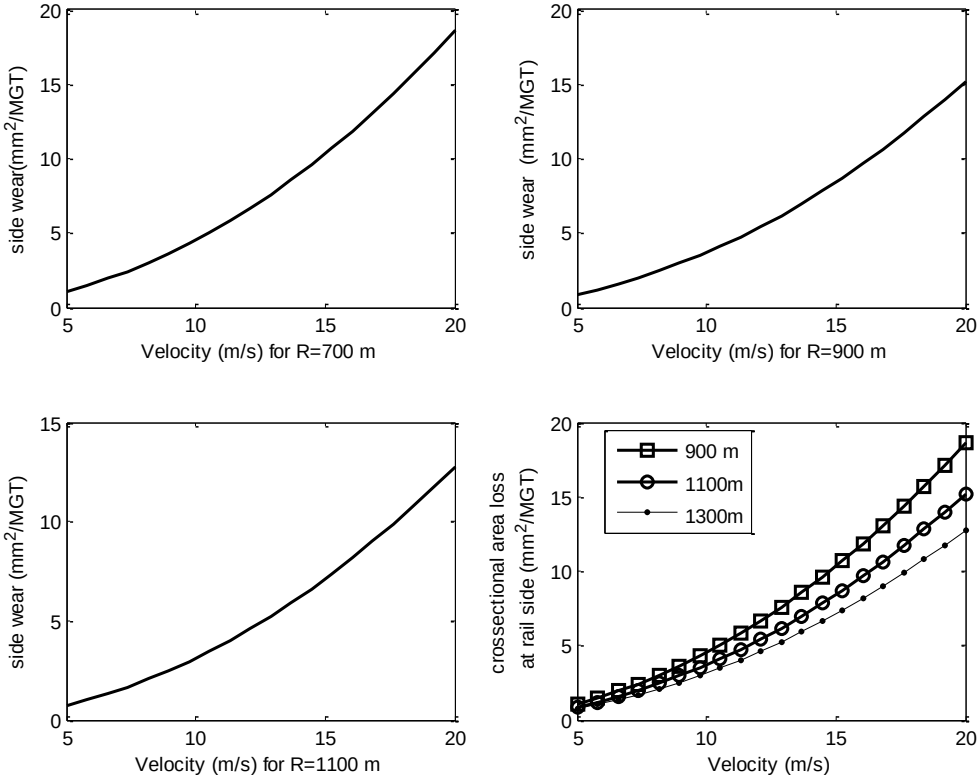

Figure 5.11: the Graph Shows Cross-Sectional area Loss as a Function of Speed of the Vehicle in Different Radius (900, 1100 And 1300m) of a Track at Right Rail Side on Horizontal Curved Rail

5.2.1.5 Predicting rail life as a function of velocity on Horizontal curved track

From **fig 5.12** the traffic tonnage decreases with decrease of radius and increases of forward velocity.

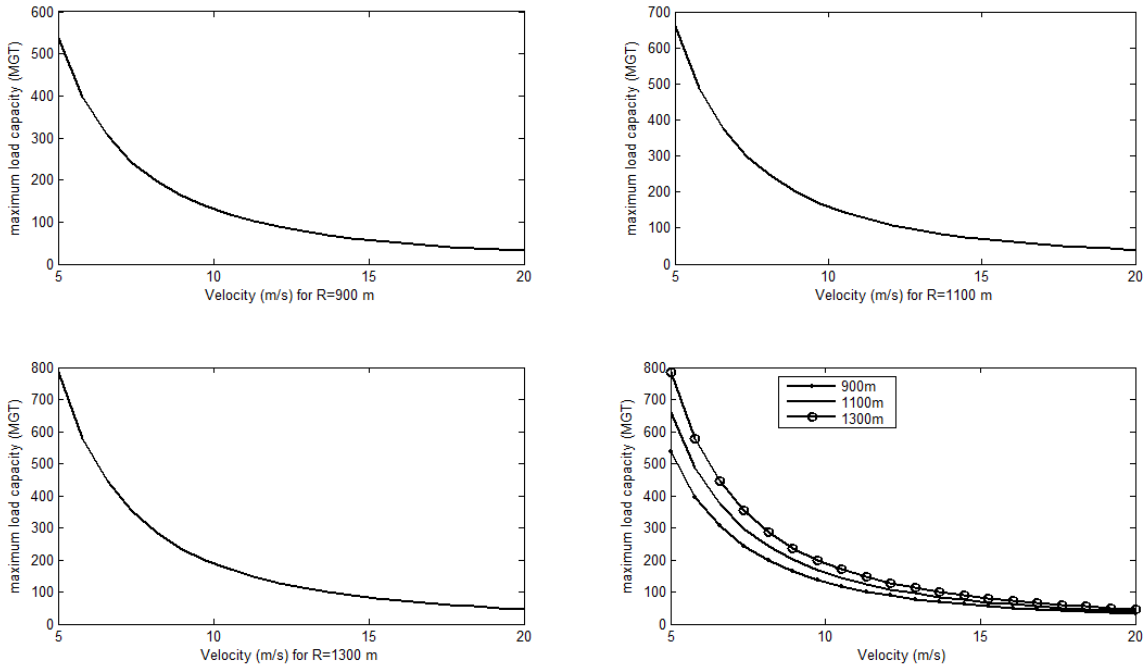

Figure 5.12: the Graph Shows Predicting the Maximum Tonnage of Rail using Right Side Cross-Sectional Area Loss as Function of Velocity

5.2.2 Canted curved rail Analysis

5.2.2.1 Friction property as a function of radius

From **fig.5.13** the following can be generalized to friction property of right rail as a function radius. When the vehicle moves above equilibrium it increases with decrease of radius, it is almost constant which around half of axle loads at equilibrium speed and increases with increase of radius at vehicle velocity below equilibrium. The more the velocity of the vehicle the friction force at right rail also high. Both lines seem to converge to large radius, which corresponds to a configuration with no rail side contact. The slope of the line of friction force in absolute value is high as radius decreases. The friction property at the left rail has a property of **fig. 5.14.** When the vehicle moves below equilibrium, it increases with decrease of radius, it is almost constant which around half of axle loads at equilibrium speed and increases with increase of radius at vehicle velocity above equilibrium.

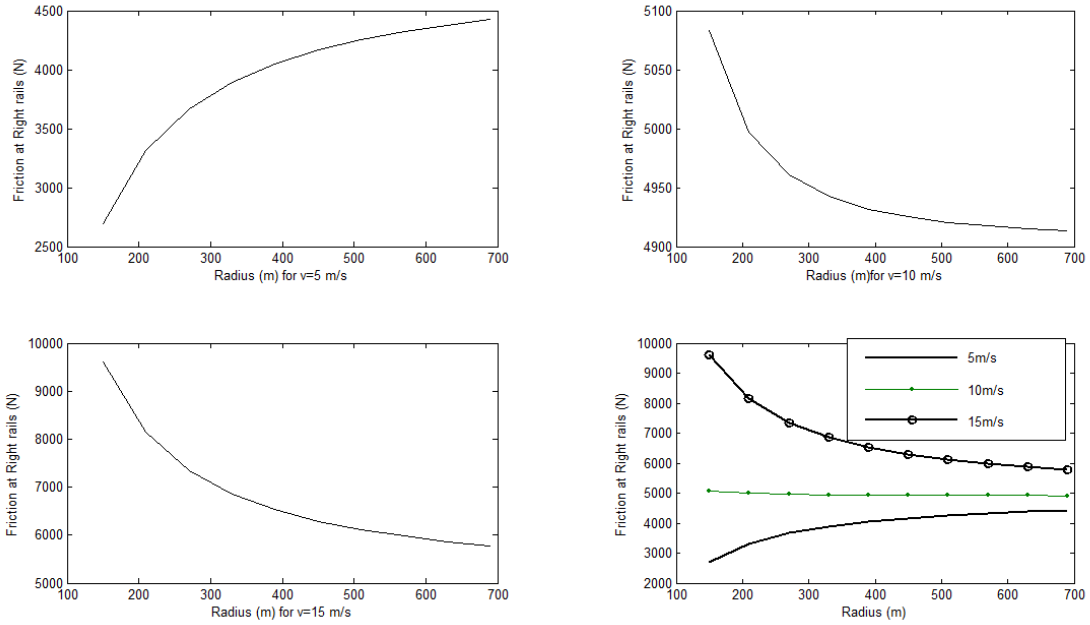

Figure 5.13: Graph Shows the Effect of Radius Curves on Right Rail Friction Property at Different Forward Velocity (5, 10, And 15) for Canted Curved Track

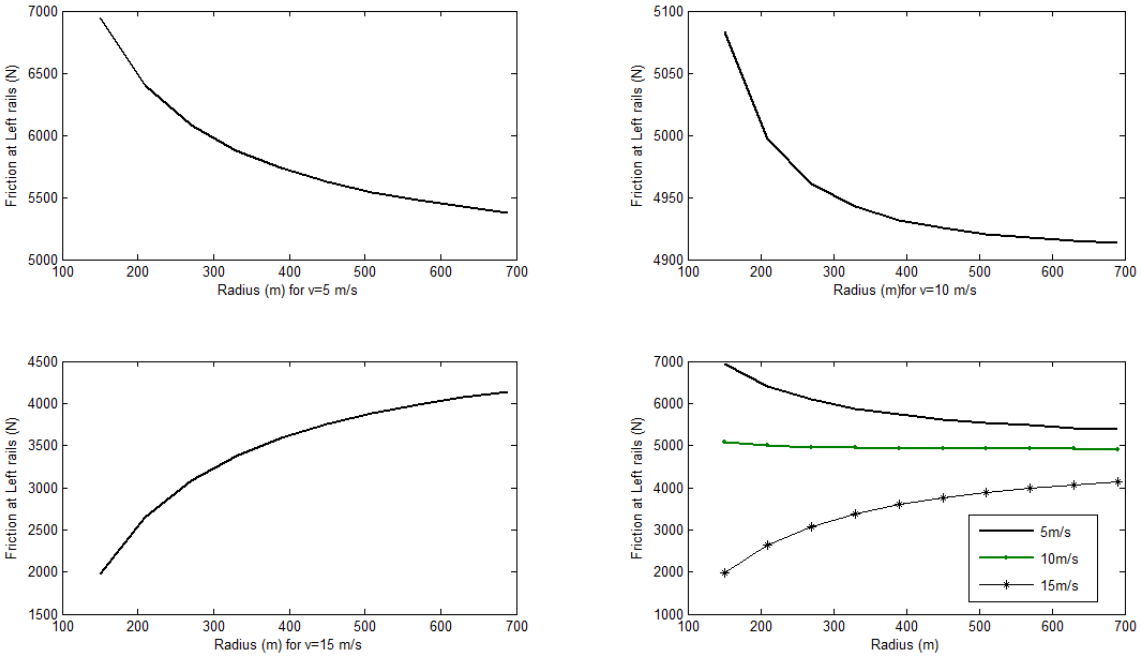

Figure 5.14: Graph Shows the Effect of Radius Curves on Left Rail Friction Property at Different Forward Velocity (5, 10, And 15) for Canted Curved Rail

5.2.2.2 Wear as a function of radius

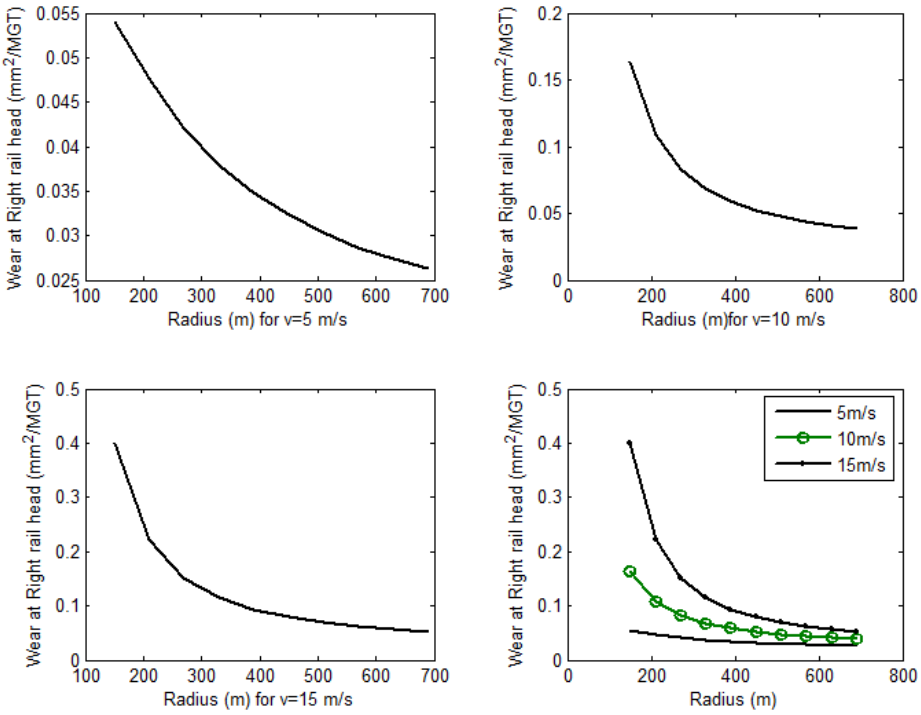

Figure 5.15: the Graph Shows Right Rail Head Cross-Sectional Area Loss as a Function of Radius of Curved Track in Different Forward Velocity (5, 10, And 15) for Canted Curved Rail

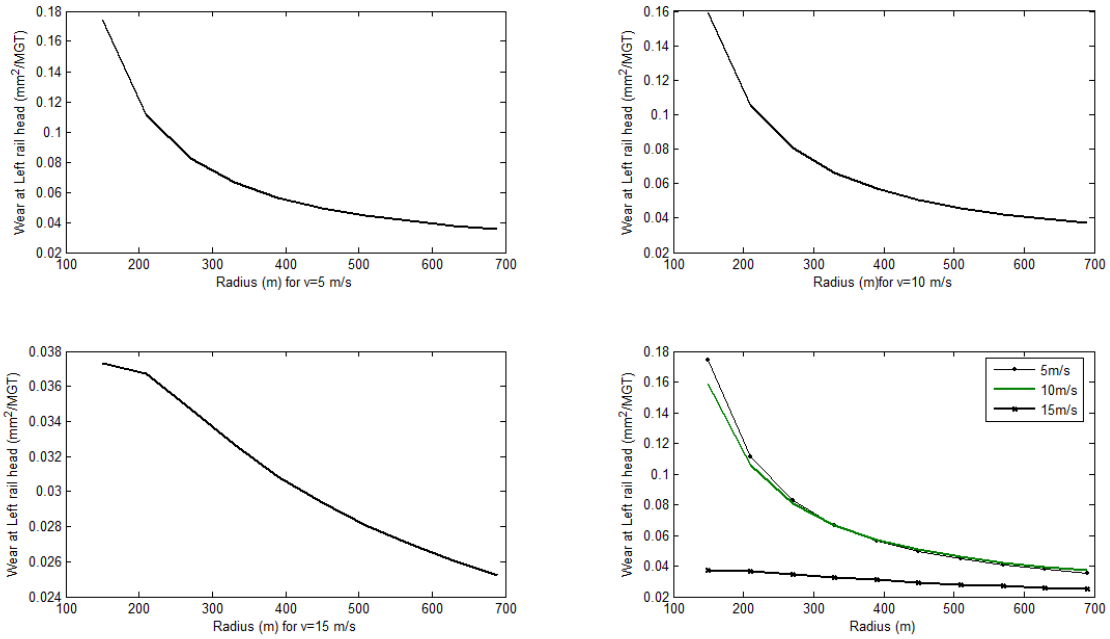

Figure 5.16: the Graph Shows Left Rail Head Cross-Sectional Area Loss as a Function of Radius of Curved Track in Different Forward Velocity (5, 10, And 15) for Canted Curved Rail

The cross-sectional area loss at right rail head of a canted curved for 10 tone axle as shown at **fig. 5.15** and can be summarized as the right rail head wear have different property with the vehicle speed (less than and greater than equilibrium speed). When the vehicle speed is above equilibrium speed the right rail is highly damaged as the radius becomes sharper but for the vehicle speed lower than equilibrium speed the wear has decreases with decrease of radius. The (the rate of change) slope of the curves increases as radius decreases for vehicle velocity above equilibrium speed. The cross-sectional area loss at Left rail head of a canted curved for 10 tone axle as shown from the graph above **fig. 5.16** can be summarized as the left rail head wear have a property of decreasing with increase of curve radius. The higher the vehicle speed the less head wear at left rail head. The slope of the curves decreases as radius increases. The cross-sectional area loss at right rail of a canted curved for 10 tone axles is shown in **fig. 5.17** and can be summarized by as Right rail side wear is happened when the vehicle is moving faster than the designed (equilibrium) speed. The right rail side wears decreases as the radius of a track increases. The slop increases as the radius of the curve decreases. The side cross-sectional area loss at left rail of a canted curved track for 10 tone axle loads is shown above **fig. 5.18** can be summarized as Left rail side is happened when the vehicle is moving slower than the designed (equilibrium) speed. The Left rail side wears decreases as the radius of a track increases. The slope increases as the radius decreases.

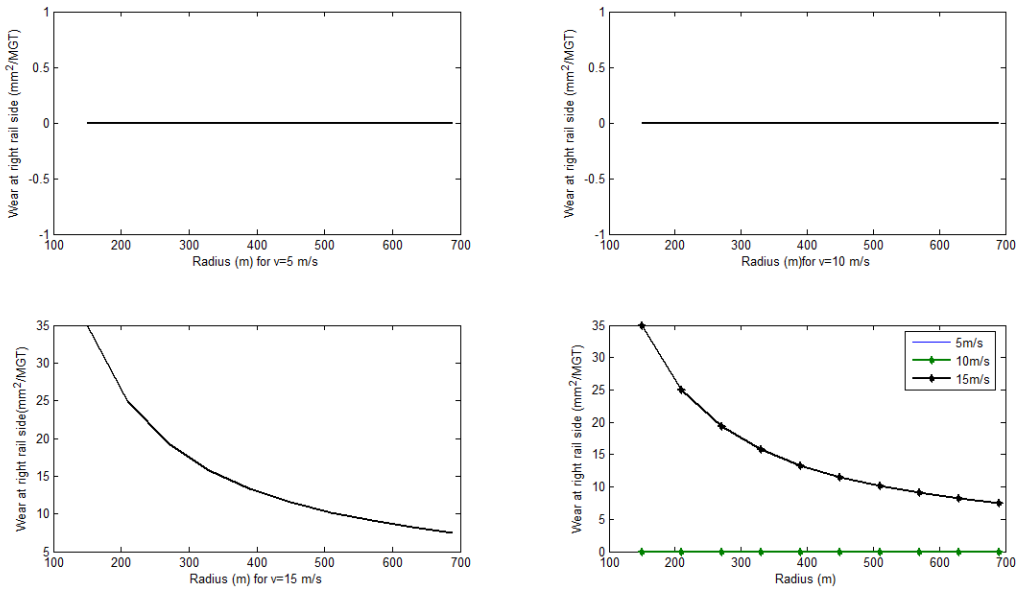

Figure 5.17: the Graph Shows Cross-Sectional Area Loss at Right Rail Side as a Function of Radius of Curved Track in Different Forward Velocity (5, 10, And 15) for Canted Curved Rail

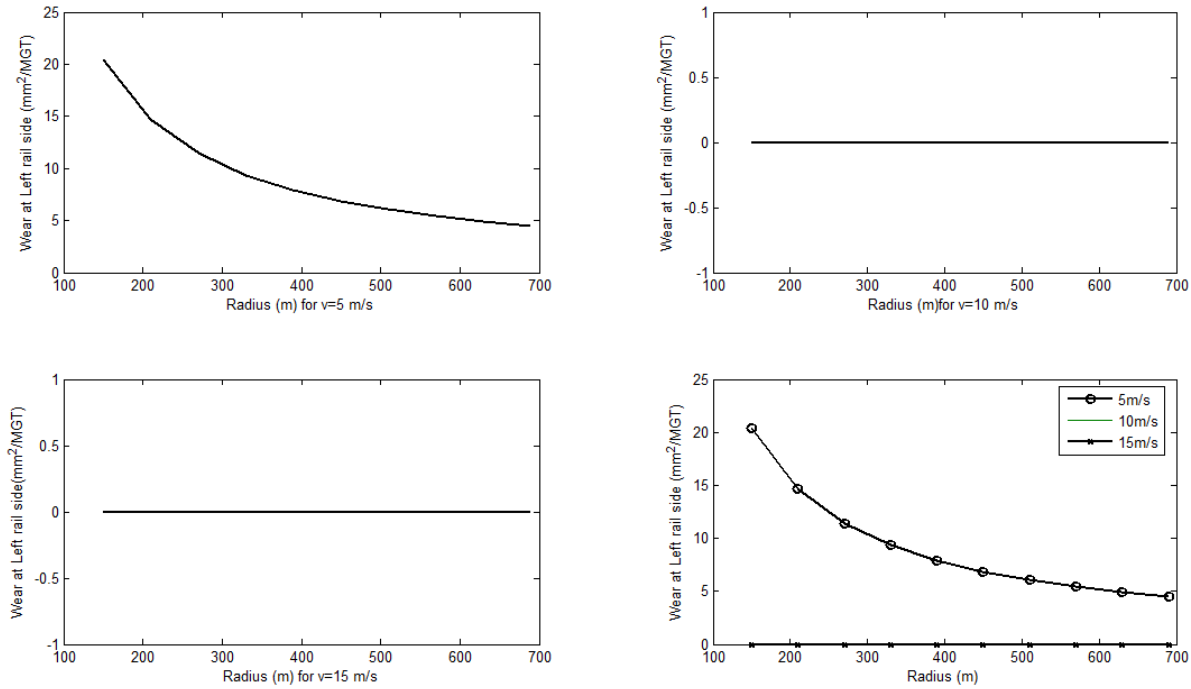

Figure 5.18: the Graph Shows Cross-Sectional Area Loss at Left Rail Side as a Function of Radius of Curved Track in Different Forward Velocity (5, 10, And 15) for Canted Curved Rail

5.2.2.3 Predicting rail life as a function of radius on canted curved track

In this case both rails are responsible for rail damaging processes and analyzed using fig. **5.19.** It is possible to conclude that at vehicle equilibrium velocity there is no side wears and at this time using stress theories will predict the life of the rail since the rail head cross-sectional area loss is not that much significant to determine the life of the wear. There is a linear relationship of increasing capacity of traffics as the radius increases. The Left side at above equilibrium velocity is less exposed to damage with the same traffics so interchanging the rails helpful to lengthen the service life of the rail.

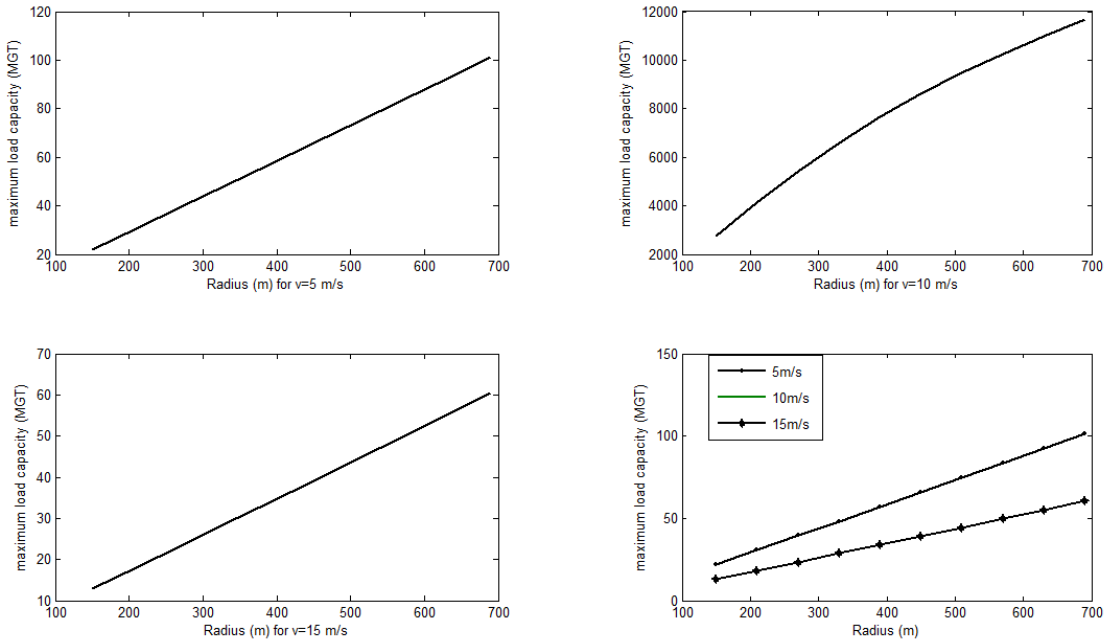

Figure 5.19: the Graph Shows Predicting the Maximum Tonnage of Rail using Both Sides Cross-Sectional Area Loss's as Function of Radius. (5m/s for left rail and 15m/s right side)

5.2.2.4 Friction property as a function of velocity

The figure below shows (**fig. 5.20**) the friction property at right rail with a function of velocity at different radius. The rate of change of friction forces decreases as the vehicle speed as approaches to equilibrium vehicle speed (10m/s). The friction forces on the right rail increase the forward velocity increases. The rate of change of these forces increases as the track curvature increases with the same velocity. The figure below shows (**fig. *5.21***) the friction property at left rail with a function of velocity at different radius. The friction forces on the left rail decreases as the forward velocity increases. The rate of change of these forces increases as the track curvature increases with the same velocity. The rate of change of friction increases as the forward velocity increases.

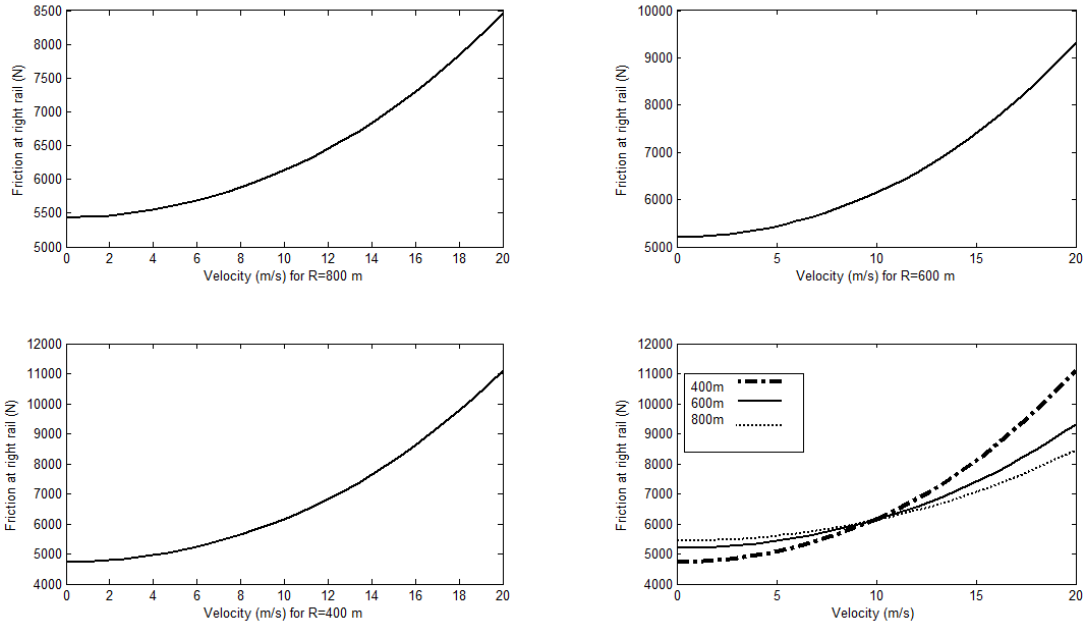

Figure 5.20: the Graph Shows the Effect of Forward Velocity on Friction Property of Right Rails at Different Radius Curves (400,600,800m) for Canted Curved Rail

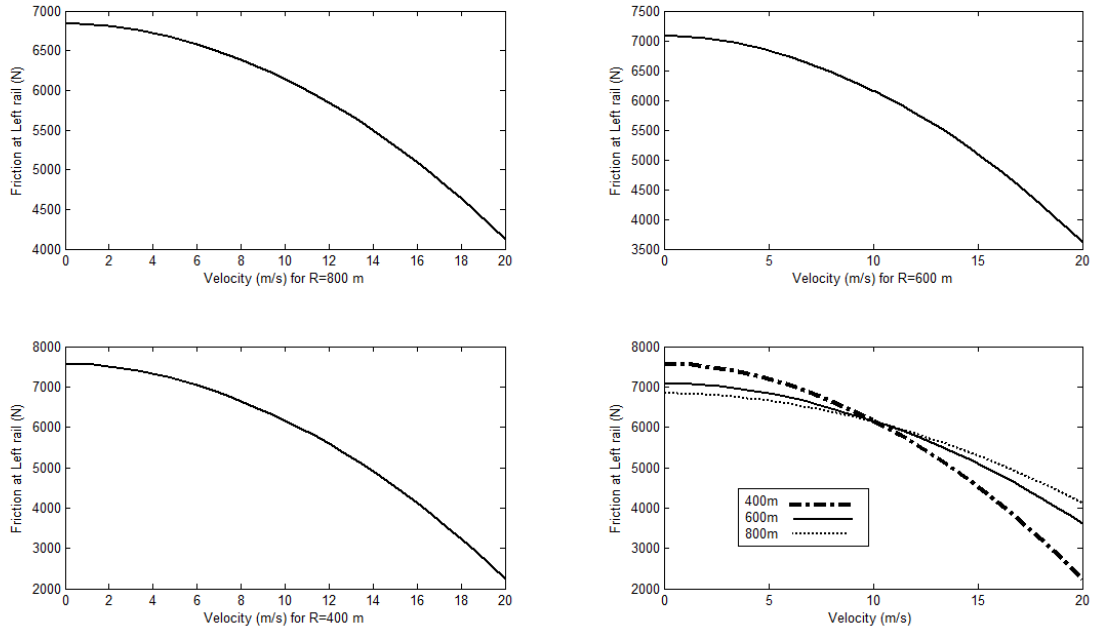

Figure 5.21: the Graph Shows the Effect of Forward Velocity on Friction Property of Left Rails at Different Radius Curves (400,600,800m) for Canted Curved Rail

5.2.2.5 Wear property as a function of velocity on canted curved rail

The cross-sectional area loss at right rail head of a canted curved for 10 tone axle as a function of velocity using different radius tracks are shown at **fig. 5.22** and can be summarized as the right rail head wear increases as the forward velocity increase. Rate of change wear is increased as the track radius deceases within the same velocity. The cross-sectional area loss at left rail head of a canted

curved for 10 tone axle as a function of velocity using different radius tracks are shown at **fig. 5.23** and can be summarized as the left rail head wear increases up to equilibrium speed then decreases with high rate when the vehicle is moving with speed above equilibrium speed. The slope of the curves increases as the vehicle is moving far from equilibrium speed. At large curved track there is minimum slope. The wear at the vehicle velocity beyond equilibrium speed is very low when compared the vehicle moving below equilibrium speed. The side cross-sectional area loss at right rail of a canted curved for 10 tone axle as a function of velocity using different radius tracks are shown at **fig. *5.24*** and can be summarized as the forward velocity increases the right rail side is exposed for high wear. As the radius becomes sharper right rail side exposed to sever wear for vehicle speed above equilibrium speed. For vehicle with speed less than equilibrium speed (10m/s) there is no right side wear. The side cross-sectional area loss at left rail of a canted curved for 10 tone axle as a function of velocity using different radius tracks are shown at **fig. *5.25*** and can be summarized as the forward velocity decreases the left rail side is exposed for high wear. As the radius becomes sharper left rail side exposed to sever wear for vehicle speed below equilibrium speed. For vehicle with speed above than equilibrium speed (10m/s) there is no left side wear.

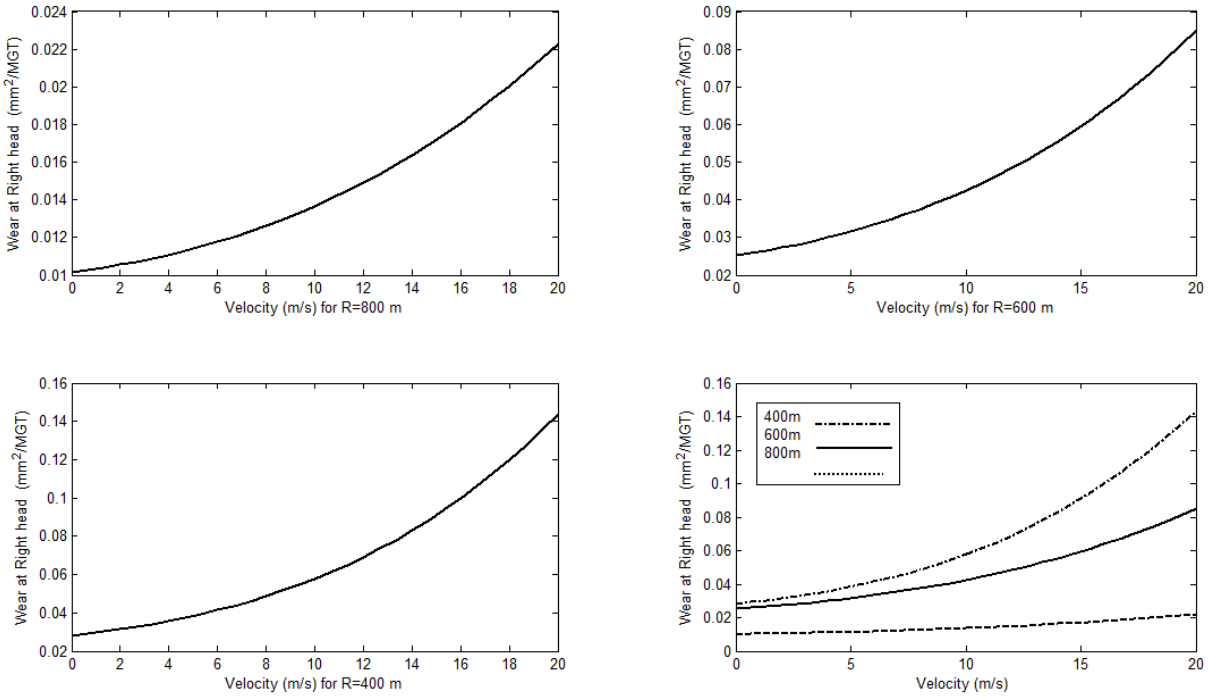

Figure 5.22: the Graph Shows Cross-Sectional Area Loss as a Function of Speed of the Vehicle in Different Radius of a Curve at Right Rail Head On Canted Rail

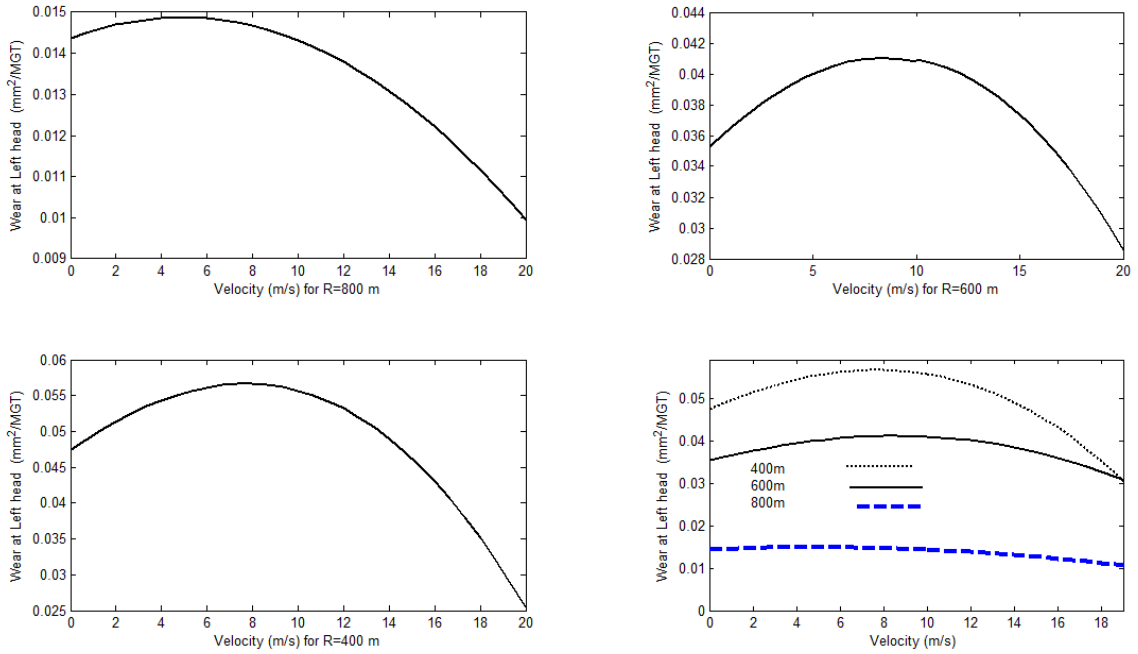

Figure 5.23: the Graph Shows Cross-Sectional Area Loss as a Function of Speed of the Vehicle in Different Radius of a Track at Left Rail Head on Canted Rail

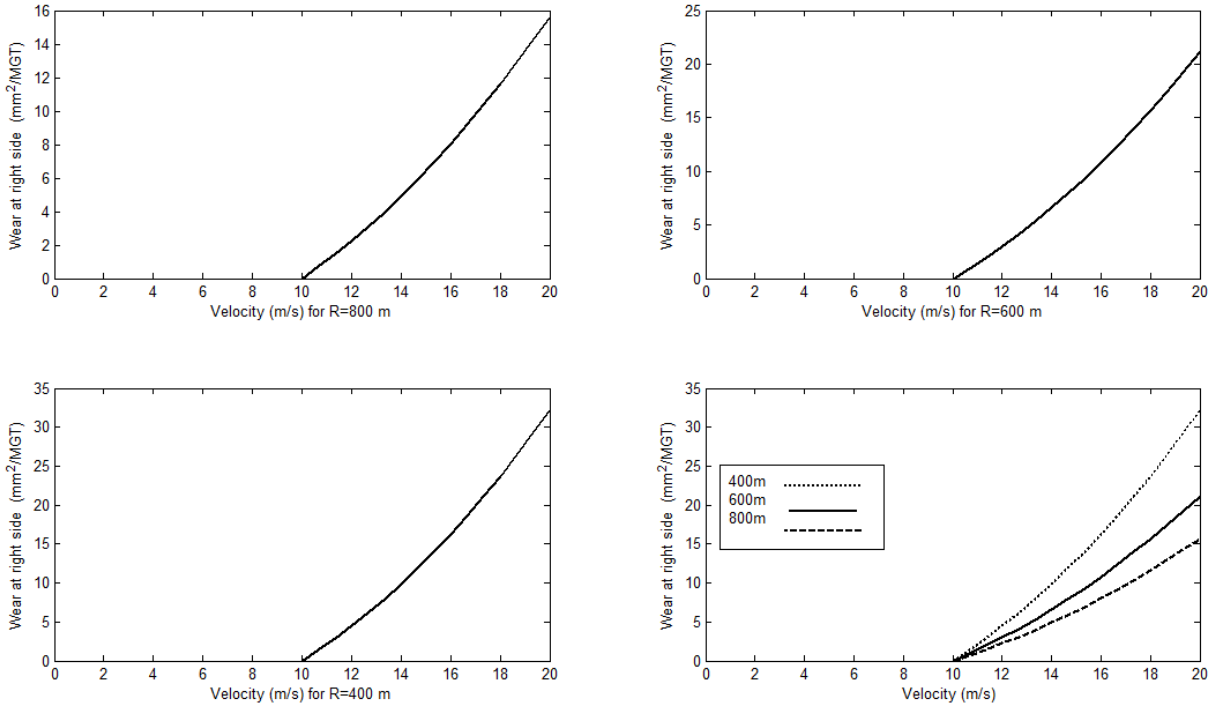

Figure 5.24: the Graph Shows Cross-Sectional Area Loss as a Function of Speed of the Vehicle in Different Radius of a curve at Right Rail Side on Canted Rail

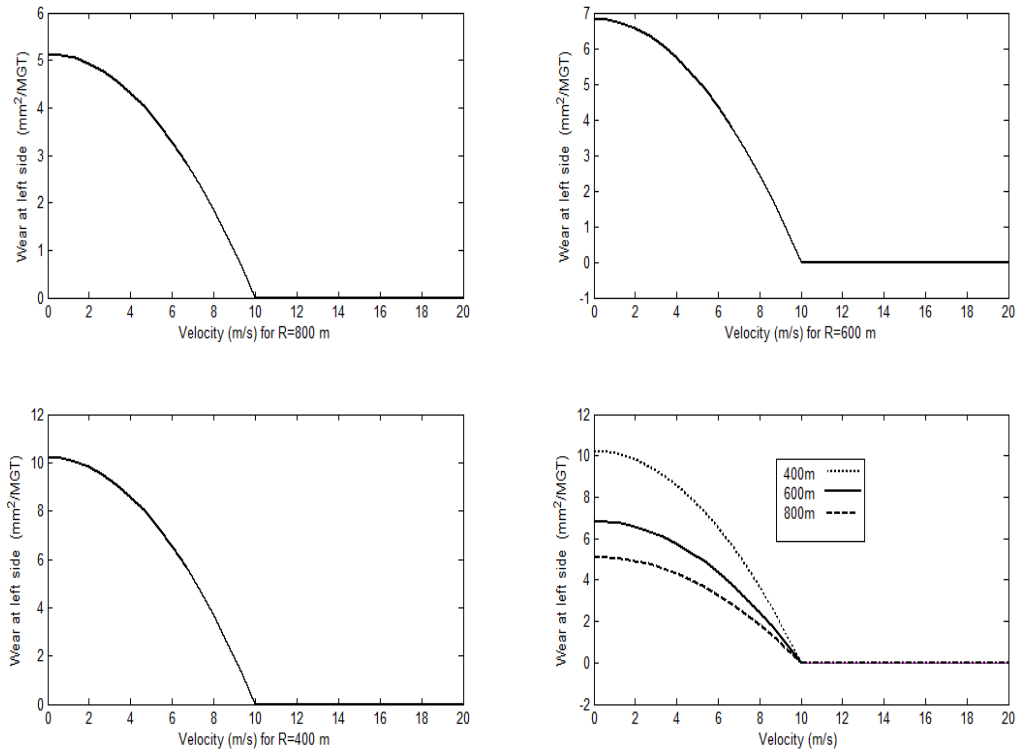

Figure 5.25: the Graph Shows Cross-Sectional Area Loss as a Function of Speed of the Vehicle in Different Radius of a Track at Left Rail Side on Canted Rail

5.2.2.6 Predicting rail life as a function of velocity on canted curved track

Using **fig. 5.26** it is possible to conclude that at vehicle equilibrium velocity there is no side wear and at this time using stress theories will predict the life of the rail since the rail head cross-sectional area loss is not that much significant to determine the life of the wear. There is a linear relationship of increasing capacity of traffics as the radius increases. The Left side at below equilibrium velocity is less exposed to damage with the same traffics so interchanging the rails helpful to lengthen the service life of the rail.

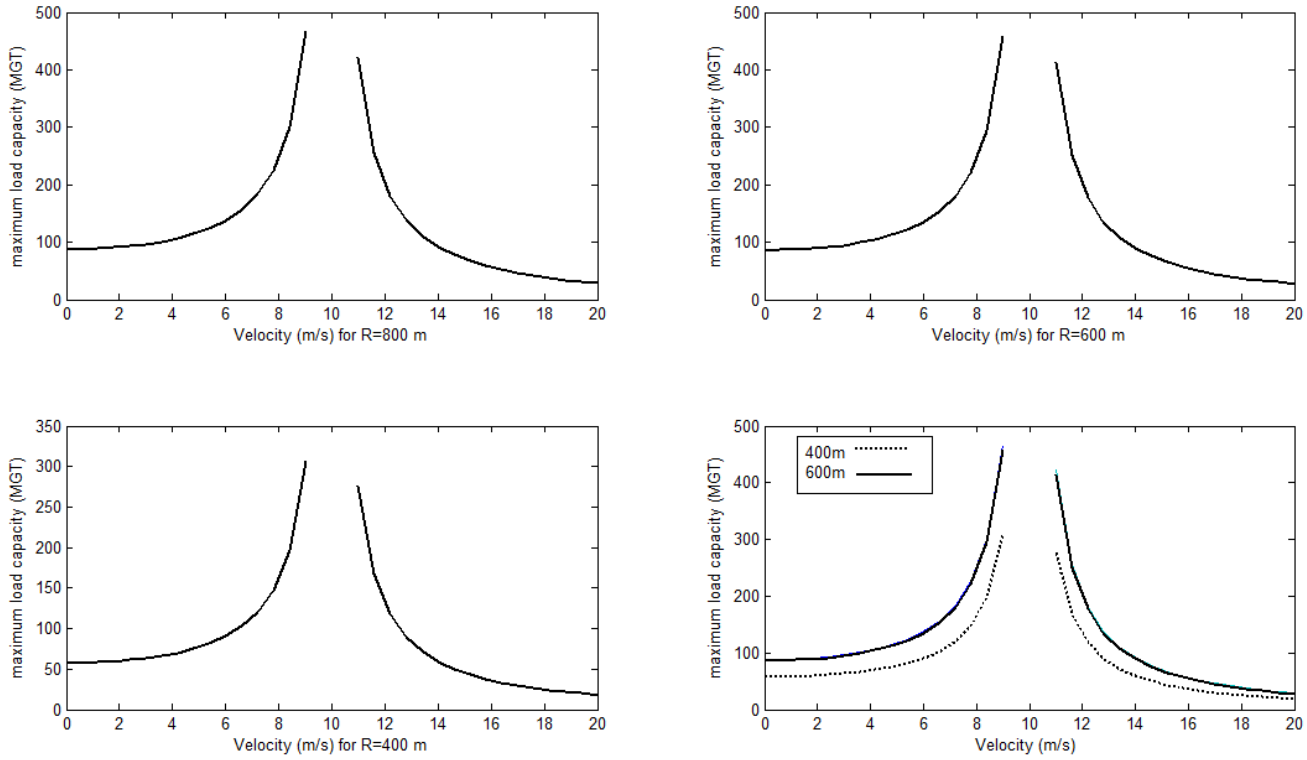

Figure 5.26: the Graph Shows Predicting the Maximum Tonnage of Rail Using both Side Cross-Sectional Area Loss's as Function of Velocity

5.2.2.5 Friction property as a Function of Superelvation Deficiency for Constant Radius track (600m)

From (**fig. 5.27**) the friction property at right rail with a function of superelvation deficiency at radius equals to 600 m. The friction force on the right rails increases.as the superelvation deficiency increases. There is a direct and a linear relationship between superelvation and friction at right rail. Similarly from (**fig. 5.28**) the friction property at left rail with a function of superelvation deficiency at radius equals to 600 m. The friction force on the left rail decreases as the superelvation deficiency increases thus implies friction property of left rail inversely proportional to superelvation deficiency.

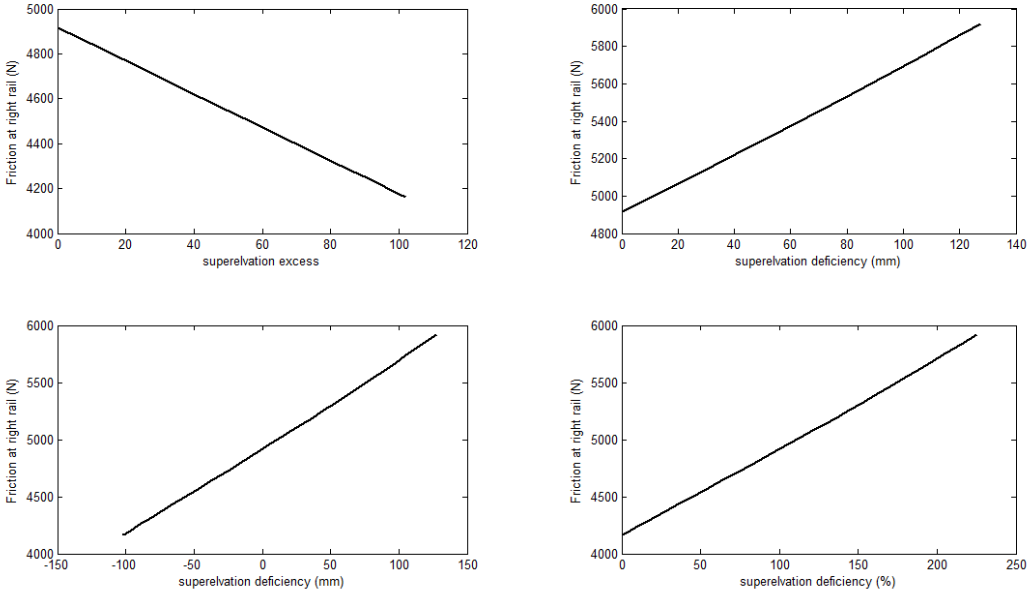

Figure 5.27: The Graph Shows the Influence of Superelvation Deficiency at Right Rail Friction

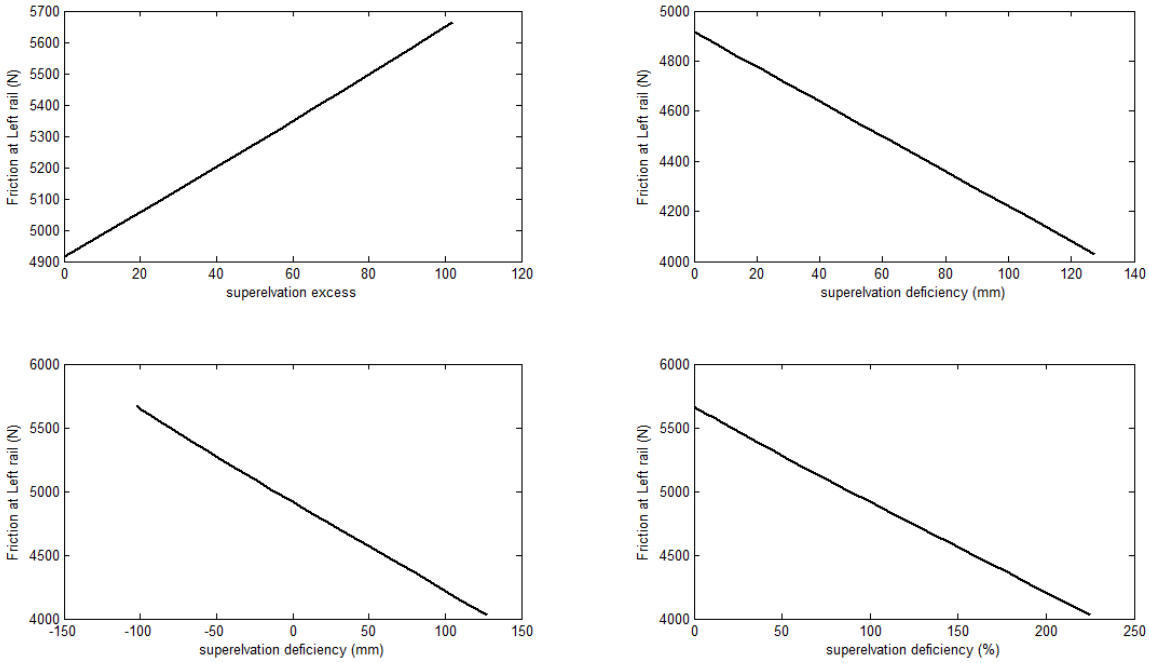

Figure 5.28: the Graph Shows the influence of Superelvation at Left Rail Friction

5.2.2.6 Wear property as a function of superelevation deficiency

From **fig.5.29** the cross-sectional area loss at right rail head with a function of superelvation deficiency at radius equals to 600 m. The wear at right rail head is higher at superelvation excess than superelvation deficiency. Wear on the right rail head increases as the superelvation deficiency increases. Right rail head exposed for series damage with higher superelevation deficiency. There is an interesting nature wear at right rail head is affected more in case of cant deficiency than cant

excess. From **fig.5 30** the cross-sectional area loss at left rail head with a function of superelvation deficiency at radius equals to 600 m. Similarly to the above of wear conditions of left rail head higher at left side rail flange contact than at right side to wheel flange contact which is a transitional point below equilibrium to above equilibrium velocity. It shows a great reduction on severity wear when the vehicle is moving with and above equilibrium speed. Wear on the left rail head decreases as the superelvation deficiency increases. The wear conditions of left rail have interesting behaviour for the vehicle is moving at speed below equilibrium at high superelevation excess the wear at left rail is minimum and increases to a certain value then decreases. From **fig. 5.31** below shows that cross-sectional area loss at side of right rail with a function of superelvation deficiency at radius equals to 600 m. The wear on the side of right rail increase as the superelvation deficiency increases. There is a direct and a linear relationship between superelvation and side wear of right rail. At and below balanced superelvation there is no side wear of right rail. From **fig.5. 32** shows that cross-sectional area loss at side of left rail with a function of superelvation deficiency at radius equals to 600 m. The wear on the left rail decreases as the superelvation deficiency increases (increases with excess of superelvation). The wear at left rail side is happened when only there is superelvation excess. There is an inversely proportionality between superelvation and wear at left rail.

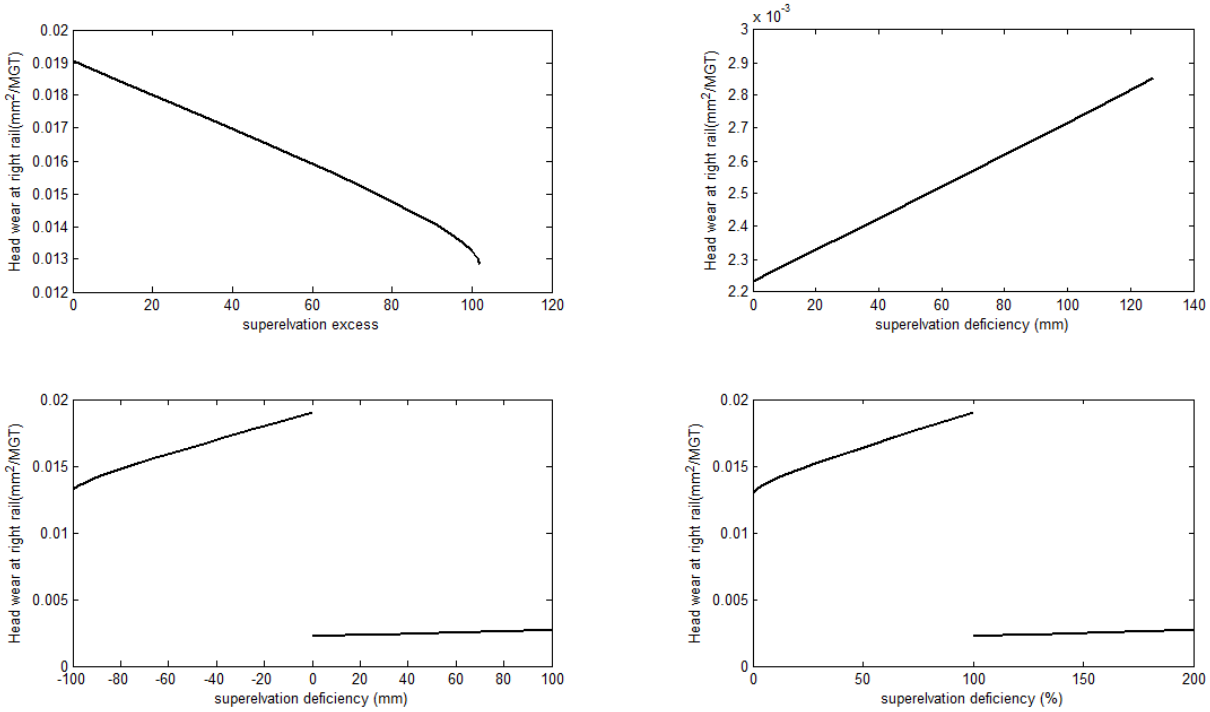

Figure 5.29: the Graph Shows Cross-Sectional Area Loss at Right Rail Head as a Function of Superelvation Deficiency

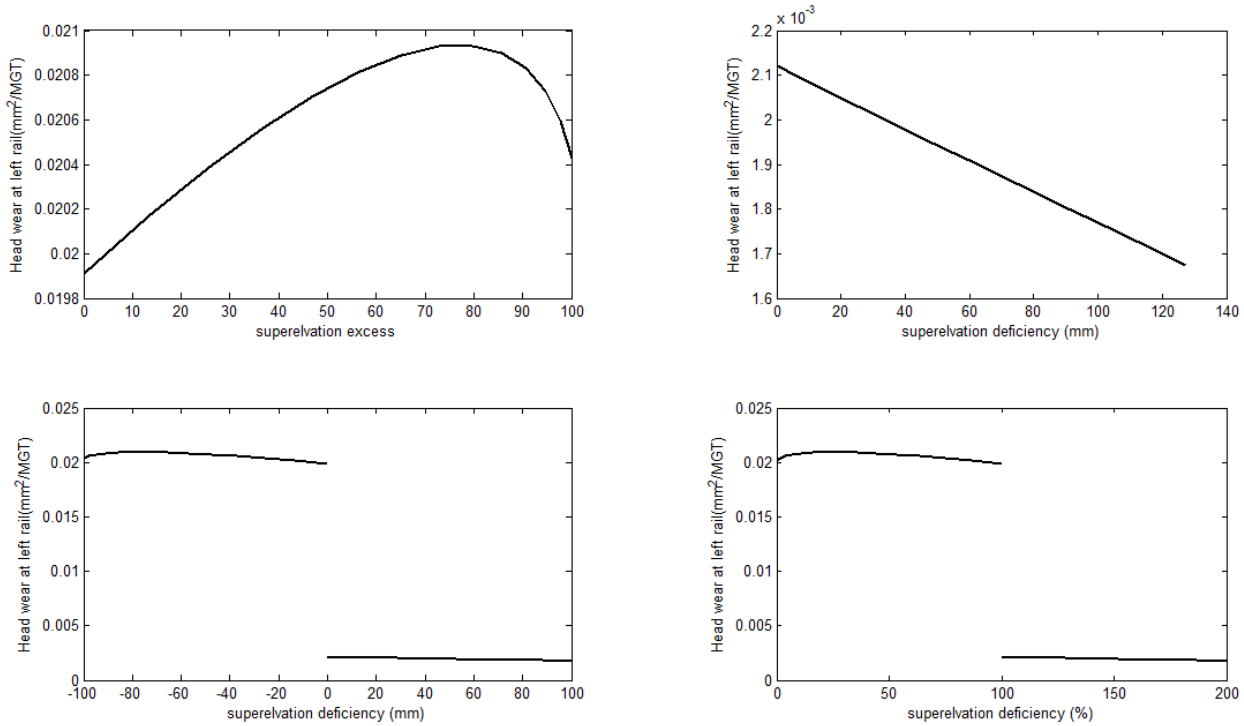

Figure 5.30: the Graph Shows Cross-Sectional Area Loss at Left Rail Head as a Function of Superelvation Deficiency

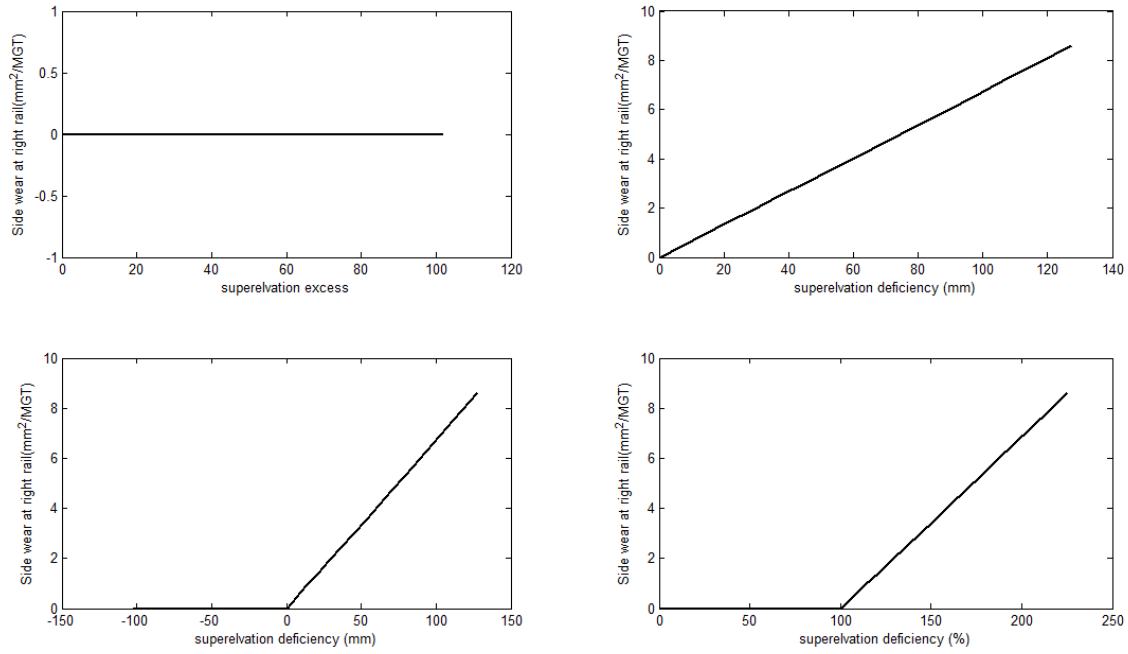

Figure 5.31: the Graph Shows Cross-Sectional Area Loss at Right Rail Side as a Function of Superelvation Deficiency

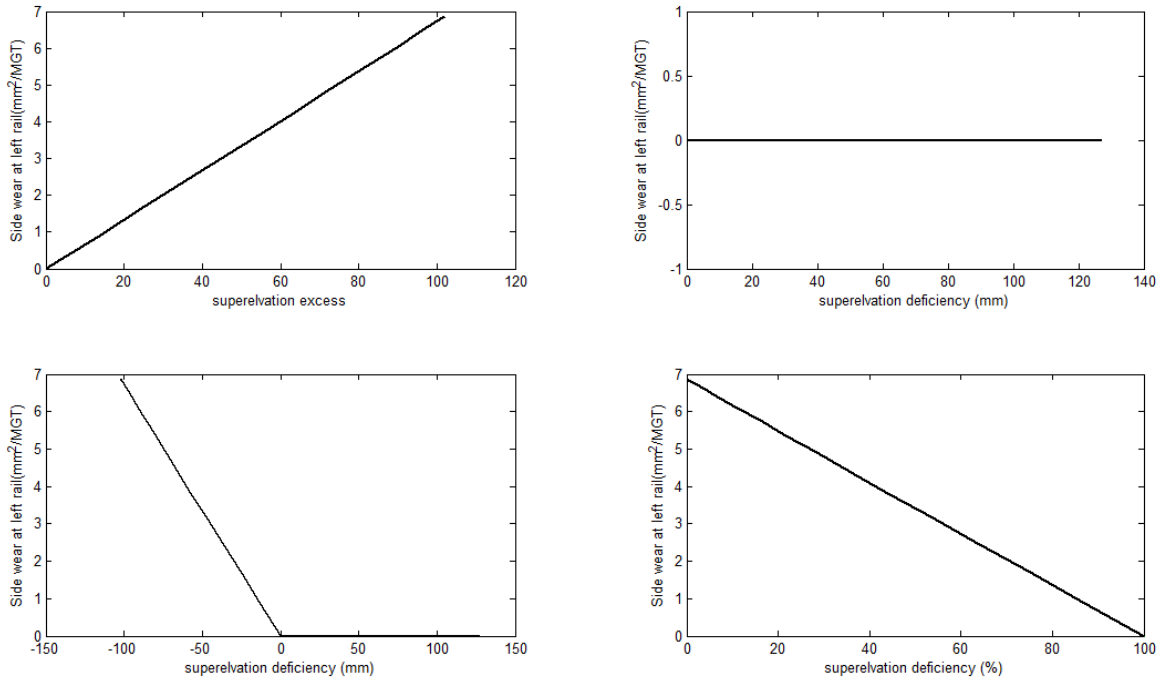

Figure 5.32: the Graph Shows Cross-Sectional Area Loss at Left Rail Side as a Function of Superelvation Deficiency

CHAPTER 6

6. CONCLUSION AND RECOMMENDATIONS

6.1 Conclusion

A major question of the study is how the velocity of the vehicle and the radius of the track are influencing the friction at contact and damaging due to wear at rail head and side during curve negotiation. These require understanding of mechanisms of kinematic motion on curved and generation of contact forces in between the wheel and the rail. The kinematic analysis deals with the differences in between the arc length of inner rail and outer rail which are supposed to be covered by the vehicle within the same time. The slip conditions on curved track is differed from tangent track due to centrifugal force. Analyzing curved track dynamic response for changing speed of the vehicle and radius of track using mathematical model requires assumptions. The dynamics in the vehicle to the rail was analyzed using a quasi-static approach which at instant time the vehicle is loaded vertically by its weight and laterally by centrifugal force. This lateral force behaves differently for horizontal curved track and canted curved track. On horizontal curved track the lateral force is only supported by small roll angle which is a factor of lateral displacement, conicity and gauge width and the direction is always horizontally towards outer rail. Whereas on the canted curved track the lateral centrifugal force is balanced by using centripetal force and its direction may be inwards and outwards depending on velocity and weight of the vehicle. It is applied on outer rails while the vehicle is moving above equilibrium speed and it is applied at the inner rail while the vehicle is moving below equilibrium speed. In case of horizontal curved track the only force which can resist lateral centrifugal force is the elevation difference at two rails which produced by the tapered wheels. The elliptical dimensions were interpolated using lateral displacement from known tabulated values. Friction and wear analysis uses the equations of slip and force which is found from a curved geometry and a vehicle speed. It uses different conditions for analysis of the friction and wear due to it depends on a large number of parameters such as: geometry of a track, vehicle speed, contamination properties, surface roughness, wheel and rail profiles, material properties and external load. It helps to obtain targeted results by avoiding other factors and to simplify the solution processes. The kinematic theoretical relations are formed from the differences in perimeter of the two rails. And dynamic analysis relates the geometric parameterizes with vehicle loads. Friction and wear are the effect of this dynamic interaction between wheel of the vehicle and the curved rail. All mechanisms of friction and wear modeled as adhesive mechanisms. Wear model uses Archard method and wear coefficients are found in literature for standard UIC 60 rail,

interpolating the values by using slip and contact pressures. The model integrates vehicle motions with rail geometrical parameters then it is used determine friction and wear conditions of the rail at each vehicle passing over the rail at different radius of the track. The result shows a very good agreement since wear of a rail associates with different factors the exact similarity to practical data is not expected. It is possible for predicting rail life and friction conditions of contact patch due to the differences made on curved geometry and the rule made for speed restrictions. The increase in radius of the rail has exponentially decrease the wear and friction conditions at constant velocity on horizontal curved track at both rail head, and the outer rail side is damaged severely as the forward velocity increases. The inner and outer rail friction and wear interchangeably increases as the vehicle speed is out of equilibrium velocity. The outer rail damages more than the inner rail when the vehicle is moving above equilibrium speed and the reverse happen when the vehicle moves below equilibrium speed. The superelvation deficiency is linearly proportional for right rail wear and inversely proportional for left rail. Generally knowing the effects of this parameter on overall system helps for understanding the mechanism and can be added for practical rail way design.

6.2 Recommendations

The rolling stock companies, rail road designer's and related business owners are recommended as follows:-

- Curved rail geometry requires more attention than that of tangent track due to an additional centrifugal force
- It is possible to obtain low friction using analyses of vehicle speed and geometry of a track.
- Severity of wear can be reduced using equilibrium speed of the vehicle.
- Interchanging of inner rail and outer rail can be considered as a means to lengthen the service life of the rail at horizontal curved track since the side wear is only occur at outer rail.
- Superelvation of the track is a mandatory for small radius curves to avoid excessive wear at high speeds.
- The rail life predictions on the curved track have to include the wear rate in addition to stress and fatigue.
- The driver must implement a vehicle speed restriction if otherwise that leads to excessive wear of the contacting surface and high friction.

6.3 Future Work

However, there are some good achievements were obtained, there are other works remaining which are equally influence wear and friction conditions rails like curve radius and speed of the vehicle. To obtain a complete, general generalization to the point of rail tribology the following works are remaining

- The influence of vertical curved geometry
- The influence of starting, braking and accelerating of a vehicle
- The influence of lubrication conditions on rail friction and wear properties.

References

1. Kumar, S. (2006). A Study of the Rail Degradation Process to Predict Rail Breaks. Lulea University of Technology Division of Operation and Maintenance Engineering. Lulea: Sweden.
2. Lewis, R., Dwyer-Joyce, R.S., Bruni, S., Ekberg, A., Cavalletti, M., Belknani, K. (nd).A New CAE Procedure for Railway Wheel Tribological Design. 14th International Wheelset Congress. USA.(White Rose Consortium ePrints Repository: (http://eprints.whiterose.ac.uk/archive/00000781/)
3. Swan, P. G. & Fitton, J. C.(2010).The South African Institute of Tribology SA Tribology Project 2010. South African Institute of Tribology. South Africa.
4. Fukagai, S., Ban, T., Namura, A., Ishida, M., Ogata, M., Aoki, F. &Arai T. (nd). Development of Friction Moderating System to Improve Wheel/Rail Interface in Sharp Curves. Railway Technical Research Institute. Tokyo, Japan.
5. Matsumoto, K., Tomeoka, M., Suda, Y, Nakai, T &Tanimoto, M. (nd).Development of Onboard Friction Control System for Tokyo Subway. Railway Technical Research Institute. Osaka, Japan.
6. Reddy, V. (2004). Modelling and Analysis of Rail Grinding & Lubrication strategies for controlling (RCF) and Rail Wear. Submitted for partial fulfillment of master of applied science. Queensland University.
7. Waara, P. (2001). Lubricant influence on flange wear in sharp railroad curves, Industrial lubrication and tribology, Vol 53, No. 4 pp 161-168.
8. Telliskivi, T., Olofsson, U., Sellgren U. & Kruse P. (nd).A tool and a method for FE analysis of wheel and rail interaction. Machine Elements, Department of Machine Design Royal Institute of Technology (KTH). Stockholm: Sweden
9. Lewis, R. and Olofsson, U. (2004). Mapping rail wear regimes and transitions. Wear, 257 (7-8). pp. 721-729]. Stockholm, Sweden.
10. Sadeghi J. & Akbari, B. (2006). Field investigation on effects of railway track geometric parameters on rail wear. Journal of Zhejiang University science. Iran
11. Olofsson, U. & Lewis, R. (nd). Tribology of wheel rail contact. Hand book of Railway vehicle Dynamics.
12. Evans J, & Iwnicki, S.D. (ND) Vehicle Dynamics and the Wheel/Rail. Rail Technology Unit, Manchester Metropolitan University, Department of Engineering & Technology. Manchester, United Kingdom. http://www.railtechnologyunit.com

13. Reddy, V. (2007). Development of An integrated model for assessment of operational risks in rail track. Submitted to Queensland University of technology for degree of Doctor of Philosophy. Queensland University of Technology.
14. Lindahl, M. (2001). A literature survey and simulation of dynamic vehicle response track geometry for high speed trains. Royal institute of Railway technology. Sweden
15. Popovici, R. (2010). Friction in wheel–Rail contacts. Ph.D. thesis, University of twente. Wohrmann printing service .Zutphen, Netherlands.
16. Jendel, T. (2002). Prediction of wheel profile wear—comparisons with field measurements. Division of Railway Technology, Department of Vehicle Engineering, Royal Institute of Technology (KTH), Teknikringen 8, 10044 Stockholm, Sweden Wear Volume 253, Issues 1–2, pp 89–99
17. Thompson, D.J., Monk-steel, A.D., & Jones, J.C. (2003). Railway noise curve squall Roughness Growth, Friction and wear. Prepared for the railway safety and standards board. The institute of sound and vibration Research. The University of Southampton.
18. Australian Rail track corporation LTD. (2006). Rail Defects Handbook Some Rail Defects, their Characteristics, Causes and Control. Engineering practice manual.
19. Innotrack (2009), the state of the art of the simulation of vehicle track interaction as a method for determining track degradation rates. Simulation of vehicle track interaction Part 2 .Project no. TIP5-CT-2006-031415
20. Johnson, D.M. (2006). Gauging Issues, by Taylor and Francis Group, LLC
21. http://en.wikipedia.org/Degree_of_curvature

APPENDIX

Appendix A: Definitions

Wear: damage to one or both surfaces, involving loss or displacement of material from a contacting surface.

Hardness of materials: - defined as the resistance to penetration of a material by an indenter.

Fatigue: - Most material will fracture when a small load is applied repeatedly.

Inertia force: a tendency of an object to continue its condition. If there changing direction the object tends to continue changing direction.

**Degree of the curve (D): ** the number of the angles subtended by 30.5 m chord of a curve.

Angle of attack: -angle between the wheel and the rail made by wheel to shift direction of movement.

Superelvation: the difference in elevation between the two edges of the track, allows vehicles travelling through the turn to go at higher speeds than would normally be possible.

Superelvation deficiency: - The difference in height between applied elevation and a higher equilibrium superelvation that the vehicle can travel with no lateral force and the angle called cant deficiency.

Superelvation excess: -The difference in height between applied elevation and a lower equilibrium superelvation that the vehicle can travel with no lateral force and the angle called cant excess.

Equilibrium superelvation (cant): - The track superelvation (cant) needed to neutralize the horizontal acceleration due to curving.

Horizontal plane: - Plane of earth horizon.

Tractive Effort: the force applied to the rail by the wheel of the train to cause movement

Derailment: - overturning of the vehicle

Quasi-static condition: Condition which is static under a certain period, here typically in a circular curve. The equations are formulated based on the assumptions of constant radius at constant velocity of the vehicle.

Equilibrium rolling line: the position where the rolling radius difference balances the difference in the lengths of the rails.

Centripetal force: a component of weight acting towards the lower rail when the vehicle moving on canted track.

Balancing speed; where the cant is exactly balances the lateral acceleration.

Adhesion: the grip or force of attachment, produced by friction between the wheels and rails. It is required to keep the wheels from slipping.

Inner rail: The rail closer to the center of track

Outer rail: rail farther away from the center of curve.

Creep: Creep forces are generated at the wheel/rail contact patch, by the much localized action of the wheel rolling on the rail.

Two-point contact; the situation (include contact between the wheel flange and rail gauge face in addition to the rolling contact at the rail head.

Sharp Curved track: the length of curve radius below 300m

Medium Curved track: the length of curve radius between 300 and 800m

Large Curved track: the length of curve radius above800m

MGT: the amount of traffic in terms of million gross tone mass flow over the rail annually

Appendix B: MAT LAB PROGRAM

```
%Horizontal curved track as a function of radius
yieldstrength=1350;G=70.9*10^9; sy=yieldstrength;
m=10000; %axle load 10 tone
g=9.81;%gravity
w=m*g/4;%weight per wheel
conicity=0.05;%conicity angle per radian
ro=0.460;%nominal radius of the wheel
L=0.750;% half of the gauge length
R=[500:100:1500];% where there is 5mm lateral displacement
lateralshift=(ro*L./(R*conicity))*1000;% lateral displacement
maxlateralshift=5;% before flange contact
y1=5;
if lateralshift<5;
   phi=asind(lateralshift.*conicity/(10^3*L));
else
   phi=asind(y1.*conicity/(10^3*L));
end
Veq=sqrt(R.* w.*(phi)./m);
vl1=1;% velocity in m/s
v2=5;% velocity in m/s
vr3=10;% velocity in m/s
%interpolating contact patch axis dimensions
y=[-5 -4 -3 -2 -1 0 1 2 3 4 5];
a1l=[6.5e-3 6.5e-3 6.5e-3 6.3e-3 6.0e-3 5.4e-3 7.8e-3 7.7e-3 7.6e-3 7.4e-3 7.1e-3];
```

```
b1l=[6.4e-3 6.4e-3 6.4e-3 7.1e-3 8.2e-3 10.7e-3 3.4e-3 3.5e-3 3.7e-3 4.1e-3 4.9e-3];

a1r=[7.1e-3 7.4e-3 7.6e-3 7.7e-3 7.8e-3 5.4e-3 6.0e-3 6.3e-3 6.5e-3 6.5e-3 6.5e-3];

b1r=[4.9e-3 4.1e-3 3.7e-3 3.5e-3 3.4e-3 10.7e-3 8.2e-3 7.1e-3 6.4e-3 6.4e-3 6.4e-3];

al1=interp1(-y,a1l,-1*y1,'linear');

al2=interp1(-y,a1l,-1*y1,'linear');

al3=interp1(-y,a1l,-1*y1,'linear');

bl1=interp1(-y,b1l,-1*y1,'linear');

bl2=interp1(-y,b1l,-1*y1,'linear');

bl3=interp1(-y,b1l,-1*y1,'linear');

ar1=interp1(y,a1r,y1,'linear');

ar2=interp1(y,a1r,y1,'linear');

ar3=interp1(y,a1r,y1,'linear');

br1=interp1(y,b1r,y1,'linear');

br2=interp1(y,b1r,y1,'linear');

br3=interp1(y,b1r,y1,'linear');

%%%%%%%%%%%%%%%%%%%%%

longslipright=abs(-L./R)+(conicity*lateralshift*10^-3/ro);%

longslipleft=abs((L./R)+(-conicity*lateralshift*10^-3/ro));%

%%%%%%%%%%%%%%%%%%%%%%%%%%%%%%%%%%%%%%%%%%%%%%%

attackang=acos(1-longslipleft);

lateralslip=attackang;

spin=sind(conicity)/ro;

% %%%%%%%%%%%%%%%%%%%%%%%%%%%%%%%%%%%%%%%%%

%forces

Fy1=m*vl1.^2./R;%lateral force at horizontal track
```

```
Fy2=m*v2.^2./R-w*sind(phi);%lateral force at horizontal track

Fy3=m*vr3.^2./R-w*sind(phi);%lateral force at horizontal track

Fz1=w*cosd(phi);%normal force at horizontal track

Fz2=w*cosd(phi);%normal force at horizontal track

Fz3=w*cosd(phi);%normal force at horizontal track

FAK1=0.5*Fz1-1.1*Fy1;%normal force at left rail

FAK2=0.5*Fz2-1.1*Fy2;%normal force at left rail

FAK3=0.5*Fz3-1.1*Fy3;%normal force at left rail

FBK1=0.5*Fz1+1.1*Fy1;% normal force at right rail

FBK2=0.5*Fz2+1.1*Fy2;% normal force at right rail

FBK3=0.5*Fz3+1.1*Fy3;% normal force at right rail

FBj1=Fy1;%right side force

FBj2=Fy2;%right side force

FBj3=Fy3;%right side force

FAj1=0;%there is no force towards left rail side

FAj2=0;%there is no force towards left rail side

FAj3=0;%there is no force towards left rail side

%%%%%%%%%%%%%%%%%%%%%%%%%%%%%%%%%%%%%%%%%%%%%

Plh1=FAK1./(pi.*al1.*bl1*10^6);

Prh1=FBK1./(pi.*ar1.*br1*10^6);

Prs1=FBj1./(0.85.*pi.*ar1.*br1*10^6);

Plh2=FAK2./(pi.*al2.*bl2*10^6);

Prh2=FBK2./(pi.*ar2.*br2*10^6);

Prs2=(FBj2)./(0.85.*pi.*ar2.*br2*10^6);

Plh3=FAK3./(pi.*al3.*bl3*10^6);
```

```
Prh3=FBK3./(pi.*ar3.*br3*10^6);

Prs3=(FBj3)./(0.85.*pi.*ar3.*br3*10^6);

%wears coefficients

v1slip=abs(vl1.*longslipright);%slip at v=1& for wear coefficients

v2slip=abs(v2.*longslipright);%slip at v=5& for wear coefficients

v3slip=abs(vr3.*longslipright);%slip at v=10& fo

v1slipl=abs(vl1.*longsliplеft);%slip at v=1& for wear coefficients

v2slipl=abs(v2.*longsliplеft);%slip at v=5& for wear coefficients

v3slipl=abs(vr3.*longsliplеft);%slip at v=10& for wear coefficients

sir1=v1slip;%right

sir2=v2slip;%right

sir3=v3slip;%right

rir1=Prh1./sy;

rir2=Prh2./sy;

rir3=Prh3./sy;

sil1=v1slipl;

sil2=v2slipl;

sil3=v3slipl;

ril1=Plh1./sy;

ril2=Plh2./sy;

ril3=Plh3./sy;

rrs1=Prs1./sy;

rrs2=Prs2./sy;

rrs3=Prs3./sy;

sideslip=1;
```

```
srs=sideslip;

%%%%%%%%%%%%%%%%%%%%%%%%%%%%%%%%%%%%%%%%%%

S=[0,0.2,0.21,0.7,0.71,1];

Kw=[1*10^-5,10* 10^-5,30* 10^-5,40* 10^-5,1*10^-4,10* 10^-5];

r=[0,0.8,1];

Ks=[1*10^-5,10* 10^-5,400*10^-5];

%%%%%%%%%%%%%%%%%%%%%%%%%%%%%%%%%%%%%%%%%%

Kr11=interp1(S,Kw,sir1,'linear');Kr12=interp1(r,Ks,rir1,'linear');

Kr21= interp1(S,Kw,sir2,'linear');Kr22=interp1(r,Ks,rir2,'linear');

Kr31= interp1(S,Kw,sir3,'linear');Kr32=interp1(r,Ks,rir3,'linear');

Kl11=interp1(S,Kw,sil1,'linear');Kl12=interp1(r,Ks,ril1,'linear');

Kl21=interp1(S,Kw,sil2,'linear');Kl22=interp1(r,Ks,ril2,'linear');

Kl31=interp1(S,Kw,sil3,'linear'); Kl32=interp1(r,Ks,ril3,'linear');

Ksr11=interp1(S,Kw,srs,'linear');Ksr12=interp1(r,Ks,rrs1,'linear');

Ksr21=interp1(S,Kw,srs,'linear');Ksr22=interp1(r,Ks,rrs2,'linear');

Ksr31=interp1(S,Kw,srs,'linear');Ksr32=interp1(r,Ks,rrs3,'linear');

% for right side using averages

Wearcoefficientsr1= (Ksr11+ Ksr12)./2;

Wearcoefficientsr2= (Ksr21+ Ksr22)./2;

Wearcoefficientsr3= (Ksr31+ Ksr32)./2;

Wearcoefficientr1= (Kr11+ Kr12)./2;

Wearcoefficientr2= (Kr21+ Kr22)./2;

Wearcoefficientr3= (Kr31+ Kr32)./2;

% for rail side at either side

Wearcoefficientl1=(Kl11+ Kl12)./2;
```

```
Wearcoefficientl2=(Kl21 +Kl22)./2;
Wearcoefficientl3=(Kl31+ Kl32)./2;
wearsright1=(FBj1).*(sideslip.*Wearcoefficientsr1)./(yieldstrength);
wearsright2=(FBj2).*(sideslip.*Wearcoefficientsr2)./(yieldstrength);
wearsright3=(FBj3).*(sideslip.*Wearcoefficientsr3)./(yieldstrength);
Rightwear1=longslipright.*(FBK1.*Wearcoefficientr1)./(yieldstrength);
Rightwear2=longslipright.*(FBK2.*Wearcoefficientr2)./(yieldstrength);
Rightwear3=longslipright.*(FBK3.*Wearcoefficientr3)./(yieldstrength);
Leftwear1=longslipright.*(FAK1.*Wearcoefficientl1)./(yieldstrength);
Leftwear2=longslipright.*(FAK2.*Wearcoefficientl2)./(yieldstrength);
Leftwear3=longslipright.*(FAK3.*Wearcoefficientl3)./(yieldstrength);
%%%%%%%%%%%%%%%%%%%%%%%%%%%%%%%%%%%%%%%%%%%%%
mu=0.4; %friction mu=0.4
FB1=sqrt((FBK1.^2)+(FBj1.^2));FB2=sqrt(FBK2.^2+FBj2.^2);FB3=sqrt(FBK3.^2+FBj3.^2);
FA1=sqrt((FAK1.^2));FA2=sqrt(FAK2.^2);FA3=sqrt(FAK3.^2);
ffA1=mu.*FA1;ffA2=mu.*FA2;ffA3=mu.*FA3;
ffB1=mu.*FB1;ffB2=mu.*FB2;ffB3=mu.*FB3;
%%%%%%%%%%%%%%%%%%%%%%%%%%%%%%%%%%%%%%%%%%%%
%assumptions equal amount of wear depth limits (11mm)
limitdepth=11;
depth1=0.75*wearsright1*10^5/(pi*2*br2*10^3);
depth2=0.75*wearsright2*10^5/(pi*2*br2*10^3);
depth3=0.75*wearsright3*10^5/(pi*2*br3*10^3);
%%%%%%%%%%%%%%%%%%%%%%%%%%%%%%%%%%%%%%%%%%%%
%Horizontal curved track as a function of vehicle speed
```

```
%%%%%%%%%%%%%%%%%%%%%%%%%%%%%%%%%%%%

% graph shows cross-sectional area loss as a function of speed of the vehicle...

% in different radius of a track at rail side on horizontal curved track

v=linspace(5,20,20);

yieldstrength=1350;

sy=yieldstrength;

m=10000;

g=9.81;

w=m*g/4;

conicity=0.05;

ro=0.460;

L=0.750;

R1=900;

R2=1100;

R3=1300;

lateralshift1=(ro*L./(R1*conicity))*1000;

lateralshift2=(ro*L./(R2*conicity))*1000;

lateralshift3=(ro*L./(R3*conicity))*1000;

if lateralshift1<=5

   y1=lateralshift1;

else

   y1=5;

end

if lateralshift2<5

   y2=lateralshift2;
```

```
else
    y2=5;
end
if lateralshift3<5
    y3=lateralshift3;
else
    y3=5;
end
phi1=y1*conicity/(10^3*L);
phi2=y2*conicity/(10^3*L);
phi3=y3*conicity/(10^3*L);
Veq1=sqrt(R1*w*sind(phi1)./m);
Veq2=sqrt(R2*w*sind(phi2)./m);
Veq3=sqrt(R3*w*sind(phi3)./m);
%interpolating contact patch axis dimensions
y=[-5 -4 -3 -2 -1 0 1 2 3 4 5];
a1l=[6.5e-3 6.5e-3 6.5e-3 6.3e-3 6.0e-3 5.4e-3 7.8e-3 7.7e-3 7.6e-3 7.4e-3 7.1e-3];
b1l=[6.4e-3 6.4e-3 6.4e-3 7.1e-3 8.2e-3 10.7e-3 3.4e-3 3.5e-3 3.7e-3 4.1e-3 4.9e-3];
a1r=[7.1e-3 7.4e-3 7.6e-3 7.7e-3 7.8e-3 5.4e-3 6.0e-3 6.3e-3 6.5e-3 6.5e-3 6.5e-3];
b1r=[4.9e-3 4.1e-3 3.7e-3 3.5e-3 3.4e-3 10.7e-3 8.2e-3 7.1e-3 6.4e-3 6.4e-3 6.4e-3];
al1=interp1(-y,a1l,-1*y1,'linear');
al2=interp1(-y,a1l,-1*y2,'linear');
al3=interp1(-y,a1l,-1*y3,'linear');
bl1=interp1(-y,b1l,-1*y1,'linear');
bl2=interp1(-y,b1l,-1*y2,'linear');
```

```
bl3=interp1(-y,b1l,-1*y3,'linear');
ar1=interp1(y,a1r,y1,'linear');
ar2=interp1(y,a1r,y2,'linear');
ar3=interp1(y,a1r,y3,'linear');
br1=interp1(y,b1r,y1,'linear');
br2=interp1(y,b1r,y2,'linear');
br3=interp1(y,b1r,y3,'linear');
%%%%%%%%%%%%%%%%%%%%
longslipright1=(-L./R1)+(-conicity* lateralshift1*10^-3/ro);%
longslipright2=(-L./R2)+(-conicity* lateralshift2*10^-3/ro);%
longslipright3=(-L./R3)+(-conicity* lateralshift3*10^-3/ro);%
longslipleft1=(L./R1)+(conicity* lateralshift1*10^-3/ro);%
longslipleft2=(L./R2)+(conicity* lateralshift2*10^-3/ro);%
longslipleft3=(L./R3)+(conicity* lateralshift3*10^-3/ro);%
%%%%%%%%%%%%%%%%%%%%%%555
attackang1=acos(1- longslipright1);
attackang2=acos(1- longslipright2);
attackang3=acos(1- longslipright3);
lateralslip1= attackang1;
lateralslip2= attackang2;
lateralslip3= attackang3;
spin=sind(conicity)/ro;% spin due to conicity
%Forces
Fy1=m*v.^2./R1-w*(phi1);
Fy2=m*v.^2./R2-w*(phi2);
```

```
Fy3=m*v.^2./R3-w*(phi3);

Fz1= w*cosd(phi1);

Fz2 =w*cosd(phi1);

Fz3 =w*cosd(phi1);

%normal load (vector sum of gravity and centrifugal load)

FAK1=0.5*Fz1-1.1*Fy1;%normal force at left rail

FAK2=0.5*Fz2-1.1*Fy2;%normal force at left rail

FAK3=0.5*Fz3-1.1*Fy3;%normal force at left rail

FBK1=0.5*Fz1+1.1*Fy1;% normal force at right rail

FBK2=0.5*Fz2+1.1*Fy2;% normal force at right rail

FBK3=0.5*Fz3+1.1*Fy3;% normal force at right rail

FBj1=Fy1;

FBj2=Fy2;

FBj3=Fy3;

FAj1=Fy1-Fy1;

FAj2=Fy2-Fy1;

FAj3=Fy3-Fy1;

a=atand(Fy1./Fz2);% contact angle

spinl=sind(a)/ro;% spin due to flange contact

spinr=sind(a)/ro;% spin due to  flange contact

%contact pressure

Plh1=FAK1./(pi.*al1.*bl1*10^6);

Prh1=FBK1./(pi.*ar1.*br1*10^6);

Prs1=(FBj1)./(0.85.*pi.*ar1.*br1*10^6);

Plh2=FAK2./(pi.*al2.*bl2*10^6);
```

```
Prh2=FBK2./(pi.*ar2.*br2*10^6);

Prs2=(FBj2)./(0.85.*pi.*ar2.*br2*10^6);

Plh3=FAK3./(pi.*al3.*bl3*10^6);

Prh3=FBK3./(pi.*ar3.*br3*10^6);

Prs3=(FBj3)./(0.85.*pi.*ar3.*br3*10^6);

%wears coefficients

sir1=v.*abs(longslipright1);

sir2=v.*abs(longslipright2);

sir3=v.*abs(longslipright3);

rir1=Prh1./sy;

rir2=Prh2./sy;

rir3=Prh3./sy;

sil1= v.*abs(longslipleft1);

sil2= v.*abs(longslipleft2);

sil3= v.*abs(longslipleft3);

srs=1;

%ratio b/n pressure to strength

ril1=Plh1./sy;

ril2=Plh2./sy;

ril3=Plh3./sy;

rrs1=Prs1./sy;

rrs2=Prs2./sy;

rrs3=Prs3./sy;

%%%%%%%%%%%%%%%%%%%%%%%%%%%%%%%%%%%%%%%%%%%%%

S=[0,0.2,0.21,0.7,0.71,1];
```

```
Kw=[1*10^-5,10* 10^-5,40* 10^-5,40* 10^-5,1*10^-5,10* 10^-5];

r=[0,0.8,1];

Ks=[1*10^-5,10*10^-5,400*10^-5];

%%%%%%%%%%%%%%%%%%%%%%%%%%%%%%%%%%%%%%%%%%%%%%%

%right head

Kr11=interp1(S,Kw,sir1,'linear');Kr12=interp1(r,Ks,rir1,'linear');

Kr21=interp1(S,Kw,sir2,'linear');Kr22=interp1(r,Ks,rir2,'linear');

Kr31=interp1(S,Kw,sir3,'linear');Kr32=interp1(r,Ks,rir3,'linear');

%left railhead coefficients

Kl11=interp1(S,Kw,sil1,'linear'); Kl12=interp1(r,Ks,ril1,'linear');

Kl21=interp1(S,Kw,sil2,'linear');Kl22=interp1(r,Ks,ril2,'linear');

Kl31=interp1(S,Kw,sil3,'linear');Kl32=interp1(r,Ks,ril3,'linear');

%right-side wear coefficients

Ksr11=interp1(S,Kw,srs,'linear');Ksr12=interp1(r,Ks,rrs1,'linear');

Ksr211=interp1(S,Kw,srs,'linear');Ksr222=interp1(r,Ks,rrs2,'linear');

Ksr311=interp1(S,Kw,srs,'linear');Ksr332=interp1(r,Ks,rrs3,'linear');

%%%%%%%%%%%%%%%%%%%%%%%%%%%%%%%%%%%%%%%%%%%%%%%

Wearcoefficientl1=(Kl11+Kl12)./2;%mean values of k from pressure and slip interpolate

Wearcoefficientl2=(Kl21+Kl22)./2; %mean values of k from pressure and slip

Wearcoefficientl3=(Kl31+Kl32)./2; %mean values of k from pressure and slip

Wearcoefficientr1=(Kr11+Kr12)./2; %mean values of k from pressure and slip

Wearcoefficientr2=(Kr21+Kr22)./2; %mean values of k from pressure and slip

Wearcoefficientr3=(Kr31+Kr32)./2; %mean values of k from pressure and slip

Wearcoefficientsr1=(Ksr11+Ksr12)./2; %mean values of k from pressure and slip

Wearcoefficientsr2=(Ksr211+Ksr222)./2; %mean values of k from pressure and slip
```

```
Wearcoefficientsr3=(Ksr311+Ksr332)./2; %mean values of k from pressure and slip
yieldstrength=sy;
sideslip=1;
%%%%%%%%%%%%%%%%%%%%%%%%%%%%%%%%%
wearsright1=abs(FBj1).*(sideslip.*Wearcoefficientsr1)./(yieldstrength);
wearsright2=abs(FBj2).*(sideslip.*Wearcoefficientsr2)./(yieldstrength);
wearsright3=abs(FBj3).*(sideslip.*Wearcoefficientsr3)./(yieldstrength);
Rightwear1=abs(longslipright1).*(FBK1.*Wearcoefficientr1)./(yieldstrength);
Rightwear2=abs(longslipright2).*(FBK2.*Wearcoefficientr2)./(yieldstrength);
Rightwear3=abs(longslipright3).*(FBK3.*Wearcoefficientr3)./(yieldstrength);
Leftwear1=abs(longslipleft1).*(FAK1.*Wearcoefficientl1)./(yieldstrength);
Leftwear2=abs(longslipleft2).*(FAK2.*Wearcoefficientl2)./(yieldstrength);
Leftwear3=abs(longslipleft3).*(FAK3.*Wearcoefficientl3)./(yieldstrength);
%%%%%%%%%%%%%%%%%%%%%%%%%%%%%%%%
%friction mu=0.4,
mu=0.4;
FB1=sqrt((FBK1.^2)+(FBj1.^2));FB2=sqrt(FBK2.^2+FBj2.^2);FB3=sqrt(FBK3.^2+FBj3.^2);
FA1=sqrt((FAK1.^2)+(FAj1.^2));FA2=sqrt(FAK2.^2+FAj2.^2);FA3=sqrt(FAK3.^2+FAj3.^2);
ffA1=mu.*FA1;ffA2=mu.*FA2;ffA3=mu.*FA3;
ffB1=mu.*FB1;ffB2=mu.*FB2;ffB3=mu.*FB3;
%%%%%%%%%%%%%%%%%%%%%%%%%%%%%%%%%%%%%
%assumptions wear depth limits (11mm)
limitdepth=11;
depth1=0.75*wearsright1*10^5/(pi*2*br2*10^3);
depth2=0.75*wearsright2*10^5/(pi*2*br2*10^3);
```

```
depth3=0.75*wearsright3*10^5/(pi*2*br3*10^3);

%%%%%%%%%%%%%%%%%%%%%%%%%%%%%%%%%%%%%%%%

% Canted curved rail as a function of radius

% As function of radius in canted track

R=linspace(150,690,10);

yieldstrength=1350;

sy=yieldstrength;

%vehicle loads

m=10000;

g=9.81;

w=m*g/4;% axle load

%wheelset dimensions

conicity=0.05;%wheel conicity(rad)

ro=0.460;%nominal wheel radius(m)

L=0.750;% half of the distance b/n the center of rails (m)

% canted track properties

conicity=0.05;

r=0.460;

L=0.750;

veq=10;

vl1=5;v2=10;vr3=15;

cant=atand(m*veq^2./(w.*R));

yl1=0;y2=10;yr3=10;

lateralshift1=yl1;

lateralshift2=y2;
```

```
lateralshift3=yr3;

%interpolating contact patch axis dimensions

c=[0 1 2 3 4 5 6 7 8 9 10];

f=[-10,-9,-8,-7,-6,-5,-4,-3,-2,-1,0];

a2l=[6.5e-3 6.5e-3 6.5e-3 6.3e-3 6.0e-3 5.4e-3 7.8e-3 7.7e-3 7.6e-3 7.4e-3 7.1e-3];

b2l=[6.4e-3 6.4e-3 6.4e-3 7.1e-3 8.2e-3 10.7e-3 3.4e-3 3.5e-3 3.7e-3 4.1e-3 4.9e-3];

a2r=[6.5e-3 6.5e-3 6.5e-3 6.3e-3 6.0e-3 5.4e-3 7.8e-3 7.7e-3 7.6e-3 7.4e-3 7.1e-3];

b2r=[6.4e-3 6.4e-3 6.4e-3 7.1e-3 8.2e-3 10.7e-3 3.4e-3 3.5e-3 3.7e-3 4.1e-3 4.9e-3];

al1=interp1(f,a2l,-yl1,'linear');al2=interp1(f,a2l,-y2,'linear');al3=interp1(f,a2l,-yr3,'linear');

bl1=interp1(f,b2l,-yl1,'linear');bl2=interp1(f,b2l,-y2,'linear');bl3=interp1(f,b2l,-yr3,'linear');

ar1=interp1(c,a2r,yl1,'linear');ar2=interp1(c,a2r,y2,'linear');ar3=interp1(c,a2r,yr3,'linear');

br1=interp1(c,b2r,yl1,'linear');br2=interp1(c,b2r,y2,'linear');br3=interp1(c,b2r,yr3,'linear');

%%%%%%%%%%%%%%%%%%%%%%%%%%%%%%%%%%%%%%%%%%%%%%

longsliprightl =(-L./R)+(-conicity* lateralshift1*10^-3 /ro);

longslipright =(-L./R)+(-conicity* lateralshift2*10^-3 /ro);

longsliprightr =(-L./R)+(-conicity* lateralshift3*10^-3 /ro);

longslipleftl=(L./R)+(conicity* lateralshift1*10^-3 /ro);

longslipleft=(L./R)+(conicity* lateralshift2*10^-3 /ro);

longslipleftr =(L./R)+(conicity* lateralshift3*10^-3 /ro);

attackangl =acos(1- longslipleftl);

attackang =acos(1- longslipleft);

attackangr=acos(1- longslipleftr);

lateralslipl= attackangl;

lateralslip= attackang;

lateralslipr= attackangr;
```

```
spin=sind(conicity)/ro;% spin due to conicity
%Forces
Fyl1=(m*vl1.^2.*cosd(cant)./(R))-(w.*sind(cant));
Fy2=(m*v2.^2.*cosd(cant)./(R))-(w.*sind(cant));
Fyr3=((m*vr3.^2.*cosd(cant)./(R))-(w.*sind(cant)));
%%%%%%%%%%%%%%%%%%%%%%%%%%%%%%%%%%%%%%%%%%%%%%%%%%%%%%%%
Fz1=(m*vl1.^2.*sind(cant)./(R))+(w.*cosd(cant));
Fz2=(m*v2.^2.*sind(cant)./(R))+(w.*cosd(cant));
Fz3=(m*vr3.^2.*sind(cant)./(R))+(w.*cosd(cant));
Fzl1=(m*vl1.^2.*sind(cant)./(R))+(w.*cosd(cant));
Fz2=(m*v2.^2.*sind(cant)./(R))+(w.*cosd(cant));
Fzr3=(m*vr3.^2.*sind(cant)./(R))+(w.*cosd(cant));
%%%%%%%%%%%%%%%%%%%%%%%%%%%%%%%%%%%%%%%%%%%%%%%%%%%%%%%%
FAK1=0.5.*Fz1-1.1.*Fyl1;
FAK2=0.5.*Fz2-1.1.*Fy2;
FAK3=0.5.*Fz3-1.1.*Fyr3;
FBK1=0.5.*Fz1+1.1.*Fyl1;
FBK2=0.5.*Fz2+1.1.*Fy2;
FBK3=0.5.*Fz3+1.1.*Fyr3;
FAJ1=-Fyl1;
FAJ2=Fy2-Fy2;
FAj2=FAJ2;
FAj1=FAJ1;
FAJ3=Fyr3-Fyr3;
FAj3=FAJ3;
```

```
FBj1=Fyl1-Fyl1;

FBj2=Fy2-Fy2;

FBj3=Fyr3;

% normal forces at v=5m/s

FBkl=FBK1;

FBJl=FBj1;

FAkl=FAK1;

FAJl=Fyl1-Fyl1;

FBl=sqrt((FBkl.^2)+(FBJl.^2));

FAl=sqrt((FAkl.^2)+(FAJl.^2));

% normal forces at v=10m/s

FBk2=FBK2;

FAk2=FAK2;

FAJ2=Fy2-Fy2;

FBJ2=Fy2-Fy2;

FB2=sqrt((FBk2.^2)+(FBJ2.^2));

FA2=sqrt((FAk2.^2)+(FAJ2.^2));

% normal forces at v=15m/s

FBk3=FBK3;

FBJ3=Fyr3;

FAk3=FAK3;

FAJ3=0;

FB3=sqrt(FBk3.^2+FBJ3.^2);

FA3=sqrt(FAk3.^2+FAJ3.^2);

%contact pressure
```

```
Plh1=FAK1./(pi.*al1.*bl1*10^6);

Plh2=FAK2./(pi.*al2.*bl2*10^6);

Plh3=FAK3./(pi.*al3.*bl3*10^6);

Prh1=FBK1./(pi.*ar1.*br1*10^6);

Prh2=FBK2./(pi.*ar2.*br2*10^6);

Prh3=FBK3./(pi.*ar3.*br3*10^6);

Prs1=(FBj1)./(0.85.*pi.*ar1.*br1*10^6);

Prs2=(FBj2)./(0.85.*pi.*ar2.*br2*10^6);

Prs3=(FBj3)./(0.85.*pi.*ar3.*br3*10^6);

Pls1=abs(FAj1)./(0.85.*pi.*al1.*bl1*10^6);

Pls2=abs(FAj2)./(0.85.*pi.*al2.*bl2*10^6);

Pls3=abs(FAj3)./(0.85.*pi.*al3.*bl3*10^6);

%wears coefficients

sir1= vl1.*longslipleftl;

sir2= v2.*longslipleft;

sir3= vr3.*longslipleftr;

rir1=Prh1./sy;

rir2=Prh2./sy;

rir3=Prh3./sy;

sil1= vl1.*abs(longslipleftl);

sil2= v2.*abs(longslipleft);

sil3= vr3.*abs(longslipleftr);

ril1=Plh1./sy;

ril2=Plh2./sy;

ril3=Plh3./sy;
```

```
rrs1=Prs1./sy;

rrs2=Prs2./sy;

rrs3=Prs3./sy;

sideslip=1;

sls=sideslip;

srs=sideslip;

rls1=Pls1./sy;

rls2=Pls2./sy;

rls3=Pls3./sy;

%%%%%%%%%%%%%%%%%%%%%%%%%%%%%%%%%%%%%%%%%%%%%%%%%%%%

S=[0,0.2,0.21,0.7,0.71,1];

Kw=[1*10^-5,10* 10^-5,30* 10^-5,40* 10^-5,1*10^-5,10* 10^-5];

r=[0,0.8,1];

Ks=[1*10^-5,10*10^-5,400*10^-5];

%%%%%%%%%%%%%%%%%%%%%%%%%%%%%%%%%%%%%%%%%%%%%%%%%%%%%

Kr11=interp1(S,Kw,sir1,'linear');Kr12=interp1(r,Ks,rir1,'linear');

Kr21= interp1(S,Kw,sir2,'linear');Kr22=interp1(r,Ks,rir2,'linear');

Kr31= interp1(S,Kw,sir3,'linear');Kr32=interp1(r,Ks,rir3,'linear');

Kl11=interp1(S,Kw,sil1,'linear');Kl12=interp1(r,Ks,ril1,'linear');

Kl21=interp1(S,Kw,sil2,'linear');Kl22=interp1(r,Ks,ril2,'linear');

Kl31=interp1(r,Ks,sil3,'linear'); Kl32=interp1(r,Ks,ril3,'linear');

Ksr11=interp1(S,Kw,srs,'linear');Ksr12=interp1(r,Ks,rrs1,'linear');

Ksr21=interp1(S,Kw,srs,'linear');Ksr22=interp1(r,Ks,rrs2,'linear');

Ksr31=interp1(S,Kw,srs,'linear');Ksr32=interp1(r,Ks,rrs3,'linear');

Ksl11=interp1(S,Kw,sls,'linear');Ksl12=interp1(r,Ks,rls1,'linear');
```

```
Ksl21=interp1(S,Kw,sls,'linear');Ksl22=interp1(r,Ks,rls2,'linear');

Ksl31=interp1(S,Kw,sls,'linear');Ksl32=interp1(r,Ks,rls3,'linear');

% for right side

Wearcoefficientsr1=(Ksr11+ Ksr12)./2;

Wearcoefficientsr2=(Ksr21+ Ksr22)./2;

Wearcoefficientsr3=(Ksr31+ Ksr32)./2;

% for left side

Wearcoefficientsl1=(Ksl11+ Ksl12)./2;

Wearcoefficientsl2=(Ksl21+ Ksl22)./2;

Wearcoefficientsl3=(Ksl31+ Ksl32)./2;

% for rail side at either side

Wearcoefficientr1= (Kr11+ Kr12)./2;

Wearcoefficientr2= (Kr21+ Kr22)./2;

Wearcoefficientr3= (Kr31+ Kr32)./2;

% for rail side at either side

Wearcoefficientl1=(Kl11+Kl12)./2;

Wearcoefficientl2=(Kl21+Kl22)./2;

Wearcoefficientl3=(Kl31+Kl32)./2;

wearsright1=abs(FBj1).*(sideslip.*Wearcoefficientsr1)./(yieldstrength);

wearsright2=abs(FBj2).*(sideslip.*Wearcoefficientsr2)./(yieldstrength);

wearsright3=abs(FBj3).*(sideslip.*Wearcoefficientsr3)./(yieldstrength);

wearsleft1=(FAJ1).*(sideslip.*Wearcoefficientsl1)./(yieldstrength);

wearsleft2=abs(FAJ2).*(sideslip.*Wearcoefficientsl2)./(yieldstrength);

wearsleft3=abs(FAJ3).*(sideslip.*Wearcoefficientsl3)./(yieldstrength);

Rightwear1=abs(longslipright).*(FBK1.*Wearcoefficientr1)./(yieldstrength);
```

```
Rightwear2=abs(longslipright).*(FBK2.*Wearcoefficientr2)./(yieldstrength);

Rightwear3=abs(longslipright).*(FBK3.*Wearcoefficientr3)./(yieldstrength);

Leftwear1=abs(longslipleft).*(FAK1.*Wearcoefficientl1)./(yieldstrength);

Leftwear2=abs(longslipleft).*(FAK2.*Wearcoefficientl2)./(yieldstrength);

Leftwear3=abs(longslipleft).*(FAK3.*Wearcoefficientl3)./(yieldstrength);

%%%%%%%%%%%%%%%%%%%%%%%%%%%%%%%%%%%%%%%%%%%%%%%%%%

mu=0.4;%wear coefficients

FB1=sqrt((FBkl.^2)+(FBJl.^2));FB2=sqrt((FBk2.^2)+(FBJ2.^2));FB3=sqrt(FBk3.^2+FBJ3.^2);

FA1=sqrt((FAkl.^2)+(FAJl.^2));FA2=sqrt((FAk2.^2)+(FAJ2.^2));FA3=sqrt(FAk3.^2+FAJ3.^2);

ffA1=mu.*FA1;ffA2=mu.*FA2;ffA3=mu.*FA3;

ffB1=mu.*FB1;ffB2=mu.*FB2;ffB3=mu.*FB3;

%%%%%%%%%%%%%%%%%%%%%%%%%%%%%%%%%%%%%%%%%%%%%%%%%

ffA1=mu.*FA1;ffA2=mu.*FA2;ffA3=mu.*FA3;

ffB1=mu.*FB1;ffB2=mu.*FB2;ffB3=mu.*FB3;

%%%%%%%%%%%%%%%%%%%%%%%%%%%%%%%%%%%%%%%%%%%%%%%%%

limitdepth=11;

depth1=0.75*wearsleft1*10^5/(pi*2*bl1*10^3);

depthF=0.75*Rightwear2*10^5/(pi*2*bl1*10^3);

depth5=0.75*wearsright3*10^5/(pi*2*br2*10^3);

%%%%%%%%%%%%%%%%%%%%%%%%%%%%%%%%%%%%%%%%%%%%%%%%%

%Canted curved rail as a function of vehicle speed

% effects of speed with in different curve radius canted rail

vl=linspace(0,9,16);%speed of the vehicle below equilibrium(m/s)

vr=linspace(11,20,16);%speed above equilibrium(m/s)

yieldstrength=1350;
```

```
sy=yieldstrength;
%vehicle loads
m =10000;
g=9.81;
w=m*g/4;
conicity=0.05;
ro=0.460;%nominal wheel radius(m)
L=0.750;% half of the distance b/n the center of rails (m)
% canted track (3 deg.), 350m (5 deg.), (7 deg.)
R1=800;
R2=600;
R3=400;
veq=10;%equilibrium velocity of the vehicle (m/s)
cant1=atand(m*veq^2/(w*R1));%cant angle radius
cant2=atand(m*veq^2/(w*R2));
cant3=atand(m*veq^2/(w*R3));
yc1=0;yc2=10;yc3=10;% wheelset lateral displacement (mm)
lateralshift1= yc1;%(ro*L./(R1*conicity))*1000*cosd(cant1);
lateralshift2= yc2;%(ro*L./(R2*conicity))*1000*cosd(cant2);
lateralshift3= yc3;%(ro*L./(R3*conicity))*1000*cosd(cant3);
%interpolating contact patch axis dimensions
c=[0 1 2 3 4 5 6 7 8 9 10]; %known lateral shift from the inner most of the left rail
f=[-10,-9,-8,-7,-6,-5,-4,-3,-2,-1,0];% it uses to relate left side positions with right sides
a2l=[6.5e-3 6.5e-3 6.5e-3 6.3e-3 6.0e-3 5.4e-3 7.8e-3 7.7e-3 7.6e-3 7.4e-3 7.1e-3];
b2l=[6.4e-3 6.4e-3 6.4e-3 7.1e-3 8.2e-3 10.7e-3 3.4e-3 3.5e-3 3.7e-3 4.1e-3 4.9e-3];
```

```
a2r=[6.5e-3 6.5e-3 6.5e-3 6.3e-3 6.0e-3 5.4e-3 7.8e-3 7.7e-3 7.6e-3 7.4e-3 7.1e-3];
b2r=[6.4e-3 6.4e-3 6.4e-3 7.1e-3 8.2e-3 10.7e-3 3.4e-3 3.5e-3 3.7e-3 4.1e-3 4.9e-3];
al1=interp1(f,a2l,-yc1,'linear');al2=interp1(f,a2l,-yc2,'linear');al3=interp1(f,a2l,-
yc3,'linear');%horizontal left rail
bl1=interp1(f,b2l,-yc1,'linear');bl2=interp1(f,b2l,-yc2,'linear');bl3=interp1(f,b2l,-
yc3,'linear');%horizontal left rail
ar1=interp1(c,a2r,yc1,'linear');ar2=interp1(c,a2r,yc2,'linear');ar3=interp1(c,a2r,yc3,'linear');%horizonta
l right rail
br1=interp1(c,b2r,yc1,'linear');br2=interp1(c,b2r,yc2,'linear');br3=interp1(c,b2r,yc3,'linear');%horizont
al right rail
longslipright1=(-L./R1)+(-conicity* lateralshift1*10^-3 /ro);
longslipright2=(-L./R2)+(-conicity* lateralshift2*10^-3 /ro);
longslipright3=(-L./R3)+(-conicity* lateralshift3*10^-3 /ro);
longslipleft1=(L./R1)+(conicity* lateralshift1*10^-3 /ro);
longslipleft2=(L./R2)+(conicity* lateralshift2*10^-3 /ro);
longslipleft3=(L./R3)+(conicity* lateralshift3*10^-3 /ro);
attackang1=acos(1- longslipright1);attackang2=acos(1- longslipright2);attackang3=acos(1-
longslipright3);
lateralslip1= attackang1;lateralslip2= attackang2;lateralslip3= attackang3;
spin=sind(conicity)/ro;% spin due to conicity
%%%%%%%%%%%%%%%%%%%%%%%%%%%%%%%%%%%%%%%%%%%%%%%%%%%%%%%%%%
vl1slip=vl.*abs(longslipright1);%slip
vl2slip=vl.*abs(longslipright2);%slip
vl3slip=vl.*abs(longslipright3);%slip
%%%%%%%%%%%%%%%%%%%%%%%%%%%%%%%%%%%%%%%%%%%%%%%%%%%%%%%%%%
```

```
vr1slip=vr.*abs(longslipright1);%slip

vr2slip=vr.*abs(longslipright2);%slip

vr3slip=vr.*abs(longslipright3);%slip

%%%%%%%%%%%%%%%%%%%%%%%%%%%%%%%%%%%%%%%%%%%%%%%

%contact forces for lateral components and for friction conditions

% lateral low velocity ranges

Fyl1=(m*vl.^2.*cosd(cant1)./R1)-(w.*sind(cant1));

Fyl2=(m*vl.^2.*cosd(cant2)./R2)-(w.*sind(cant2));

Fyl3=(m*vl.^2.*cosd(cant3)./R3)-(w.*sind(cant3));

% lateral high velocity ranges

Fyr1=(m*vr.^2.*cosd(cant1)./R1)-(w.*sind(cant1));

Fyr2=(m*vr.^2.*cosd(cant2)./R2)-(w.*sind(cant2));

Fyr3=(m*vr.^2.*cosd(cant3)./R3)-(w.*sind(cant3));

% normal low velocity ranges

Fz1l=(m*vl.^2.*sind(cant1)./(R1))+w*cosd(cant1);

Fz2l=(m*vl.^2.*sind(cant2)./(R2))+w*cosd(cant2);

Fz3l=(m*vl.^2.*sind(cant3)./(R3))+w*cosd(cant3);

% normal high velocity ranges

Fz1r=(m*vr.^2.*sind(cant1)./(R1))+w*cosd(cant1);

Fz2r=(m*vr.^2.*sind(cant2)./(R2))+w*cosd(cant2);

Fz3r=(m*vr.^2.*sind(cant3)./(R3))+w*cosd(cant3);

%% Normal  force components for R=800

FBKl1=(0.5*Fz1l)+(1.1*Fyl1);FBjl1=Fyl1-Fyl1;FBKr1=0.5*Fz1r+1.1*Fyr1;FBjr1=Fyr1;

FAKl1=(0.5*Fz1l)-(1.1*Fyl1);FAjl1=Fyl1;FAKr1=0.5*Fz1r-1.1*Fyr1;FAjr1=0;

FBl1=sqrt((FBKl1.^2)+(FBjl1.^2));FBr1=sqrt(FBKr1.^2+FBjr1.^2);
```

```
FAl1=sqrt((FAKl1.^2)+(FAjl1.^2));FAr1=sqrt(FAKr1.^2+FAjr1.^2);
%%  Normal  force components for R=600
FBKl2=0.5*Fz2l+1.1*Fyl2;FBjl2=Fyl2-Fyl2;FBKr2=0.5*Fz2r+1.1*Fyr2;FBjr2=Fyr2;
FAKl2=0.5*Fz2l-1.1*Fyl2;FAjl2=Fyl2;FAKr2=0.5*Fz3r-1.1*Fyr2;FAjr2=Fyr2-Fyr2;
FBl2=sqrt((FBKl2.^2)+(FBjl2.^2));FBr2=sqrt(FBKr2.^2+FBjr2.^2);
FAl2=sqrt((FAKl2.^2)+(FAjl2.^2));FAr2=sqrt(FAKr2.^2+FAjr2.^2);
% Normal  force components for R=400
FBKl3=0.5*Fz3l+1.1*Fyl3;FBjl3=Fyl3-Fyl3;FBKr3=0.5*Fz3r+1.1*Fyr3;FBjr3=Fyr3;
FAKl3=0.5*Fz3l-1.1*Fyl3;FAjl3=Fyl3;FAKr3=0.5*Fz3r-1.1*Fyr3;FAjr3=Fyr3-Fyr3;
FBl3=sqrt((FBKl3.^2)+(FBjl3.^2));FBr3=sqrt(FBKr3.^2+FBjr3.^2);
FAl3=sqrt((FAKl3.^2)+(FAjl3.^2));FAr3=sqrt(FAKr3.^2+FAjr3.^2);
%%%%%%%%%%%%%%%%%%%%%%%%%%
mu=0.5;
%friction  R=800
ffAl1=mu.*FAl1;ffAh1=mu.*FAr1;
ffBl1=mu.*FBl1;ffBh1=mu.*FBr1;
%friction R=600
ffAl2=mu.*FAl2;ffAh2=mu.*FAr2;
ffBl2=mu.*FBl2;ffBh2=mu.*FBr2;
%friction R=400
ffAl3=mu.*FAl3;ffAh3=mu.*FAr3;
ffBl3=mu.*FBl3;ffBh3=mu.*FBr3;
FAjl1=-Fyl1;FAjr1=Fyr2-Fyr2;
FBjl1=Fyl1-Fyl1;FBjr1=Fyr1;
FAjl2=-Fyl2;FAjr2=Fyr2-Fyr2;
```

```
FBjl2=Fyl2-Fyl2;FBjr2=Fyr2;

FAjl3=-Fyl3; FAjr3=Fyr3-Fyr3;

FBjl3=Fyl3-Fyl3;FBjr3=Fyr3;

%contact pressure for canted track left rail heads

Plhl1=FAKl1./(pi.*al1.*bl1*10^6); Plhr1=FAKr1./(pi.*al1.*bl1*10^6);

Plhl3=FAKl3./(pi.*al3.*bl3*10^6); Plhr3=FAKr3./(pi.*al3.*bl3*10^6);

Plhl2=FAKl2./(pi.*al2.*bl2*10^6); Plhr2=FAKr2./(pi.*al2.*bl2*10^6);

%left rail side

Pls1= FAjl1./(0.85.*pi.*al1.*bl1*10^6);%contact pressure at rail side left (Prs)(N/mm^2)

Pls2= FAjl2./(0.85.*pi.*al2.*bl2*10^6);%contact pressure at rail side left (Prs)(N/mm^2)

Pls3= FAjl3./(0.85.*pi.*al3.*bl3*10^6);%contact pressure at rail side left (Prs)(N/mm^2)

%right rail head

Prhl1=FBKl1./(pi.*ar1.*br1*10^6); Prhr1=FBKr1./(pi.*ar1.*br1*10^6);

Prhl2=FBKl2./(pi.*ar2.*br2*10^6); Prhr2=FBKr2./(pi.*ar2.*br2*10^6);

Prhl3=FBKl3./(pi.*ar3.*br3*10^6); Prhr3=FBKr3./(pi.*ar3.*br3*10^6);

%right rail side

Prs1=(FBjr1)./(0.85.*pi.*ar1.*br1*10^6);%contact pressure at rail side right (Pls)(N/mm^2)

Prs2=(FBjr2)./(0.85.*pi.*ar2.*br2*10^6);%contact pressure at rail side right (Pls)(N/mm^2)

Prs3=(FBjr3)./(0.85.*pi.*ar3.*br3*10^6);%contact pressure at rail side right (Pls)(N/mm^2)

%%%%%%%%%%%%%%%%%%%%%%%%%%%%%%%%%%%%%%%%%%%%

%right rail wear coefficients

sirl1=vl1slip; sirr1=vr1slip;

sirl2=vl2slip; sirr2=vr2slip;

sirl3=vl3slip; sirr3=vr3slip;

rirl1=Prhl1./sy; rirr1=Prhr1./sy;
```

```
rirl2=Prhl2./sy; rirr2=Prhr2./sy;

rirl3=Prhl3./sy; rirr3=Prhr3./sy;

rrs1=Prs1./sy;

rrs2=Prs2./sy;

rrs3=Prs3./sy;

sideslip=1;

sls=sideslip;

srs=sideslip;

%left wear

rls1=Pls1./sy;

rls2=Pls2./sy;

rls3=Pls3./sy;

sill1=vl1slip; silr1=vr1slip;

sill2=vl2slip; silr2=vr2slip;

sill3=vl3slip; silr3=vr3slip;

sls=1;%slip

rill1=Plhl1./sy; rilr1=Plhr1./sy;

rill2=Plhl2./sy; rilr2=Plhr2./sy;

rill3=Plhl3./sy; rilr3=Plhr3./sy;

%%%%%%%%%%%%%%%%%%%%%%%%%%%%%%%%%%%%%%%%%%%%

S=[0,0.2,0.21,0.7,0.71,1];

Kw=[1*10^-5,10* 10^-5,30* 10^-5,40* 10^-5,1*10^-5,10* 10^-5];

r=[0,0.8,1];

Ks=[1*10^-5,10* 10^-5,400*10^-5];

%%%%%%%%%%%%%%%%%%%%%%%%%%%%%%%%%%%%%%%%%%%%
```

```
%right head
Kr1l1=interp1(S,Kw,sirl1,'linear');Kr1l2=interp1(r,Ks,rirl1,'linear');
Kr1r1=interp1(S,Kw,sirr1,'linear');Kr1r2=interp1(r,Ks,rirr1,'linear');
Kr2l1=interp1(S,Kw,sirl2,'linear');Kr2l2=interp1(r,Ks,rirl2,'linear');
Kr2r1=interp1(S,Kw,sirr2,'linear');Kr2r2=interp1(r,Ks,rirr2,'linear');
Kr3l1=interp1(S,Kw,sirl3,'linear');Kr3l2=interp1(r,Ks,rirl3,'linear');
Kr3r1=interp1(S,Kw,sirr3,'linear');Kr3r2=interp1(r,Ks,rirr3,'linear');
%left railhead coefficients
Kl1l1=interp1(S,Kw,sill1,'linear'); Kl1l2=interp1(r,Ks,rill1,'linear');
Kl1r1=interp1(S,Kw,silr1,'linear'); Kl1r2=interp1(r,Ks,rilr1,'linear');
Kl2l1=interp1(S,Kw,sill2,'linear');Kl2l2=interp1(r,Ks,rill2,'linear');
Kl2r1=interp1(S,Kw,silr2,'linear');Kl2r2=interp1(r,Ks,rilr2,'linear');
Kl3l1=interp1(S,Kw,sill3,'linear');Kl3l2=interp1(r,Ks,rill2,'linear');
Kl3r1=interp1(S,Kw,silr3,'linear');Kl3r2=interp1(r,Ks,rilr2,'linear');
%right-side wear coefficients
Ksr11=interp1(S,Kw,srs,'linear');Ksr12=interp1(r,Ks,rrs1,'linear');
Ksr211=interp1(S,Kw,srs,'linear');Ksr222=interp1(r,Ks,rrs2,'linear');
Ksr311=interp1(S,Kw,srs,'linear');Ksr332=interp1(r,Ks,rrs3,'linear');
%left-side wear coefficients
Ksl11=interp1(S,Kw,sls,'linear'); Ksl12=interp1(r,Ks,rls1,'linear');
Ksl21=interp1(S,Kw,sls,'linear'); Ksl22=interp1(r,Ks,rls2,'linear');
Ksl31=interp1(S,Kw,sls,'linear'); Ksl32=interp1(r,Ks,rls3,'linear');
%%%%%%%%%%%%%%%%%%%%%%%%%%%%%%%%%%%%%%%%%%%%
Wearcoefficientll1=(Kl1l1+Kl1l2)./2; Wearcoefficientlr1=(Kl1r1+Kl1r2)./2;
Wearcoefficientll2=(Kl2l1+Kl2l2)./2; Wearcoefficientlr2=(Kl2r1+Kl2r2)./2;
```

```
Wearcoefficientll3=(Kl3l1+Kl3l2)./2; Wearcoefficientlr3=(Kl3r1+Kl3r2)./2;
Wearcoefficientrl1=(Kr1l1+Kr1l2)./2; Wearcoefficientrr1=(Kr1r1+Kr1r2)./2;
Wearcoefficientrl2=(Kr2l1+Kr2l2)./2; Wearcoefficientrr2=(Kr2r1+Kr2r2)./2;
Wearcoefficientrl3=(Kr3l1+Kr3l2)./2; Wearcoefficientrr3=(Kr3r1+Kr3r2)./2;
%%%%%%%%%%%%%%%%%%%%%%%%%%%%%%%%%%%%%%%%%%%%
Rightwear1l=abs(longslipright1).*(FBKl1.*Wearcoefficientrl1)./(yieldstrength);
Rightwear2l=abs(longslipright2).*(FBKl2.*Wearcoefficientrl2)./(yieldstrength);
Rightwear3l=abs(longslipright3).*(FBKl3.*Wearcoefficientrl3)./(yieldstrength);
Rightwear1r=abs(longslipright1).*(FBKr1.*Wearcoefficientrr1)./(yieldstrength);
Rightwear2r=abs(longslipright2).*(FBKr2.*Wearcoefficientrr2)./(yieldstrength);
Rightwear3r=abs(longslipright3).*(FBKr3.*Wearcoefficientrr3)./(yieldstrength);
Leftwear1l=abs(longslipleft1).*(FAKl1.*Wearcoefficientll1)./(yieldstrength);
Leftwear2l=abs(longslipleft2).*(FAKl2.*Wearcoefficientll2)./(yieldstrength);
Leftwear3l=abs(longslipleft3).*(FAKl3.*Wearcoefficientll3)./(yieldstrength);
Leftwear1r=abs(longslipleft1).*(FAKr1.*Wearcoefficientlr1)./(yieldstrength);
Leftwear2r=abs(longslipleft2).*(FAKr2.*Wearcoefficientlr2)./(yieldstrength);
Leftwear3r=abs(longslipleft3).*(FAKr3.*Wearcoefficientlr3)./(yieldstrength);
%%%%%%%%%%%%%%%%%%%%%%%%%%%%%%%%%%%%%%%%%%%%
Wearcoefficientsr1=(Ksr11+Ksr12)./2;
Wearcoefficientsr2=(Ksr211+Ksr222)./2;
Wearcoefficientsr3=(Ksr311+Ksr332)./2;
Wearcoefficientsl1=(Ksl11+ Ksl12)./2;
Wearcoefficientsl2=(Ksl21+ Ksl12)./2;
Wearcoefficientsl3=(Ksl31+ Ksl12)./2;
%%%%%%%%%%%%%%%%%%%%%%%%%%%%%%%%%%%%%%%%%%%%
```

```
wearsrightr1=(FBjr1).*(sideslip.*Wearcoefficientsr1)./(yieldstrength);
wearsrightl1=(FBjl1).*(sideslip.*Wearcoefficientsr1)./(yieldstrength);
wearsrightr2=(FBjr2).*(sideslip.*Wearcoefficientsr2)./(yieldstrength);
wearsrightl2=(FBjl2).*(sideslip.*Wearcoefficientsr2)./(yieldstrength);
wearsrightr3=(FBjr3).*(sideslip.*Wearcoefficientsr3)./(yieldstrength);
wearsrightl3=(FBjl3).*(sideslip.*Wearcoefficientsr3)./(yieldstrength);
%leftside
wearsleftl1=(FAjl1).*(sideslip.*Wearcoefficientsl1)./(yieldstrength);
wearsleftr1=(FAjr1).*(sideslip.*Wearcoefficientsl1)./(yieldstrength);
wearsleftl2=(FAjl2).*(sideslip.*Wearcoefficientsl2)./(yieldstrength);
wearsleftr2=(FAjr2).*(sideslip.*Wearcoefficientsl2)./(yieldstrength);
wearsleftl3=(FAjl3).*(sideslip.*Wearcoefficientsl3)./(yieldstrength);
wearsleftr3=(FAjr3).*(sideslip.*Wearcoefficientsl3)./(yieldstrength);
%assumptions equal amount of wear depth limits (11mm)
limitdepth=11;
depth1=0.75*wearsleftl1*10^5/(pi*2*bl1*10^3);
depth2=0.75*wearsleftl2*10^5/(pi*2*bl2*10^3);
depth3=0.75*wearsleftl3*10^5/(pi*bl3*2*10^3);
depth4=0.75*wearsrightr1*10^5/(pi*2*bl1*10^3);
depth5=0.75*wearsrightr2*10^5/(pi*2*bl2*10^3);
depth6=0.75*wearsrightr3*10^5/(pi*2*bl3*10^3);
%%%%%%%%%%%%%%%%%%%%%%%%%%%%%%%%%%%%%%%%%%%%%%%%%%%%%%%
% Canted curved rail as a function of superelvation
%friction and cross-sectional area loss as a function superelvation deficiency at constant radius
yieldstrength=1350;
```

```
m =10000;

g=9.81;

w=m*g/4;

conicity=0.05;

ro=0.460;

L=0.750;

% canted track properties

R=600; %constant radius

%%%%%%%%%%%%%%%%%%%%%%%%%%%%%%%%%%%%%%%%%%%%%%

veq=10;%equilibrium velocity of the vehicle (m/s)

cant=atand(m*veq^2/(w*R));%cant angle

lateralshift=(ro*L./(R*conicity))*1000*cosd(cant);

ycl=0;yc=lateralshift;ycr=10;

%vehicle tends to move at inner rail side (low velocity)

lateralshiftl= ycl;

%vehicle tends to move at outer rail side (high velocity)

lateralshiftr= ycr;

%%%%%%%%%%%%%%%%%%%%%%%%%%%%%%%%%%%%%%%%%%%%%%

ht=2*L*m*veq^2/(w*R)*1000;% superelvation of the track

%%%%%%%%%%%%%%%%%%%%%%%%%%%%%%%%%%%%%%%%%%%%%%

vl=linspace(0,10,16);%speed of the vehicle below equilibrium(m/s)

vr=linspace(10,15,16);%speed above equilibrium(m/s)

%slips for canted

longsliprightl= (-L./R)+(-conicity* lateralshiftl*10^-3 /ro); % while  inner rail is in flange contact

longsliprightr= (-L./R)+(conicity* lateralshiftr*10^-3 /ro);% wheelsets try to use conicity
```

```
longslipleftl= (L./R)+(conicity* lateralshiftl*10^-3 /ro); % while  inner rail is in flange contact

longslipleftr= (L./R)+(-conicity* lateralshiftr*10^-3 /ro);% wheelsets try to use conicity

sideslipl=1;

sideslipr=1;

%forces

Fyl=(m*vl.^2.*cosd(cant)./(R))-(w.*sind(cant));

Fyr=(m*vr.^2.*cosd(cant)./(R))-(w.*sind(cant));

Fzl= ((m*vl.^2.*sind(cant)./(R))+ w.*cosd(cant));

Fzr= ((m*vr.^2.*sind(cant)./(R))+ w.*cosd(cant));

FAKl=0.5.*Fzl-1.1.*Fyl;

FAKr=0.5.*Fzr-1.1.*Fyr;

FBKl=0.5.*Fzl+1.1.*Fyl;

FBKr=0.5.*Fzr+1.1.*Fyr;

FBjl=Fyl-Fyl;

FBjr=Fyr;

FAjr=Fyl-Fyl;

FAjl=Fyl;

dl=ht-(2*L*m*vl.^2/(w*R)*1000);% superelvation excess

dr=(2*L*m*vr.^2/(w*R)*1000)-ht;% superelvation deficiency

p=100;%

pe=p*(-dl)/ht+p;pf=p*(dr)/ht+p;

ycl=0;

ycr=10;

%%%%%%%%%%%%%%%%%%%%%%%%%%%%%%%%%%%%%%%%%%%%%%%%

%Known contact patch axis dimensions
```

```
c=[0 1 2 3 4 5 6 7 8 9 10];
f=[-10,-9,-8,-7,-6,-5,-4,-3,-2,-1,0];
a2l=[6.5e-3 6.5e-3 6.5e-3 6.3e-3 6.0e-3 5.4e-3 7.8e-3 7.7e-3 7.6e-3 7.4e-3 7.1e-3];
b2l=[6.4e-3 6.4e-3 6.4e-3 7.1e-3 8.2e-3 10.7e-3 3.4e-3 3.5e-3 3.7e-3 4.1e-3 4.9e-3];
a2r=[6.5e-3 6.5e-3 6.5e-3 6.3e-3 6.0e-3 5.4e-3 7.8e-3 7.7e-3 7.6e-3 7.4e-3 7.1e-3];
b2r=[6.4e-3 6.4e-3 6.4e-3 7.1e-3 8.2e-3 10.7e-3 3.4e-3 3.5e-3 3.7e-3 4.1e-3 4.9e-3];
%interpolating contact patch axis dimensions
%to  the inner flange contact
all=interp1(f,a2l,0,'linear');
bll=interp1(f,b2l,0,'linear');
arl=interp1(c,a2r,0,'linear');
brl=interp1(c,b2r,0,'linear');
% to the outer flange contact
alr=interp1(f,a2l,-10,'linear');
blr=interp1(f,b2l,-10,'linear');
arr=interp1(c,a2r,10,'linear');
brr=interp1(c,b2r,10,'linear');
% for canted track
Plh1=FAKl./(pi.*all.*bll*10^6);%contact pressure left Plh(N/mm^2)
Prh1=FBKl./(pi.*arl.*brl*10^6);%contact pressure at right rail(Prh)(N/mm^2)
Prs1=(FBjl)./(0.85.*pi.*arl.*brl*10^6);%contact pressure at rail sideright (Pls)(N/mm^2)
Pls1=abs(FAjl)./(0.85.*pi.*all.*bll*10^6);%contact pressure at rail sideleft (Prs)(N/mm^2)
Plh2=FAKr./(pi.*alr.*blr*10^6);%contact pressure left Plh(N/mm^2)
Prh2=FBKr./(pi.*arr.*brr*10^6);%contact pressure at right rail(Prh)(N/mm^2)
Prs2=(FBjr)./(0.85.*pi.*arr.*brr*10^6);%contact pressure at rail sideright (Pls)(N/mm^2)
```

```
Pls2=abs(FAjr)./(0.85.*pi.*alr.*blr*10^6);%contact pressure at rail sideleft (Prs)(N/mm^2)

%left rail wear coefficients

sy = yieldstrength;

sls=sideslipl;%slip

rls1=Pls1./sy;

rls2=Pls2./sy;

%wears coefficients

%right rail wear coefficients

sir1= vl.*longslipleftl;

sir2=vr.* longslipleftr;

rir1=Prh1./sy;

rir2=Prh2./sy;

sil1= vl.*longslipleftl;

sil2=vr.* longslipleftr;

srs=1;

%ratio b/n pressure to strength

ril1=Plh1./sy;

ril2=Plh2./sy;

rrs1=Prs1./sy;

rrs2=Prs2./sy;

%%%%%%%%%%%%%%%%%%%%%%%%%%%%%%%%%%%%%%%%%%%%%%%

S=[0,0.2,0.21,0.7,0.71,1];

Kw=[1*10^-5,10* 10^-5,30* 10^-5,40* 10^-5,1*10^-5,10* 10^-5];

r=[0,0.8,1];

Ks=[1*10^-5,10* 10^-5,400*10^-5];
```

```
%%%%%%%%%%%%%%%%%%%%%%%%%%%%%%%%%%%%%%%%%%%%%%%%
%right head
Kr11=interp1(S,Kw,sir1,'linear');Kr12=interp1(r,Ks,rir1,'linear');
Kr21=interp1(S,Kw,sir2,'linear');Kr22=interp1(r,Ks,rir2,'linear');
%left railhead coefficients
Kl11=interp1(S,Kw,sil1,'linear'); Kl12=interp1(r,Ks,ril1,'linear');
Kl21=interp1(S,Kw,sil2,'linear');Kl22=interp1(r,Ks,ril2,'linear');
% right-side wear coefficients
Ksr11=interp1(S,Kw,srs,'linear');Ksr12=interp1(r,Ks,rrs1,'linear');
Ksr211=interp1(S,Kw,srs,'linear');Ksr222=interp1(r,Ks,abs(rrs2),'linear');
%left-side wear coefficients
Ksl11=interp1(S,Kw,sls,'linear'); Ksl12=interp1(r,Ks,rls1,'linear');
Ksl21=interp1(S,Kw,sls,'linear'); Ksl22=interp1(r,Ks,rls2,'linear');
%%%%%%%%%%%%%%%%%%%%%%%%%%%%%%%%%%%%%%%%%%%%%%%%
% for cant excess
Wearcoefficientl1=(Kl11+Kl12)./2;
Wearcoefficientr1=(Kr11+Kr12)./2;
Wearcoefficientsr1=(Ksr11+Ksr12)./2;
Wearcoefficientsl1=(Ksl11+ Ksl12)./2;
wearsrightl=abs(FBjl).*(sideslipl.*Wearcoefficientsr1)./(yieldstrength);
wearsleftl=abs(FAjl).*(sideslipl.* Wearcoefficientsl1)./(yieldstrength);
Rightwearl=abs(longsliprightl).*(FBKl.* Wearcoefficientr1)./(yieldstrength);
Leftwearl=abs(longslipleftl).*(FAKl.* Wearcoefficientl1)./(yieldstrength);
%%%%%%%%%%%%%%%%%%%%%%%%%%%%%%%%%%%%%%%%%%%%%%%%
%cant deficiency
```

```
Wearcoefficientl2=(Kl21+Kl22)./2;

Wearcoefficientr2=(Kr21+Kr22)./2;

Wearcoefficientsr2=(Ksr211+Ksr222)./2;

Wearcoefficientsl2=(Ksl21+ Ksl12)./2;

wearsrightr=abs(FBjr).*(sideslipr.*Wearcoefficientsr2)./(yieldstrength);

wearsleftr=abs(FAjr).*(sideslipr.* Wearcoefficientsl2)./(yieldstrength);

Rightwearr=abs(longsliprightr).*(FBKr.* Wearcoefficientr2)./(yieldstrength);

Leftwearr=abs(longslipleftr).*(FAKr.* Wearcoefficientl2)./(yieldstrength);

%%%%%%%%%%%%%%%%%%%%%%%%%%%%%%%%%%%%%%%%%%%

% Normal component of forces at the two rails

mu=0.4;

FBl=sqrt((FBKl.^2)+(FBjl.^2));FBr=sqrt(FBKr.^2+FBjr.^2);

FAl=sqrt((FAKl.^2)+(FAjl.^2));FAr=sqrt(FAKr.^2+FAjr.^2);

ffAl=mu.*FAl;ffAr=mu.*FAr;

ffBl=mu.*FBl;ffBr=mu.*FBr;

%%%%%%%%%%%%%%%%%%%%%%%%%%%%%%%%%%%%%%%%%%%%

% Plotting commands

% horizontal with radius wear at right rail head

A= Rightwear1*10^5;B= Rightwear2*10^5;C= Rightwear3*10^5;

subplot(221), plot(R,A)

xlabel('Radius (m) for v=1 m/s'),ylabel('Wear at Right rail side (mm^2/MGT)')

subplot(222), plot(R,B)

xlabel('Radius (m)for v=5 m/s'),ylabel('Wear at Right rail side (mm^2/MGT)')

subplot(223), plot(R,C)

xlabel('Radius (m) for v=10 m/s'),ylabel('Wear at Right rail side (mm^2/MGT)')
```

```
subplot(224),plot(R,A,R,B,R,C)
xlabel('Radius (m)'),ylabel('Wear at Right rail side (mm^2/MGT)')
%%%%%%%%%%%%%%%%%%%%%%%%%%%%%%%%%%%%%%%%%%%%%%%%%%%%%%
% horizontal with radius left head wear
A=Leftwear1*10^5;B=Leftwear2*10^5;C=Leftwear3*10^5;
subplot(221), plot(R,A)
xlabel('Radius (m) for v=1 m/s'),ylabel('Wear at Left head  (mm^2/MGT)')
subplot(222), plot(R,B)
xlabel('Radius (m)for v=5 m/s'),ylabel('Wear at Left head  (mm^2/MGT)')
subplot(223), plot(R,C)
xlabel('Radius (m) for v=10 m/s'),ylabel('Wear at Left head (mm^2/MGT)')
subplot(224),plot(R,A,R,B,R,C)
xlabel('Radius (m)'),ylabel('Wear at Left head (mm^2/MGT)')
%%%%%%%%%%%%%%%%%%%%%%%%%%%%%%%%%%%%%%%%%%%%%
%horizontal with radius right side wear
A=wearsright1*10^5;B=wearsright2*10^5;C=wearsright3*10^5;
subplot(221), plot(R,A)
xlabel('Radius (m) for v=1 m/s'),ylabel('Wear at Right rail side (mm^2/MGT)')
subplot(222), plot(R,B)
xlabel('Radius (m)for v=5 m/s'),ylabel('Wear at Right rail side (mm^2/MGT)')
subplot(223), plot(R,C)
xlabel('Radius (m) for v=10 m/s'),ylabel('Wear at Right rail side (mm^2/MGT)')
subplot(224),plot(R,A,R,B,R,C)
xlabel('Radius (m)'),ylabel('Wear at Right rail side (mm^2/MGT)')
% horizontal with velocity wear at right rail side
```

```
subplot(221), plot(v,A)
xlabel('Velocity (m/s) for R=700 m'),ylabel('side wear(mm^2/MGT)')
subplot(222), plot(v,B)
xlabel('Velocity (m/s) for R=900 m'),ylabel('side wear  (mm^2/MGT)')
subplot(223), plot(v,C)
xlabel('Velocity (m/s) for R=1100 m'),ylabel('side wear (mm^2/MGT)')
subplot(224),plot(v,A,v,B,v,C)
xlabel('Velocity (m/s)'),ylabel('crossectional area loss at rail side (mm^2/MGT)')
%%%%%%%%%%%%%%%%%%%%%%%%%%%%%%%%%%%%%%%%%%%%%%%%%%%
%Canted rail with radius
% canted with radius wear at right rail head
A=Rightwear1*10^5;B=Rightwear2*10^5;C=Rightwear3*10^5;
subplot(221), plot(R,A)
xlabel('Radius (m) for v=5 m/s'),ylabel('Wear at Right rail head (mm^2/MGT)')
subplot(222), plot(R,B)
xlabel('Radius (m)for v=10 m/s'),ylabel('Wear at Right rail head (mm^2/MGT)')
subplot(223), plot(R,C)
xlabel('Radius (m) for v=15 m/s'),ylabel('Wear at Right rail head (mm^2/MGT)')
subplot(224),plot(R,A,R,B,R,C)
xlabel('Radius (m)'),ylabel('Wear at Right rail head (mm^2/MGT)')
% canted with radius wear at left rail head
A=Leftwear1*10^5;B=Leftwear2*10^5;C=Leftwear3*10^5;
subplot(221), plot(R,A)
xlabel('Radius (m) for v=5 m/s'),ylabel('Wear at Left rail head (mm^2/MGT)')
subplot(222), plot(R,B)
```

```
xlabel('Radius (m)for v=10 m/s'),ylabel('Wear at Left rail head (mm^2/MGT)')
subplot(223), plot(R,C)
xlabel('Radius (m) for v=15 m/s'),ylabel('Wear at Left rail head (mm^2/MGT)')
subplot(224),plot(R,A,R,B,R,C)
xlabel('Radius (m)'),ylabel('Wear at Left rail head (mm^2/MGT)')
%canted with radius wear at right rail side
A=wearsright1*10^5;B=wearsright2*10^5;C=wearsright3*10^5;
subplot(221), plot(R,A)
xlabel('Radius (m) for v=5 m/s'),ylabel('Wear at right rail side (mm^2/MGT)')
subplot(222), plot(R,B)
xlabel('Radius (m)for v=10 m/s'),ylabel('Wear at right rail side (mm^2/MGT)')
subplot(223), plot(R,C)
xlabel('Radius (m) for v=15 m/s'),ylabel('Wear at right rail side(mm^2/MGT)')
subplot(224),plot(R,A,R,B,R,C)
xlabel('Radius (m)'),ylabel('Wear at right rail side (mm^2/MGT)')
% canted with radius wear at left rail side
A=wearsleft1*10^5;B=wearsleft2*10^5;C=wearsleft3*10^5;
subplot(221), plot(R,A)
xlabel('Radius (m) for v=5 m/s'),ylabel('Wear at Left rail side (mm^2/MGT)')
subplot(222), plot(R,B)
xlabel('Radius (m)for v=10 m/s'),ylabel('Wear at Left rail side (mm^2/MGT)')
subplot(223), plot(R,C)
xlabel('Radius (m) for v=15 m/s'),ylabel('Wear at Left rail side(mm^2/MGT)')
subplot(224),plot(R,A,R,B,R,C)
xlabel('Radius (m)'),ylabel('Wear at Left rail side (mm^2/MGT)')
```

```
% Canted rail with velocity for right and left side wears

%canted with velocity wear at right rail side

A= wearsrightl1*10^5;B= wearsrightl2*10^5;C= wearsrightl33*10^5;D= wearsrightr1*10^5;

E= wearsrightr2*10^5;F= wearsrightr3*10^5;

subplot(221), plot(vl,A,vr,D)

xlabel('Velocity (m/s) for R=800 m'),ylabel('Wear at left side  (mm^2/MGT)')

subplot(222), plot(vl,B,vr,E)

xlabel('Velocity (m/s) for R=600 m'),ylabel('Wear at left side  (mm^2/MGT)')

subplot(223), plot(vl,C,vr,F)

xlabel('Velocity (m/s) for R=400 m'),ylabel('Wear at left side  (mm^2/MGT)')

subplot(224),plot(vl,A,vl,B,vl,C,vr,D,vr,E,vr,F)

xlabel('Velocity (m/s) '),ylabel('Wear at left side  (mm^2/MGT)')

% canted with velocity wear at left rail side

A=wearsleftl1*10^5;B=wearsleftl2*10^5;C=wearsleftl3*10^5;D=wearsleftr1*10^5;

E=wearsleftr2*10^5;F=wearsleftr3*10^5;

subplot(221), plot(vl,A,vr,D)

xlabel('Velocity (m/s) for R=800 m'),ylabel('Wear at left side  (mm^2/MGT)')

subplot(222), plot(vl,B,vr,E)

xlabel('Velocity (m/s) for R=600 m'),ylabel('Wear at left side  (mm^2/MGT)')

subplot(223), plot(vl,C,vr,F)

xlabel('Velocity (m/s) for R=400 m'),ylabel('Wear at left side  (mm^2/MGT)')

subplot(224),plot(vl,A,vl,B,vl,C,vr,D,vr,E,vr,F)

xlabel('Velocity (m/s) '),ylabel('Wear at left side  (mm^2/MGT)')

%%%%%%%%%%%%%%%%%%%%%%%%%%%%%%%%%%%%%%%%%%%%%

Canted rail with superelvation deficiency
```

```
% Head wear at right rail with superelvation deficiency
A=Rightwear1*10^5;B=Rightwear2*10^5;C=Rightwear3*10^5;
subplot(221), plot(R,A)
xlabel('Radius (m) for v=1 m/s'),ylabel('Wear at Left head  (mm^2/MGT)')
subplot(222), plot(R,B)
xlabel('Radius (m)for v=10 m/s'),ylabel('Wear at Left head  (mm^2/MGT)')
subplot(223), plot(R,C)
xlabel('Radius (m) for v=10 m/s'),ylabel('Wear at Left head (mm^2/MGT)')
subplot(224),plot(R,A,R,B,R,C)
xlabel('Radius (m)'),ylabel('Wear at Left head (mm^2/MGT)')
% Head wear at left rail with superelvation deficiency
A=Leftwear1*10^5;B=Leftwear2*10^5;C=Leftwear3*10^5;
subplot(221), plot(R,A)
xlabel('Radius (m) for v=1 m/s'),ylabel('Wear at Left head  (mm^2/MGT)')
subplot(222), plot(R,B)
xlabel('Radius (m)for v=10 m/s'),ylabel('Wear at Left head  (mm^2/MGT)')
subplot(223), plot(R,C)
xlabel('Radius (m) for v=10 m/s'),ylabel('Wear at Left head (mm^2/MGT)')
subplot(224),plot(R,A,R,B,R,C)
xlabel('Radius (m)'),ylabel('Wear at Left head (mm^2/MGT)')
% Side wears at right rail with superelvation deficiency
A= wearsright1*10^5;B= wearsright2*10^5;C= wearsright3*10^5;
subplot(221), plot(R,A)
xlabel('Radius (m) for v=1 m/s'),ylabel('Wear at Left head  (mm^2/MGT)')
subplot(222), plot(R,B)
```

```
xlabel('Radius (m)for v=10 m/s'),ylabel('Wear at Left head  (mm^2/MGT)')
subplot(223), plot(R,C)
xlabel('Radius (m) for v=10 m/s'),ylabel('Wear at Left head (mm^2/MGT)')
subplot(224),plot(R,A,R,B,R,C)
xlabel('Radius (m)'),ylabel('Wear at Left head (mm^2/MGT)')
% Side wears at left rail with superelvation deficiency
A=wearsleftl*10^5;B=wearsleftr*10^5;
subplot(221), plot(dl,A)
xlabel('superelvation excess'),ylabel('Side wear at left rail(mm^2/MGT)')
subplot(222), plot(dr,B)
xlabel('superelvation deficiency (mm)'),ylabel('Side wear at left rail(mm^2/MGT)')
subplot(223), plot(-dl,A,dr,B)
xlabel('superelvation deficiency (mm)'),ylabel('Side wear at left rail(mm^2/MGT)')
subplot(224),plot(pe,A,pf,B)
xlabel('superelvation deficiency (%)'),ylabel('Side wear at left rail(mm^2/MGT)
```